Friction Compensation Using Adaptive Nonlinear Control with Persistent Excitation

by

Kathleen M. Misovec

S.B., Aeronautics and Astronautics
Massachusetts Institute of Technology(1984)

S.M. Aeronautics and Astronautics
Massachusetts Institute of Technology (1986)

Submitted to the Department of Mechanical Engineering
in partial fulfillment of the requirements for the degree of

Doctor of Philosophy

at the

Massachusetts Institute of Technology

February 1997

©Massachusetts Institute of Technology 1997. All rights reserved.

Author _____
Department of Mechanical Engineering
February 11, 1997

Certified by _____
Anuradha M. Annaswamy
Associate Professor of Mechanical Engineering
Thesis Supervisor

Accepted by _____
Professor Ain Sonin
Chairman, Department Graduate Committee

OF TECHNOLOGY

Eng

APR 1 6 1997

LIBRARIES

Friction Compensation Using Adaptive Nonlinear Control with Persistent Excitation

by

Kathleen M. Misovec

Submitted to the Department of Mechanical Engineering
on January 15, 1997, in partial fulfillment
of the requirements for the degree of
Doctor of Philosophy

Abstract

Nonlinear frictional dynamics reduce the tracking performance of machine control systems involving high-precision low-velocity tasks. We present an adaptive nonlinear friction compensation scheme which captures problematic friction effects, including Stribeck effect, hysteresis, stick-slip, presliding displacement and rising static friction. Our compensator is designed for stable compensation for the effects of the friction force due to its static, Coulomb and viscous components, while remaining robust to perturbations in friction force due to frictional lag and frictional memory. Simulation studies show that our method improves the tracking performance in low velocity tasks and overcomes the specific problems caused by nonlinear friction dynamics such as stick-slip limit cycling, hunting about a set point, and hysteresis.

A new type of error model is developed based on the design of the friction compensation scheme. The main features of this error model are that, the regression vector, a known function used to generate parameter adaptive laws, contains first and third quadrant nonlinearities, and disturbances, representing perturbations due to frictional dynamics, include Lipschitz and bounded disturbances. This error model is used to extend robust adaptive theory using persistently exciting inputs.

The main analytical result is that if the inputs are persistently exciting over a small enough subinterval with a large enough degree of persistent excitation compared to the disturbances, and if the bandwidth of the linear controller is high enough relative to the Lipschitz disturbances, then the error model system has bounded solutions. Using properties of first and third quadrant nonlinearities, we choose conditions about the subinterval in the persistent excitation condition as well as a scaling factor relating the functions in the regression vector so that a positive definite function of the system errors decreases on every interval of a certain length by an amount more than it increases over the same interval. Additionally, if the Lipschitz disturbances are small enough, an algorithm exists to compute persistent excitation conditions and tracking error and parameter error bounds for the friction compensation system. Simulations show that adding persistent excitation to the adaptive nonlinear friction compensator improves tracking performance using acceptable parameter estimates and reasonable control levels.

Thesis Supervisor: Anuradha M. Annaswamy
Title: Associate Professor of Mechanical Engineering

Acknowledgments

First of all, I would like to thank **Professor Anuradha Annaswamy**. She always made plenty of time to talk about the research in a way that is the purest form of what academia should be-questioning, open to possibilities, and dedicated to working through the uncertainties and difficulties in pursuit of the solutions to problems that are both challenging and practical. I have benefitted enormously from her numerous insights in these discussions. In addition to her technical expertise, I have rarely found the level of integrity and character that in a person I have found in her, and I could always trust that through times that were sometimes stressful for me. Watching her approach research with calmness, patience and dedication was a valuable lesson for me. I want to thank her especially for giving me the chance to work with her, for being open to allowing me to construct a program that worked for me, and for letting me grow and find my way. Finally, her immense enthusiasm and excitement made our work together fun.

I would like to thank the members of my committee. Thanks to **Professor Haruhiko Asada** for helping me make my explanations clearer, and helping me gain perspective by his appreciation for broader issues and implications, and taking the time to discuss the work with me and share his technical and physical insights. I would also like to thank him for organizing valuable programs and research discussions for students and professors in different labs that encourage interaction, communication and educational exchanges. Thanks to **Professor Munther Dahleh** for his wonderful classes on nonlinear control and his quick elucidation of the deeper issues of any technical problem. I really appreciate his taking the time to talk to me about my work and giving me support and encouragement that really helped me. And thanks to **Professor Zaichun Feng** for taking a genuine interest in my work and for his thoughtful and helpful discussions on my problem and his own work in nonlinear mechanics, and also for his physical insights.

I would like to thank my family for their constant love, encouragement, and support: My father, **Dr. Andrew P. Misovec**, my earliest teacher, for introducing me to mathematics and science, for teaching me to persist and for always taking the time to listen and encourage me. My mother **Margaret Misovec** for caring about me so much and being thoughtful, supportive, encouraging and kind. My brothers **Andrew C. Misovec** and **Michael Misovec** for always being there for me and for taking the time to listen and offer encouragement. **Shelley and Justin** for being there and for making things fun. My grandmother and uncle **Mary and Paul Misovec** for the countless wonderful and generous things that they have done for me over the years. The **Telliers**, **Rene, Patricia and Jimmy**, for their kindness and support and for a home away from home that was really a comfort to me.

Others who have had tremendous impact on me include **Dr. Bruce Johnson**, who was my friend as well as my mentor at SatCon Technology Corporation. I have always

regarded all that I learned from him as one of the largest parts of my education. I am also immensely grateful to **Professor Ain Sonin**. Talking to him helped me to gain perspective and helped me to learn how to try to appreciate and enjoy 'life's existential uncertainties.'

I would like to thank **Dr. Rienk Bakker, Dr. Steingrimur Karason, Fredrik Skantze, and Dr. Ssu-Hsin Yu** for making the adaptive control group a stimulating, educational and collaborative environment. And **Aleksandar Kojic, Chayakorn Thanomsat, and Jennifer Rumsey** for continuing in that tradition.

I would like to thank everybody at **SatCon Technology Corporation** for educational and financial support. The people that I worked with at SatCon were a real team with tremendous innovative abilities, creativity and technical insights. They generously supported my endeavors and taught me invaluable lessons. I would especially like to thank **Dave Eisenhaure** for giving me the opportunity to work there. And thanks also to **Dick Hockney**, **Dr. Jim Downer**, **Bill Bonnice**, **Jim Goldie**, **Dr. Mike Gerver**, **Dr. Dick Torti**.

And there were many helpful people at MIT including the following: **Professor Richard Melrose**, who gave me a taste and appreciation for mathematical analysis along with a wonderful collection of philosophical quotes and jokes. Now I can always be happy when I'm confused because 'confusion is the start of understanding.' **Professor Derek Rowell**, who was a fun Professor to TA for, and I think his class demonstrations of second order systems with a rubber band and a coffee cup were the greatest! **Professor Jean-Jacques Slotine** for being helpful and taking an interest in my work and my program. **Professor James Williams**, for getting me to laugh and for paving a courageous way for the special issues faced by students of underrepresented groups. **Professor Dave Trumper**, who was a great TA before being a professor, for his kind support.

Finally, the generous help and support from **Leslie Regan, Kate Melvin, Kari Kulaszewicz, Joan Kravit, and Peggy Garlick** are greatly appreciated. I want to thank Leslie especially because of her vast knowledge and experience with the department and the graduate school process. Her wisdom and kindness really helped me.

Finally, I would like to thank the following friends and people who helped me: **Dr. Sharon Roberts** for taking the time to listen, for wisdom, guidance and understanding, and for helping me learn. **Monique Gaffney Flynn**, for being a wonderful friend, who was always mega-pysched about finding fun problems in control. **Diane Ho** for her great friendship which I could always count on for wisdom and encouragement, for making Ashdown more fun, and for telling me the best stories, so great that I always found several punchlines before the real punchline. **Tara Goodman** for lots of encouragement and for being a wonderful and understanding friend. **Clau-**

dia Rodriguez for making me laugh and for warmly welcoming me to her warm, crazy and fun loving family fiestas. **Dr. Laura Adams** for making Ashdown a Virginia oasis in Boston and **Dr. J.P. Mattia** for playing bad cop, good cop and good cop,bad cop in the fight to save the dorm from the MIT administration, for his humorous commentaries on life at MIT, and for his appreciation/addiction of a good cuppa cappa. **Karen Richardson and Dr. Tom Richardson** for generously making their home a home away from home. Karen, for being a wonderful, kind and insightful friend and for taking the time to listen and Tom, for his kind advice and encouragement. **Dr. Venetka Agayn, Dr. Jee Hoon Krska, and Dr. Jennifer Wiseman** for their kindness, peacefulness and spirituality through difficult times. **Professor Vernon and Beth Ingram** for all of the important work they do to make Ashdown a community and for taking the time to help me work through grad school and dorm life. **Cedric Logan**, for taking lots of time to listen and be helpful, for being a wonderful and kind friend, and for helping me with the quirks of graphics packages. **Tara Arthur, Valarie Benezra, Juan Bruno, Yonald Cheri, Eddie Chalom, Dr. Alain Curodeau, Adam Dershowitz, Sabrina Greenberg, Rose Gulati, Johnathon Root and Steve Schultz** for their kind and helpful friendships. **Dr. K.O. Prakah-Asante** for his positive, upbeat and encouraging lectures on life, for making me laugh and for telling me wise folk stories a poor little spider named Mr. Ananasai. **Dr. Nicholas Patrick, Dr. Eddie Lanzilotta and Dave Schloerb**, for their kind and supportive friendships as we all went through this together. **Constantinos Boussios** for his great, happy and wise discussions. **Dr. Glenn Tesler, Dr. Mark Joshi and Dr. Richard Stone**, for being friends who patiently took a lot of their time to help me understand my math classes better. **Dr. Djamil Boulahbal**, for being a learn-ed TA and friend. **Dr. 'John-Tom' Johnny Thomas**, for his tremendous wisdom and his many helpful insights.

Contents

1 Introduction 15

1.1 Motivation 15

1.2 Background 17

1.3 Contributions of this Thesis 20

1.4 Synopsis 22

2 Friction: Mechanisms, Dynamic Models and Control 24

2.1 Friction Mechanisms 25

2.1.1 Presliding Displacement and Rising Static Friction 26

2.1.2 Stribeck Effect and Viscous Friction 27

2.1.3 Stick-Slip Limit Cycle 29

2.1.4 Frictional Lag and Hysteresis 30

2.2 Dynamic Models 32

2.2.1 Motivation 32

2.2.2 A Static Friction Model 33

2.2.3 A Dynamic Friction Model 35

2.3 Active Control of Systems with Friction 45

2.3.1 The Inadequacies of Linear Control 46

2.3.2 The Potential of Adaptive Nonlinear Friction Compensation 51

2.4 Chapter Summary 59

3 An Adaptive Nonlinear Compensator Design 61

3.1 Design Objective 62

3.2 Design of Adaptive Nonlinear Friction Compensator . . . 65

3.2.1 Linear Controller 68

3.2.2 Friction Estimator 68

3.3 An Error Model Approach to the Design 75

3.3.1 Why Stability of the Error Model is a Problem . . 76

3.3.2 A New Type of Error Model 79

3.3.3 The Role of Persistent Excitation for Robust Adaptation 82

3.4 Chapter Summary 92

4 Stability of the Adaptive Controller 93

4.1 Preliminaries: Properties About First and Third Quadrant Continuous Functions 95

4.1.1 A Property about First and Third Quadrant Continuous Functions 96

4.1.2 A Property About a Vector of First and Third Quadrant Continuous Functions 98

4.1.3 A Property About the Conditions Required to Apply First and Third Quadrant Function Properties 105

4.2 Preliminaries: Properties About the 'Unforced' Error Model System 109

4.3 Preliminaries: Properties Bounding the Error Model State and the Function, V, on an Interval 114

4.3.1 A Property About the Maximum Increase in V on an Interval 114

4.3.2 A Property About Upper Bounds for States and State Derivatives on an Interval 115

4.4 Robust Adaptive Approach - Use of P.E. Inputs 117

4.5 Proof of Theorem 120

4.5.1 Establish Sufficient Conditions for V to Decrease on ith Interval I_{i_D} 122

4.5.2 Choose Conditions to Make V Decrease First Interval and on Every Subsequent Intervals, Ensuring Bounded Solutions 128

4.6 Computing Theorem Conditions and Bounds for the Friction System 132

4.7 Chapter Summary 139

5 Performance of Friction Compensation Algorithm 140

5.1 Low Velocity Tracking Baseline Tasks with Friction Compensation and P.E. 142

5.1.1 Adaptive Nonlinear Friction Compensation with Sufficient P.E.: A Constant Velocity Task 142

5.1.2 Adaptive Nonlinear Friction Compensator with Sufficient P.E. for Low Velocity Task 2 - A Task with Repeated Zero Velocity Crossings 146

5.1.3 Low Velocity Tracking Task 3 with Friction Compensator and Sufficient P.E.: A Step Response . . . 150

5.2 Comparison of Nonlinear Adaptive Controller using P.E. Inputs with Nonlinear Fixed Detuned Controller 153

5.3 Robustness Simulations 154

5.4 Chapter Summary 158

6 Conclusions 160

A Boundedness of Internal Friction State, z 163

B Bounds for dynamic model perturbation effects, F_{unest}, in the friction model 165

C A Property About First and Third Quadrant Continuous Functions 167

C.1 Threshold for v 167

C.2 v does not change sign for $t \in [t_2\ t_2 + \delta_0]$ 169

C.3 Bounds for $\left| \int_{t_2}^{t_2+\delta_0} f_p(v(\tau))d\tau \right|$ 171

C.4 Proof of Property 4.1.1 171

D A Property About a Vector of First and Third Quadrant Continuous Functions 173

E A Property About the Conditions Required to Exploit First and Third Quadrant Function Properties 179

F Properties about the 'Unforced' Error Model System 182

F.1 Proof of Property 4.2.1 183

F.2 Proof of Lemma 4.2.2 187

G Properties Bounding the Error Model State and the Function, V, on an Interval 190

G.1 Proof of Property 4.3.1 190

G.2 Proof of Property 4.3.2 191

H Choice of p.e. subinterval width, δ_0, and scaling factor, k 194

List of Figures

2-1 Friction force vs. velocity at steady velocity 28

2-2 How stick slip happens 31

2-3 A control system with nonlinear dynamic friction 36

2-4 Modifications to the friction model 38

2-5 Hysteresis effects in the friction model 43

2-6 Linear controller has problems in low velocity regime 47

2-7 P.I.D controller for low velocity task 1- a constant velocity task . . . 50

2-8 P.I.D Control for low velocity task 2- a task with repeated zero velocity crossings 52

2-9 P.I.D. control for low velocity task 3 - a regulation task 53

2-10 Detuned nonlinear control using static friction estimator 56

2-11 Detuned nonlinear friction compensator using z estimator 58

2-12 The potential of adaptive nonlinear friction compensation 60

3-1 Friction compensation scheme 63

3-2 Friction compensation scheme for estimating static friction force . . . 67

3-3 Perturbations in the friction model due to dynamic effects 70

3-4 Error equation representation of closed loop friction compensation system 74

3-5 Adaptive nonlinear friction compensation with insufficient p.e. for low velocity task 1- a constant velocity task 86

3-6 Adaptive nonlinear friction compensation with insufficient p.e. for low velocity task 2- a task with repeated zero velocity crossings 88

3-7 Adaptive nonlinear friction compensation with insufficient p.e. for low velocity task 3- a regulation task 90

3-8 Adaptive nonlinear friction compensation with insufficient p.e. for low velocity task with naturally occurring p.e. 91

4-1 A useful property of first and third quadrant functions 96

4-2 Difference in the scalar function over a subinterval implies a tracking error 103

5-1 Performance improvement of the adaptive nonlinear friction compensator with sufficient p.e. for low velocity task 1- a constant velocity task 144

5-2 Adaptive nonlinear friction compensation with sufficient p.e. for low velocity task 1- a constant velocity task 145

5-3 Performance improvement of the adaptive nonlinear friction compensator with sufficient p.e. for low velocity task 2- a task with repeated zero velocity crossings 147

5-4 Adaptive nonlinear friction compensator with sufficient p.e. for low velocity task 2- a task with repeated zero velocity crossings 148

5-5 Adaptive nonlinear friction compensator with sufficient p.e. for low velocity task 2-hysteresis effects 149

5-6 Performance improvement of the adaptive nonlinear friction compensator with sufficient p.e. for low velocity task 3- a regulation task . . 151

5-7 Adaptive nonlinear friction compensator with sufficient p.e. for low velocity task 3- a regulation task 152

5-8 Tracking performance comparison for adaptive nonlinear and internal friction state estimate based friction compensators 155

5-9 Adaptive nonlinear friction compensation robustness simulation for a regulation task 157

5-10 Adaptive nonlinear friction compensator robustness simulations for baseline study Tasks 1 and 2- constant velocity and repeated zero velocity crossings 159

C-1 If v does not reach threshold value in subinterval, then the integral of v over the subinterval is less than $v_T\delta_0$ 168

F-1 Upper bound for amount of V decrease, γ, vs. T_c 188

Chapter 1

Introduction

1.1 Motivation

Friction is a force that resists the relative motion of contacting bodies. At low velocities, nonlinear contact surface mechanics cause systems to exhibit complex phenomena such as stick-slip and hysteresis. Stick-slip is a sudden transition between a stick phase, in which the bodies are not in relative motion even under the presence of an applied external force, and a slip phase, in which the bodies quickly slip relative to each other. Hysteresis is caused by a lag between a change in velocity and a change in friction force.

In control systems operating at low velocities, the friction force can dominate the effects of the control force and this produces undesirable tracking errors and limit cycling. Control applications involving high-precision, low-velocity tasks frequently exhibit unacceptable performance due to problems with friction. Modifying the control design for compensation of the effects of friction may improve tracking perfor-

mance; however, it is especially difficult due to nonlinearities of the contact surface mechanics, lack of feedback of the internal friction states, and both structural and parametric modelling uncertainty.

A variety of control techniques are available to address problems caused by friction. Passive techniques such as lubricating the surface with grease are only partially effective. Although special chemical agents can be added to the grease to reduce stick-slip effects, they are not particularly effective due to sensitivity to wear and temperature changes. An active technique is to use high bandwidth linear control. By making the control input large compared to the friction force, the friction force and consequent nonlinear behavior no longer dominate. However, high bandwidth control is undesirable because the effects of unmodelled dynamics and sensor noise become problematic at high frequencies.

Friction compensation is an alternative active control strategy in which an appropriate friction model is used to generate a friction estimate which is integrated with a controller to eliminate or reduce the effects of the friction force. The friction model utilized should be accurate enough to capture nonlinear dynamic friction effects and pertinent environmental factors in the system. High control forces are not needed in friction compensation techniques because the goal of the compensation is to match the friction forces, which are generally low in magnitude, and not to dominate them as in a high bandwidth linear design. For these reasons, friction compensation is highly promising and should not have the negative features of either passive techniques or high bandwidth linear techniques.

The potential of friction compensation relies on both accurate friction models and stability-based adaptive and nonlinear control techniques. Both fields are areas of active research. In tribology, much progress has been made in this century in understanding the physics of friction, and although many alternative models exist, they share basic common features. In control, many new methods have been developed

for nonlinear systems and for systems with uncertainty. These methods are geared towards improving performance and maintaining stability in the presence of uncertainties while using reasonable control levels. Recently, control researchers have begun to explore the new methods to try to exploit the known features of the more complex physical-based friction models in order to estimate the unknown features of friction and utilize both to obtain better performance.

1.2 Background

Several researchers have successfully illustrated the potential of friction compensation methods, yet the combination of a sufficiently complex friction model, encompassing most of the nonlinear frictional dynamic effects, and a corresponding controller which provides an adaptive nonlinear compensation has not yet been presented [13, 14, 4]. A good survey paper of friction physics, modelling and compensation techniques is presented in [2].

In [13], adaptive control has been to shown to have the potential to improve problems due to friction. In particular, modelling of the lag between change in velocity and change in friction force, often called the Dahl effect, was particularly helpful in improving performance for trajectories with repeated zero velocity crossings. However, some friction nonlinearities including the Stribeck effect were not included in this study. The Stribeck effect, discussed further in chapter 2, is the dip in the friction force vs. velocity curve when the velocity is held steady, and it is important for the accurate modelling of stick-slip onset conditions.

Nonlinear adaptive friction compensation was shown to improve tracking performance compared to a P.I.D. controller for a positioning table in [14]. The friction model used in this study was a static nonlinear map between velocity and friction force. Dynamic

effects such as frictional lag were not considered.

Unlike the models used in the previous two studies, a new friction model, presented recently in [4], captures both the Stribeck effect as well as frictional lag effects. A nonlinear compensation scheme assuming known model parameters was presented with the new model.

Extending these results to include parameter adaptation would be beneficial because performance improvement depends in part of the parameters in the model, which may be poorly known. However, because parameter adaptation for a nonlinear system is, in general, a difficult problem, an adaptive nonlinear compensator design for this friction model is a non-trivial problem. The groundwork laid in adaptive control for linear systems makes use of linear growth constraints which are not applicable to the general nonlinear problem. Although some nonlinear systems have been successfully analyzed by capitalizing on special structures [11], [25], these special structures are not present in the friction problem.

Although, designing an adaptive nonlinear compensator for the new model represents a new control analysis problem, it is a problem which fits very naturally into the framework that has developed for adaptive control of linear systems, which we now overview briefly.

In adaptive control for linear systems, the overall system is reduced to an error model. This is a nonlinear dynamic system which relates tracking errors and parameter errors. A part of the error model, called the regression vector, is a function of known system variables that, together with tracking error, is used to generate the parameter adaptive laws. Stability analysis for error models, which is important for adequate performance, must use analysis tools geared for nonlinear systems because the overall dynamic system for the tracking and parameter estimation errors is typically nonlinear.

In the late 1970's in [16], the stability of an error model was analyzed for which the regression vector is a bounded function of time. This choice of error model structure was the result an adaptive controller constructed in [15] for a linear system. At the time of the work by [16], boundedness of the regression vector for the linear adaptive control problem had not yet been proved. This problem was actively pursued and solved in the early 1980's when linear growth constraints were used to show that the corresponding regression vector, which is a linear function of the state, was indeed a bounded function of time [20], [19]. This work meant that the stability problem for the general linear adaptive control problem with output feedback had been solved.

The analysis in [16], used arguments based on persistent excitation (p.e.) to show that if the regression vector was p.e., then the error model that was considered, with the bounded regression vector, was uniformly asymptotically stable. Persistent excitation of a signal roughly means that the signal periodically excites enough of system dynamics in every direction. The intuition behind using persistent excitation analysis is that when a sufficiently rich signal is fed into a system, knowledge of the system structure can be used to predict useful characteristics of the system response. The work [16] was significant because coupled with the later results, it implied that persistently exciting inputs could be used to make parameters in the associated linear adaptive control system converge to their true values.

Unlike the linear adaptive problem, in a general nonlinear adaptive problem such as the friction compensation, the regression vector is a nonlinear function of the state and consequently, linear growth arguments used in linear adaptive control to show the regression vector is bounded can not be applied.

In the mid 1980's, research attention took a direction to focus on improving robustness properties of adaptive controllers. It had been discovered ([23], [7]), that bounded disturbances present in a linear adaptive system could make the overall adaptive system unstable by making the parameter estimates grow without bound.

In a friction compensation problem, robustness issues are of particular importance because uncertainties in the model can act as disturbances to the system. The techniques that were developed to address robustness issues for the linear adaptive problem also provide a framework for the nonlinear adaptive friction compensation problem.

Two types of robust adaptive theory were developed. Adaptive law modifications is an approach in which the adaptive laws are modified in ways which prevent parameter divergence. These methods include dead-zones ([7], [24]), maximum parameter bounds, ([12]), sigma modification ([10]), and e-modification ([18]). The other approach is the use of persistently exciting inputs. Work in [17] showed that if the level of persistent excitation is high enough compared to the level of disturbances, then the inputs counter the undesirable effects of the disturbances, and consequently boundedness of the tracking and parameter errors can be obtained.

1.3 Contributions of this Thesis

In this thesis, we will focus on position control of a simple mass with friction based on the new friction model in [4]. We design, analyze and simulate an adaptive nonlinear friction compensator and show that it is successful in improving tracking problems due to friction in low velocity control tasks. Undesirable stick slip limit cycles are eliminated, hunting about a set point is eliminated and large tracking errors are reduced. Furthermore the tracking performance improvement is gained in a stable, robust manner using reasonable levels of control.

The compensator design is motivated by the goal of estimating and compensating for the effects of friction due to it static, Coulomb and viscous components, while remaining robust to perturbations due to dynamics in the model. Compensators which estimate the entire friction force result in error models are still too difficult for

present analysis methods. The design, analysis, and simulation study of the structure and parameter adaptation laws for this adaptive nonlinear compensator is one of the contributions of this thesis.

The particular nonlinearities in the friction system result in a an error model which differs from previously studied error models in two ways. The first and more significant is that the regression vector contains nonlinear first and third quadrant functions of a state variable. The second difference is that the disturbances in our problem include both a bounded and a Lipschitz bounded disturbance whereas previous theory only addressed a bounded disturbance. A Lipschitz bounded disturbance is one which is bounded by linear growth rates. It arises because part of the unestimated part of the model is scaled by relatively fast internal friction dynamics, which scale with velocity. We show that similar to the error models used linear adaptive control which have linear regression vectors, the presence of disturbances in the new type of error model system can also cause instability. For the friction compensation design this means that the perturbations in the model due to dynamics can cause the parameter estimate errors to grow unbounded.

The main contribution of this work is a stability theorem for the new error model which implies the design of a stable adaptive nonlinear friction compensator. The stability theorem states that if the inputs to this new type of error model are persistently exciting over a small enough interval with a large enough level compared to the disturbances in the system and if the bandwidth of the linear portion of the controller is large enough compared to the Lipschitz disturbances in the system, then the error model will have bounded solutions. A second theorem guarantees that the error model solution bounds and the conditions required for stability of the friction compensation system can be computed if the Lipschitz disturbances in the system are small enough. This contribution is important because it shows that, if these perturbations are small, the conditions required in the stability theorem are guaranteed to exist.

Our approach for designing a robust adaptive controller is to use persistent excitation. Although we also examined robust adaptive approaches using adaptive law modifications, the focus in this study is on persistent excitation for two reasons. The first is that friction problems with zero-velocity crossings naturally have some persistent excitation due to the presence of periodically-occurring inputs. The second is that while persistent excitation arguments have been only sparsely used in nonlinear systems; for example, in systems that are bilinear [6], our work, in which the nonlinearity is more general but does have some special features, represents the first time persistent excitation approaches have been explored in this nonlinear adaptive control problem.

In the stability proof, the technique we use to deal with the nonlinearity in the regression vector is to exploit useful properties of first and third quadrant functions. We choose conditions about the p.e. subinterval and as well as a scaling factor so that a measure of regression vector error can be related to a measure of tracking error. Then we choose the p.e. level large enough compared to the disturbances and nonlinearities in the regression vector so that a positive definite function of the system errors decreases on every interval more than its maximum increase on the interval. The problem of a Lipschitz disturbance is handled in a similar manner to linear control problems, i.e. by making the bandwidth of the linear portion of our compensator high enough to reject the disturbance.

1.4 Synopsis

The remainder of the thesis is organized as follows. In chapter 2, we introduce the friction model in [4], which will be used as the basis for this study. We tie the model to the underlying physics of the friction process and verify by simulation that it captures the important nonlinear dynamic friction effects that are under investigation. We also examine alternative modelling techniques in order to study robustness later in

the thesis. For a linear position control system, friction effects can induce undesirable stick slip limit cycling and significant tracking errors in low velocity tasks. Three representative tasks are introduced as a baseline study for the thesis. Finally, we show that by simulation nonlinear friction compensation and nonlinear adaptive friction compensation have the potential to improve tracking performance, and we identify robustness, stability, and control requirements as design issues of importance. In chapter 3, an adaptive nonlinear friction compensator is designed for stable compensation of the static, viscous and Coulomb components of the friction and robustness to dynamic perturbations in the friction force. The overall friction compensation system reduces to a new type of nonlinear error model relating tracking error and parameter errors. We show that stability of the compensator can be affected due to the presence of the dynamic perturbations in the model which act as disturbances, and that this constitutes a new error model stability problem. We introduce persistent excitation as an approach for this issue. In chapter 4, we present a stability theorem for the error model which states that if the input to the control system is persistently exciting with a high enough degree over a small enough subinterval, and if the bandwidth is high enough relative to the Lipschitz disturbance bounds, then the adaptive algorithm will have bounded solutions. We also prove a second theorem which says that an algorithm exists to find appropriate p.e. condition which will satisfy our stability theorem for the friction system if the Lipschitz perturbations in the friction model are small enough. In chapter 5, we present simulation results for the adaptive nonlinear friction compensator using persistent excitation in the inputs. We show this method improves the tracking performance for problematic friction behavior compared to the linear controller. Furthermore, the adaptation algorithm is stable and uses reasonable control levels. In addition, we verify by simulation that our method has some robustness to possible modelling errors and unmodelled dynamics. We also present a brief the performance of the control design with a detuned nonlinear controller. Chapter 6 is the conclusions chapter.

Chapter 2

Friction: Mechanisms, Dynamic Models and Control

In this chapter, we examine the nonlinear dynamic effects of friction and the problems these effects cause in linear control systems. In the first section, we give a brief overview of the history of friction modelling. We describe friction mechanisms that have been observed and we tie each observed behavior to the underlying physical processes. We discuss the primary effects in friction literature including presliding displacement, rising static friction, varying breakaway force, Stribeck effect, stick-slip limit cycling and hysteresis effects. In the next section, we motivate and present a dynamic nonlinear friction model that is based on work by [4]. We show that static models are inadequate in explaining all of the observed friction mechanisms, and we verify that this model captures the frictional mechanisms of interest. Finally, in the third section we discuss the reasons that standard linear controller exhibits tracking performance problems in low-velocity operating regimes. We present three low-velocity tasks, which will serve as a baseline study that we return to in later chapters. We verify that the friction model we use causes the tracking errors and

undesirable limit cycling such as stick slip and hunting about a set point that have been observed experimentally.

2.1 Friction Mechanisms

Because friction, the force resisting the relative motion of contacting bodies, is present in virtually all mechanical systems, friction models, which quantitatively relate the friction force to relevant system information, have been explored for centuries. The earliest known friction model -that friction opposes motion, is proportional to load and independent of the contact area- was postulated by DaVinci in 1519 before Newton's laws were published in 1687. However, this knowledge remained hidden in his notebooks for centuries [2]. The basic effects were later rediscovered, developed, and publicized by other researchers [2]. Amontons, near the year 1699, found that friction was independent of contact area. Around 1785, Coulomb discovered that when the bodies are at rest, the friction is proportional load, and this resulted in this force being called the Coulomb friction. Later in 1833, Morin found that static friction, typically higher than Coulomb friction, is the level of applied force in steady conditions that must exceeded in order for motion to occur. Studies of fluid mechanics by Reynolds led to the viscous friction force model in 1866, in which the friction force present in greased surfaces is proportional to relative velocity. When the velocity is held steady, the friction force is a function of velocity and in most greased and ungreased surfaces there is a drop in the friction force vs. velocity curve at low velocities. This is called the Stribeck effect and was discovered in 1902.

In this century, the field of tribology, the science of rubbing surfaces, has made enormous advances towards identifying these types of behaviors and postulating dynamic friction models that more accurately explain the behaviors because they are rooted in the physics of the contact surface [3, 21, 28, 8, 2]. At the microscopic level, protrusions

in the contact surface called asperities bend in response to relative motion and act as a shear stiffness. The spring-like effect of these bending asperities exert frictional dynamic forces on the system. Additionally, the true contact area, which depends on how much these asperities come together, can be different from the apparent contact area [3]. This observation brought the physical theory closer to experimental results.

In most machine control systems, the surfaces are layered with grease in order to reduce the effects of friction. Grease consists of a solid with a fluid lubricant additive. As the surfaces move in relation to each other, the fluid lubricant comes out of the grease layer. Surfaces sliding on a fluid have less friction than solid-to-solid sliding. Grease does not always eliminate the problem because before the fluid comes out of the boundary layer, the effects of the asperities and shear in the solid boundary layer could dominate.

Examples of the types of behavior that are not adequately modelled by static models are presliding displacement, rising static friction, stick-slip and frictional lag. In the next sections, for each of these observed behavior, we will define and describe the behavior and explain how the underlying physical processes cause the behavior. In the process, we will also explain the static friction model features such as Coulomb friction, static friction constant and Stribeck effect in terms of the underlying physics.

2.1.1 Presliding Displacement and Rising Static Friction

At very low applied force levels, the friction force approximately balances applied force, producing very small (presliding) displacements. As the force level is increased, the friction force rises to match it. This observed behavior is called rising static friction. Eventually, the applied force reaches a level at which the friction can not match the applied force causing breakaway. In a static friction model, in which friction force is considered to be a function of velocity and does not include dynamic effects,

breakaway occurs when the applied friction level exceeds a fixed level which is defined as the static friction constant, F_{static}. In reality; however, the breakaway force does not depend strictly on the applied force level; instead, it also depends on the applied force rate. This behavior is called varying breakaway force.

The underlying physical process that cause these phenomenon can be understood in terms of the asperities, which act as a shear stiffness when the surfaces move relative to one another. The solid boundary layer also resists shear motion and provides damping. At low applied force levels, there is a small deflection in the asperities which are the presliding displacements, the asperities exert a shear spring-like force back on the opposing surface that holds the surfaces together. As the applied force is gradually increased, the asperities bend more to accommodate the increased load, which is the physical reason for rising static friction. As the applied force becomes larger, eventually the asperities bend too far or break. At low velocities the system behaves as a damped spring-mass system, so breakaway is a dynamic phenomena. As the applied force rate is increased, the system does not respond to the high frequencies in the input and the breakaway force is reduced.

2.1.2 Stribeck Effect and Viscous Friction

A static friction model consists of the friction force as a function of velocity when the velocity is held constant. An example is shown in figure 2-1. At zero velocities, the static friction constant, F_{static}, is the peak friction force which must be exceeded in steady conditions for sliding to occur. It is typically higher than the Coulomb friction, F_c, which is proportional to the normal load. Typically, the curve has a dip, called the Stribeck effect, as transition is made from zero to low to higher velocity friction regimes. In greased surfaces, a physical process that is partially responsible for the Stribeck effect is that entrainment of the fluid lubricant out of the grease boundary layer occurs. Because shear in a solid is typically larger than shear in

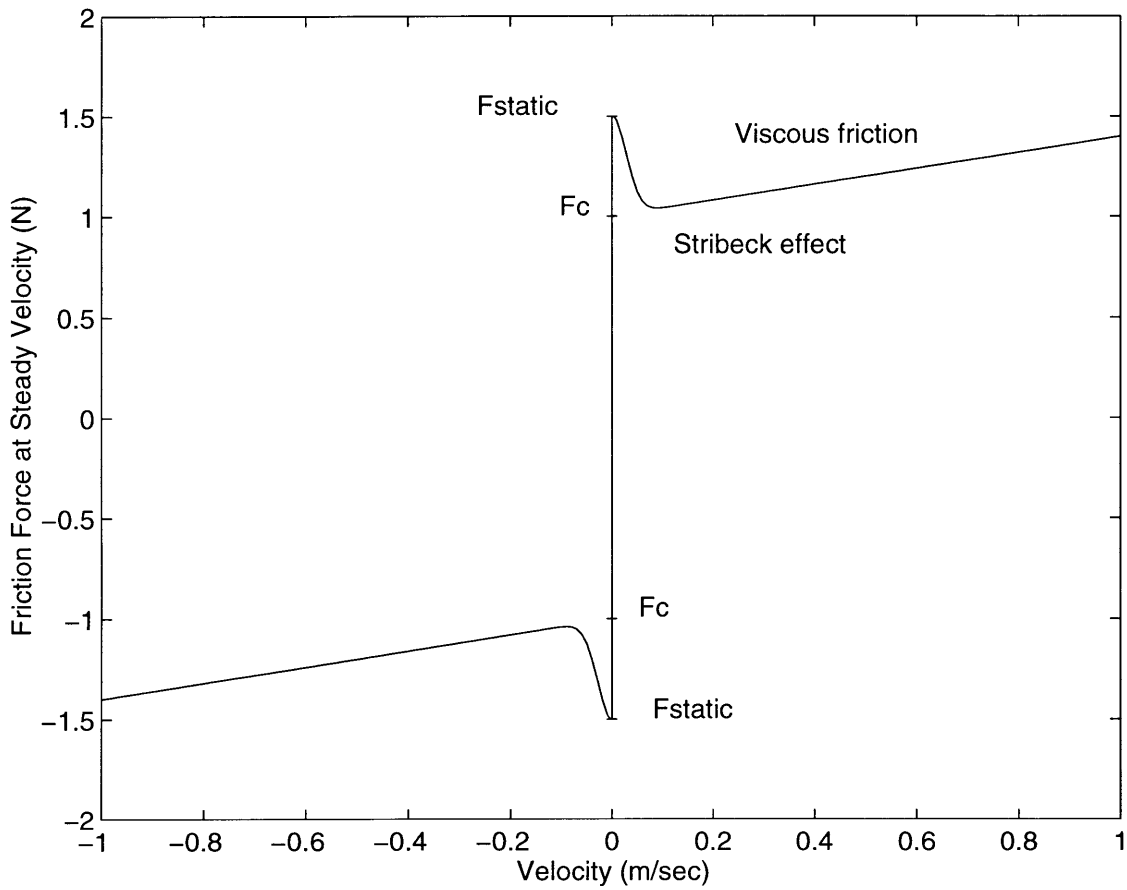

Figure 2-1: When the velocity is held constant, the friction force is a function of velocity. The peak, labelled, F_{static}, is the static friction constant, which must be exceeded in order for motion to occur in steady conditions. It is higher than the Coulomb friction, F_c. The dip in the curve is called the Stribeck effect. The viscous friction regime is at higher magnitudes of velocity, where the friction is a linear function of the velocity.

a fluid, friction force decreases as more fluid is drawn out. The Stribeck effect is also observed in ungreased metal surfaces. As the aggregate spring-like effect of the asperities diminishes with increasing velocity, the friction force, which is proportional to load for ungreased surfaces, drops.

At velocities that are not close to zero, the static friction model is linearly proportional to the velocity. This is called viscous friction.

2.1.3 Stick-Slip Limit Cycle

Stick-slip is an observed behavior which occurs in certain low-velocity conditions in which one of the bodies moving at low velocities stops and remains in 'stick' for a certain length of time, and then suddenly, quickly 'slips' before getting stuck again. This effect is responsible for the familiar unpleasant sound of chalk squeaking on a blackboard or the more pleasant (depending on who is playing) bow on a violin string. Another familiar example is a spring-loaded stapler. As the stapler is opened, the slider mechanism, that holds the staples in place is pulled by a spring. It can suddenly transition from non-motion stick to a fast slip motion and then back to stick. In machine control applications, situations can arise in low velocity regimes in which surfaces keep alternating between the stick and slip conditions, resulting in an undesirable limit cycle.

These limit cycles can occur when the Stribeck effect is present, i.e. when there is a dip in the static force vs. velocity curve [22]. Figure 2-2 shows how the physical features we discussed result in a stick slip limit cycle. A spring is attached to a mass and pulled with a constant relatively small velocity. Before the mass starts to slide, the spring force, F_s increases and the static friction force, F_f, rises to balance the spring force. In this condition, the mass is in the 'stick' position and there are small (presliding) displacements which cause the asperities to bend and balance the spring

force. As the spring force continues to increase, eventually the friction force cannot balance the spring force. At breakaway, the imbalance in the spring force and the friction force causes the mass to slip and there is a sharp increase in velocity. As the mass slides, the spring contracts, reducing the spring force until the mass stops in the stick position again.

Static friction models in which the static friction is higher than the Coulomb friction exhibit the stick-slip phenomena. This can be explained using simple friction models or phase plane diagrams [22]. However, the onset of stick slip conditions is not accurately predicted by these models because breakaway is a really a dynamic phenomena. Friction dynamics are necessary in order to accurately model the conditions that induce the behavior.

2.1.4 Frictional Lag and Hysteresis

Another behavior that is not explained by the static models is frictional lag, which was also observed by [21]. Static models predict that as the velocity changes, the friction force can change instantaneously. However, Newton's laws prohibit an instantaneous change in the friction force with velocity changes, there is a lag.

If velocity is varied sinusoidally, lag in the friction force means that if the force is plotted vs. the velocity there will be a hysteresis loop. Consider the static friction model in figure 2-1. Imagine that the velocity is varied around a very low level which is lower than the lowest part of the Stribeck dip. Instead of the static friction model as shown in figure 2-1, the actual friction force is a perturbation of this curve and the shape of this perturbation is a hysteresis loop. At low velocities when the velocity is accelerating away from zero, there is a drop in the static friction model due to the Stribeck effect. However, because the actual friction force lags the velocity, the force is slightly higher than the static friction curve. Similarly, when the velocity is decreasing,

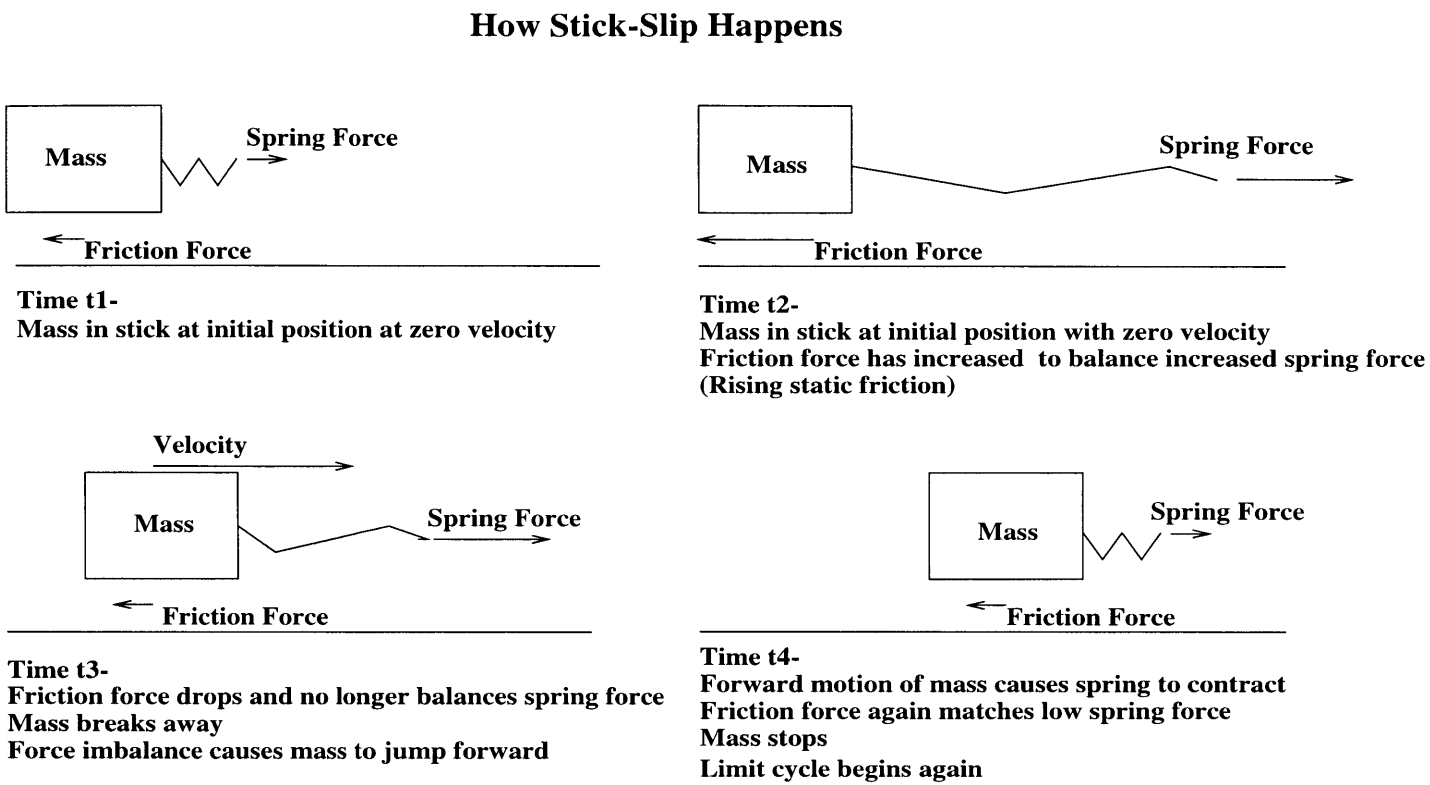

Figure 2-2: If the spring is pulled at low velocities, the friction force initially matches the spring force and the mass does not move (stick). As the spring force increases, the friction force eventually can not balance it. The mass breaks away and there is a sudden quick motion (slip) due to the unbalanced spring force. As the mass moves, tension in the spring relaxes and the low forces can again be balanced by friction so the mass re-enters the stick condition

the static force is rising but, as the friction lags, the force is slightly lower than the static friction curve. These hysteresis loops have been observed experimentally. And they have been observed to become more pronounced at higher frequencies, when the period of oscillation is small relative to the lag, which appears to be independent of oscillation frequency [9].

Frictional lag is observed in both lubricated and non-lubricated contacts. The phenomenon have been observed or studied by numerous researchers including [9], [21], [2]. The deformation of the asperities, which act as a shear stiffness contributing to the friction force, lag changes in relative velocity and contribute to the lag in friction force. In lubricated contacts, there is some evidence that the time required to modify the thickness of the lubricant film gives rise to some of the frictional memory effects; however, a physics-based model of this process is not yet available [2].

2.2 Dynamic Models

2.2.1 Motivation

These frictional mechanisms can cause tracking error problems in machine control applications that require high precision at low velocities. As explained in the previous section, static friction models do not accurately describe some of the observed friction behavior, for example presliding displacement, the onset of stick slip, and frictional lag. Because friction compensation schemes have potential to reduce these problems, control engineers have attempted to encapsulate knowledge gained from tribology to form simpler lumped parameter dynamic models suitable for control methods [5, 4, 2]. These models must accurately but simply relate a set of dynamic mathematical equations to the observed behavior of the system as well as to the physics of the system.

In this section, we present a typical static friction model, highlight its inadequacies, and then build upon that model to present a more accurate dynamic friction model developed in [4]. A slightly modified version of the model is used as the baseline for this study. We relate the elements of the baseline dynamic nonlinear friction model to the underlying physics of the contact surface and we present simulation justification that the model indeed captures the desired friction type behavior.

Because so much work has been done in friction modelling and because this model is a simplified version, questions naturally arise regarding the effects of modelling errors. Since this is important for friction compensation, in this section we also mention some alternative methods for modelling the effects. In chapter 5, we evaluate the robustness of our method by simulating the effects of some of these other types of models.

2.2.2 A Static Friction Model

Static models in which the friction force depends statically, not dynamically, on the applied load or the velocity consist of Coulomb friction, static friction, viscous friction and possibly the Stribeck effect. This type of model, which is used in most introductory engineering courses, is still adequate for many engineering applications. However, at low velocities, the observed frictional mechanisms discussed in the previous section are not adequately captured by static models. Recognition that dynamic phenomena are an important factor in accurately predicting the onset of stick slip is credited to [21]. A model which identifies and integrates several types of interacting surface phenomena is identified in [28].

Figure 2-1 shows a typical friction force velocity relationship when the velocity is held steady. The friction force opposes the direction of motion, so at low velocities, the friction force changes sign. The Coulomb friction is the friction when the bodies are

at rest and proportional to the load. The static friction constant, F_{static}, is typically higher than the Coulomb friction and in steady conditions, this is the force that must be exceeded in order for motion to occur. As the velocity transitions from low to high regimes, the drop that occurs in the steady friction value is called the Stribeck effect. At higher velocities, the dependence of the friction force to the velocity is linear. The curve shown can be described by the following static model (equation (2.1))

$$F_s(v) = b_v v + \alpha_0 sign(v) + \alpha_1 e^{-(v/v_0)^2} sign(v) \tag{2.1}$$

In this equation $F_s(v)$ represents the friction force when the velocity is steady, and v represents the relative velocity of the two interacting bodies. The signum (or sign) function, $sign(v)$, is defined as follows (equation (2.2)),

$$\begin{aligned} sign(v) &= -1 \text{ if } v < 0 \\ sign(v) &= 0 \text{ if } v = 0 \\ sign(v) &= 1 \text{ if } v > 0 \end{aligned} \tag{2.2}$$

The parameters in the equation can be related to the commonly understood friction constants. At high velocities, the friction force has a slope of b_v and is proportional to velocity, so b_v is the viscous friction parameter. At very small velocities, $|v| < v_0$, we have

$$F_{static} = \alpha_0 + \alpha_1 \tag{2.3}$$

So the sum $\alpha_0 + \alpha_1$ represents 'static' friction constant, F_{static}. We see for this plot that this peak occurs at about 1.5 N. Actually we can break this down further, in the equation above the term $\alpha_1 e^{-(v/v_0)^2} sign(v)$ is solely responsible for the dip in the figure. Therefore, α_0 represents the Coulomb friction, F_c, while α_1 represents the difference between the static friction constant and the Coulomb friction $F_{static} - F_c$.

The sharpness of the dip in the curve is related the parameter v_0. For this reason, v_0 is called the Stribeck parameter. Note that it occurs nonlinearly in equation. This is significant because adaptive control schemes have trouble with nonlinearly occurring parameters, although recent work, in which the concavity or the convexity of the nonlinearity is exploited, is promising [27] [1].

Note that while there are many different models for static friction, they have several common features: the static friction model is a function of velocity that is confined to the first and third quadrants. The model has a Coulomb friction, static friction, Stribeck dip, and a linear part at higher velocities. Some other models have modelled the Stribeck dip with a different type of function [2], but these basic features remain for the static friction model.

The static friction model does not capture the effects of presliding displacement, varying breakaway force, accurate stick slip onset conditions, and frictional lag.

2.2.3 A Dynamic Friction Model

Dynamic Model Equations

The baseline model for this study, slightly modified from that proposed by Canudas de Wit et al [4], captures all of the features that we have discussed.

Figure 2-3 shows a control system for a unitary mass system with friction.

The system can be described by the following equations (2.4).

$$\begin{aligned} \dot{x} &= v \\ \dot{v} &= u - F \\ \dot{z} &= v - \frac{\sigma_0 h(v) z}{g(v)} \end{aligned}$$

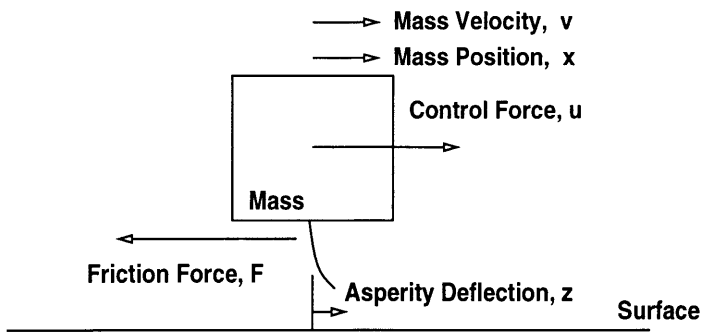

Figure 2-3: A control force, u, acting on a unitary mass is used to control the position x. The friction force, F, is a nonlinear function of velocity, v, as well as an internal friction state, z, which represents the average deflection of asperities.

$$F = \sigma_0 z + \sigma_1 \dot{z} + b_v v \tag{2.4}$$

$$\begin{aligned} h(v) &= |v| \text{ if } |v| \geq v_c \\ &= v_c \text{ if } |v| < v_c \\ &= v/sat(v) \\ g(v) &= \alpha_0 + \alpha_1 e^{-(v/v_0)^2} \end{aligned}$$

In the above equations, the mass position is represented by x; the velocity, by v, and the friction force is represented by F.

The friction model contains one internal state variable, z, representing average asperity deformation, five parameters which enter the equations of motion linearly and one parameter, the Stribeck parameter (v_0), which enters nonlinearly. Parameter values from [4] were used in this study and are presented in the table below.

Parameter Values for the Friction Model

Parameter effect	Parameter	Value
Coulomb friction	α_0	1
Static, Coulomb Difference	α_1	.5
Stribeck	v_0	.001
Viscous	b_v	.4
Asperity Stiffness	σ_0	$1e5$
Asperity Damping	σ_1	$\sqrt{(1e5)}$

REMARK 2.2.1 These equations represent dynamic equations for a unitary mass system. They could also represent normalized equations for a system in which the mass is a known parameter. The analysis we present in later chapters is currently applicable to a known or unitary mass system because it is based on a special structure in the regression vector. An unknown mass would add a feedforward term to the regression vector. Extending the results to an unknown mass system would require modifications in the stability argument.

There is a slight difference in the function $h(v)$ in this model and that in [4]. We have defined $h(v)$ using the saturation function instead of the signum function. The saturation function, defined below, is very similar to the signum (sign) function except for a very small interval near zero velocity $\begin{bmatrix} -v_c & v_c \end{bmatrix}$, the saturation function is continuous.

$$\begin{aligned} sat(v) &= sign(v) \text{ if } |v| > v_c \\ sat(v) &= \frac{v}{v_c} \text{ if } |v| \leq v_c \end{aligned} \tag{2.5}$$

The signum function on the other hand is not continuous at zero. For analysis purposes later, we want to have a continuous transition at zero velocity. We accomplish this by using the saturation function instead of the signum function. This change will allow the parameter adaptive control laws which we will define in later chapters to be continuous, ensuring that solutions for the parameter estimates exist.

The modification is not significant because the effects can be made arbitrarily small by making the v_c arbitrarily small. In this study, we used a value of one tenth the Stribeck parameter. The effects made in the function, $h(v)$, consequently, the static friction model, $F_s(v)$ are shown exaggerated in figure 2-4.

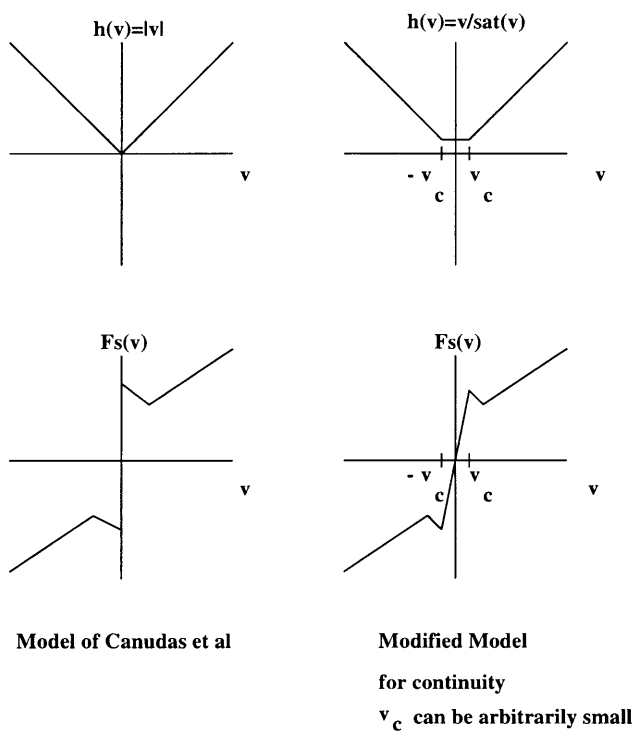

Figure 2-4: The function $h(v)$ is slightly modified from that in Canudas et al. For velocities less than or equal to an arbitrarily small velocity, v_c, then $h(v)$ is modified so that $h(v) = v_c$ instead of zero. When the velocity is held steady, this change results in the friction as continuous function of the velocity, and this assures that parameter adaptive laws defined in the next chapter will be continuous.

Dynamic Model Justification- Physical Interpretation of the Model

ELEMENTS AND MODEL BEHAVIOR

First we examine how this model behaves when the velocity is held steady. At steady velocity, the internal state variable, z, which represents the average asperity deformation, reaches a constant, z_s, which is defined below,

$$z_s = \frac{1}{\sigma_0}\frac{v}{h(v)}g(v) \tag{2.6}$$

$$z_s = \frac{1}{\sigma_0}(\alpha_0 \text{sat}\ (v) + \alpha_1 e^{-(\frac{v}{v_0})^2}\text{sat}\ (v)) \tag{2.7}$$

In this case, the friction force also reaches a steady value, $F_s(v)$, defined below,

$$F_s(v) = b_v v + \frac{v}{h(v)}g(v) \tag{2.8}$$

$$F_s(v) = b_v v + \text{sat}\ (v(\alpha_0 + \alpha_1 e^{-(\frac{v}{v_0})^2}) \tag{2.9}$$

The features of the static friction model presented in equation (2.1) and shown in figure 2-1 are recovered. The Stribeck effect is the dip in the curve. The Stribeck parameter, v_0, affects how steep the Stribeck effect is. The physical interpretation of the parameters, α_0, α_1 are the Coulomb friction and the difference between the Coulomb and static friction respectively. In this model the Coulomb friction is 1 N and the static friction constant is 1.5 N. The value of the Stribeck parameter is $v_0 = .001$, and this makes the Stribeck effect for this model sharper than is shown in the figure which used a value of $v_0 = .04$ to illustrate the shape of dip more clearly.

When there is relative motion between the mass and the surface, the asperities bend with deformation, z. This produces a force with a stiffness and damping term, $\sigma_0 z$ and $\sigma_1 \dot{z}$, respectively. Therefore in this model, the parameters, σ_0 and σ_1 represent stiffness and damping of the asperities and grease layer.

Next we examine qualitatively the dynamic features of the model. The internal state variable, z, is represented by first order nonlinear dynamics which depend on velocity.

First we consider very low velocities. Linearizing the equations near zero velocity shows that in this regime, the internal friction state, z, is lagged version of the velocity.

$$\dot{v} \simeq u - F \tag{2.10}$$

$$\dot{z} \simeq v \tag{2.11}$$

$$F \simeq \sigma_0 \frac{v}{s} + (\sigma_1 + b_v)v \tag{2.12}$$

where s is the Laplace variable. Frictional lag is present between changes in velocity and changes in friction force. Additionally in this range, the relationship between z and x is just a second order damped equation, giving rise to the phenomenon of presliding displacement, rising static friction and varying breakaway force. The relationship between applied force u and the friction force F is also second order and this why these equations can model the rising static friction. For low velocities up to about $50Hz$ due to the choice of the parameter σ_0, the linearized friction force matches the applied force. Breakaway is reached but the conditions that cause breakaway are dynamic. As the velocity is increased, the nonlinear effects also become important.

Next consider higher velocities. The dynamics of z are first order and depend on velocity as an input. At steady velocity, z, reaches a steady value as we have previously noted. If the velocity is high, z reaches this value more quickly. Additionally, we will show below that z is bounded as it is in [4]. This makes physical sense because z represents asperity deformation which should only reach a certain level before having a negligible effect.

LEMMA 2.2.1 Z IS BOUNDED *Assume, we are given bounds on the parameters, such that*

$$\begin{aligned} 0 < \alpha_0 &\leq \alpha_{0_{max}} \\ 0 < \alpha_1 &\leq \alpha_{1_{max}} \\ 0 < \sigma_{0_{min}} &\leq \sigma_{0_{max}} \end{aligned} \tag{2.13}$$

The internal friction dynamic system

$$\dot{z} = v - \frac{\sigma_0 h(v) z}{\alpha_0 + \alpha_1 e^{-(v/v_0)^2}} \tag{2.14}$$

has bounded solutions with

$$|z| \leq max(|z(t_0)|, z_{s_{max}}) \tag{2.15}$$

This can be proved using a Lyapunov function argument and the details are in an appendix (A).

Notice that at high velocities, because z is bounded and comparatively small, the viscous friction term, $b_v v$, dominates the equation as it should.

HYSTERESIS

Figure 2-5 shows hysteresis effects for the friction model under investigation. The mass is moved with a 2 Hz sinusoid, with an amplitude that is .025 m/sec, which is twenty five times the Stribeck parameter and low enough to exhibit frictional dynamic effects. The figure shows the response of the internal friction state, z, which is essentially a lagged version of the input velocity for this low velocity regime as the linearized equations (2.12) predict. The resulting friction force is a lagged version of the velocity, and it acts in a direction opposite the velocity. When the magnitude of the friction force is plotted vs. the velocity, a hysteresis loops are observed as shown in the figure. The hysteresis loops lie on top of each other in the plot. The upper curves correspond to acceleration away from zero velocity, and the lower curves correspond to deceleration towards zero velocity. This corresponds with the experimental results of [9]. The fact that the wideness of the hysteresis loop increases with increasing frequencies was also noted in [9] and is observed in this model as well as shown in the

figure.

In [9], the behavior as the velocity extremely small values was not extensively modelled. It was noted that in this region other physical variables contribute to the friction. It was however, observed that as the velocity gets smaller and smaller, stick effects cause the measured friction force to drop. The friction model we use predicts these effects and also predicts hysteresis loops at very small velocities and when zero velocity is crossed. Due to the presence of stick, these types of hysteresis loops have a different qualitative shape, but because the forces drop at these extremely small velocities they do fit with the observations in [9]. An example of this is seen later in the chapter in figure 2-8.

Stick Slip Limit Cycling

The model also exhibits stick slip limit cycling, and we will see several examples of this behavior in the next section where we examine a position control system with this friction model.

Model Limitations and Alternative Modelling Methods

In this section, we consider the implications of the fact that this model has limitations, and some of the effects may be modelled using alternative techniques. Friction compensation techniques may depend in part on the accuracy of the model so these are important issues. However, the friction compensation design we propose and analyze in later chapters is an approach that naturally has some robustness properties. In this section, we briefly present alternative modelling techniques for some of the behaviors so that later in chapter 5, we can verify that our method is robust to some of the structural types of modelling errors that may be present.

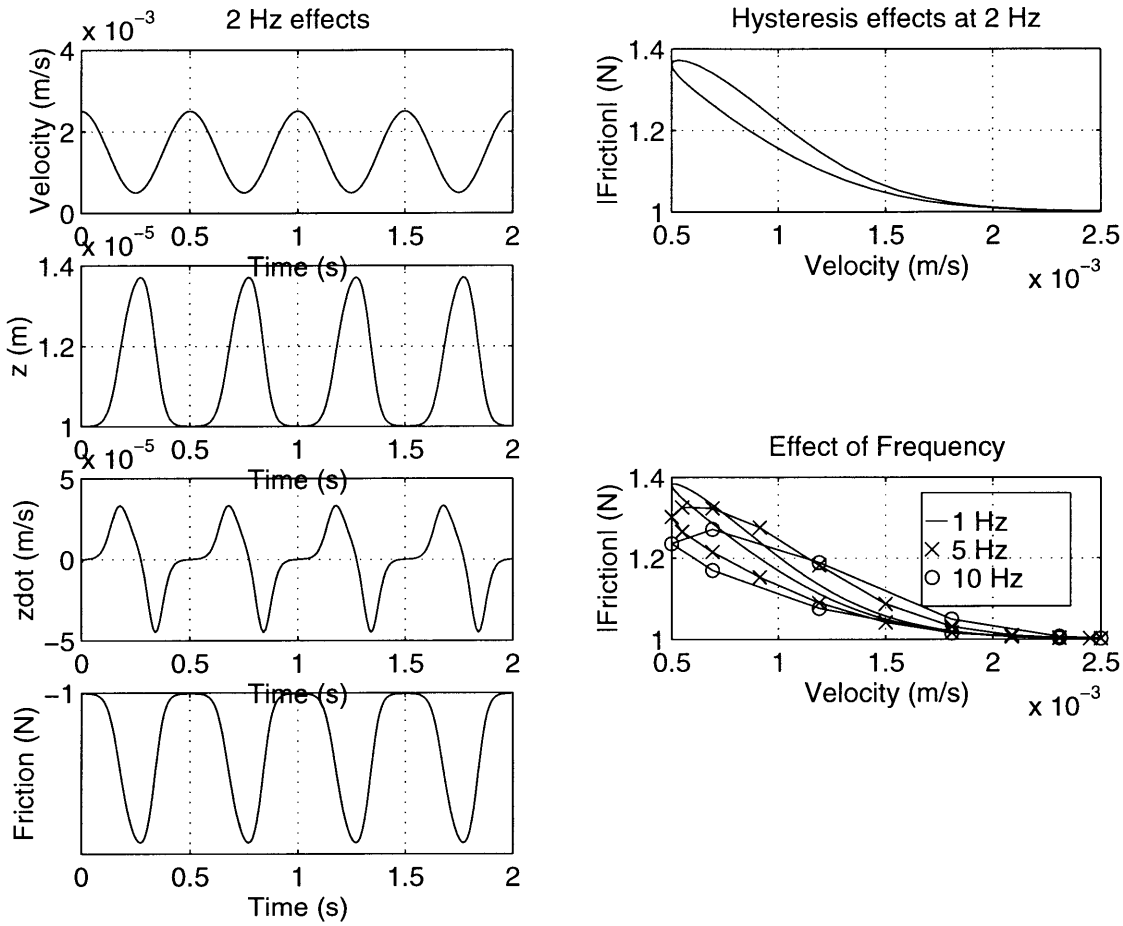

Figure 2-5: Hysteresis loops occur because friction changes lag changes in velocity. In this model, as the velocity changes, the changes in the internal friction state, z, are responsible for the lag. The hysteresis loops, which lie on top of one another, are perturbations due to friction dynamics in the static friction model. When the acceleration is away from zero velocity, and the static friction is dropping, the upper curves in the hysteresis loop are formed. During deceleration, the lower curves are formed. The wideness of the hysteresis loops increases with increasing frequency, when the period of oscillation is small relative to the lag.

The model presented above is useful because it has ties to the physical processes that have been discussed, and exhibits all of the observed behaviors, including Stribeck effect and frictional dynamic effects which have not yet been incorporated in a non-linear adaptive friction compensation scheme, and it is simple enough to consider for control purposes. Because of the lumped parameter and simplified nature, the model naturally has it limitations as does any idealized model. The entrainment process, for example, in greased surfaces is not included in the model. A modern friction model that includes more contact surface effects than the model used in this study is presented in [28].

Even among the simplified friction models currently being considered for control, there is variation in the modelling techniques; however, the basic features of the static friction model remain and the other effects are perturbations. For example, the model in [2] is a model which essentially links together several models of friction operating in different velocity regimes and is based on previous results of several different researchers.

The Stribeck effect, which is modelled using the exponential term in $g(v)$ in the model we use, can also be modelled with an alternative decreasing function such as

$$\frac{1}{1+\left(\frac{v}{v_0}\right)^2} \tag{2.16}$$

which is used in [2]. At small velocities, the differences in this term and the term used in the model above which is $e^{-(v/v_0)^2}$ are small. In fact these differences are bounded, with the peak occurring at some low velocity. The compensation design, we use is designed for robustness to bounded disturbances. Rising static friction in the model is not a state model in [2], instead it is modelled as a function of 'stick' time. Hysteresis in the model in [2] is modelled as a constant lag between change in velocity and change in friction force and is based on the model proposed by [9]. However, the experiments in [9] do not consider operation about zero velocity; instead, the experiments and

models considered are for just above 'stick'.

However, because the compensator is specifically designed for robustness to bounded or linear growth bounded (Lipschitz) disturbances, it should have some robustness properties to these types of modelling uncertainties when the differences remain small. Simulations in chapter 5 are included to verify the robustness properties of the new friction compensator. Three types of modelling uncertainties are considered which are motivated in part by the alternative modelling techniques in the literature discussed above. First the Stribeck parameter, v_0, has a ten percent error. This change is to reflect a modelling error in the steepness of the Stribeck effect. Second, the parameter, α_1, which is the difference between the static and Coulomb friction constants is time-varying. This change is made to reflect the errors that could be present in the nature of the rising static friction behavior. The third modelling error considered in chapter 5 is the inclusion of unmodelled actuator dynamics.

2.3 Active Control of Systems with Friction

In this section, first we examine the inadequacies of linear control. We explain why linear controllers have tracking problems for low velocity tasks and we present simulation results for the friction model in this chapter that illustrate these tracking problems. The simulations also serve to verify that the friction model exhibits the observed problematic behavior discussed in the previous sections in systems with friction. In the second section, we illustrate that nonlinear and nonlinear adaptive control have potential to reduce these tracking problems. We also point out some of the issues that must be addressed in these designs such as parametric uncertainty and stability robustness.

2.3.1 The Inadequacies of Linear Control

In this section, we combine the friction model with a typical representative linear controller and illustrate in detail the control challenges posed by nonlinear frictional dynamics. These will include tracking errors and undesirable limit cycles such as stick-slip and hunting. First we consider why a linear controller has tracking problems at low velocities.

Figure 2-6 shows a static friction model. The actual friction force is a perturbation of this curve due to dynamic effects. A linear controller would use a friction model linearized about a fixed velocity. The linearization has range of usefulness for which the linear controller is robust to parametric variations. A friction model linearized about zero velocity would have a range of usefulness like that shown by the dashed diagonal lines in figure 2-6. In the high velocity regimes, the friction force falls within this range so the linearization is valid in these regimes. In the low velocity regime, the friction force can fall outside the range for which the linearization is valid. A linear controller is expected have problems tracking trajectories which spend a significant portion of time in the low velocity regime.

Note that a high gain linear controller could reduce these problems because it has more robustness to parametric variations and the region of validity for the linear controller would be broader. However, there are the usual problems associated with high gain control: exciting unmodelled dynamics or sensor noise, utilizing large control inputs, etc.

Next we illustrate by simulation that a linear controller for a mass with the friction model presented in this chapter has tracking problems for low velocity tasks. We set up a baseline study of three different low-velocity tasks, in order to illustrate that friction causes the tracking problems we have discussed. These tasks are representative of the types of problematic tasks in machine control systems. Throughout the

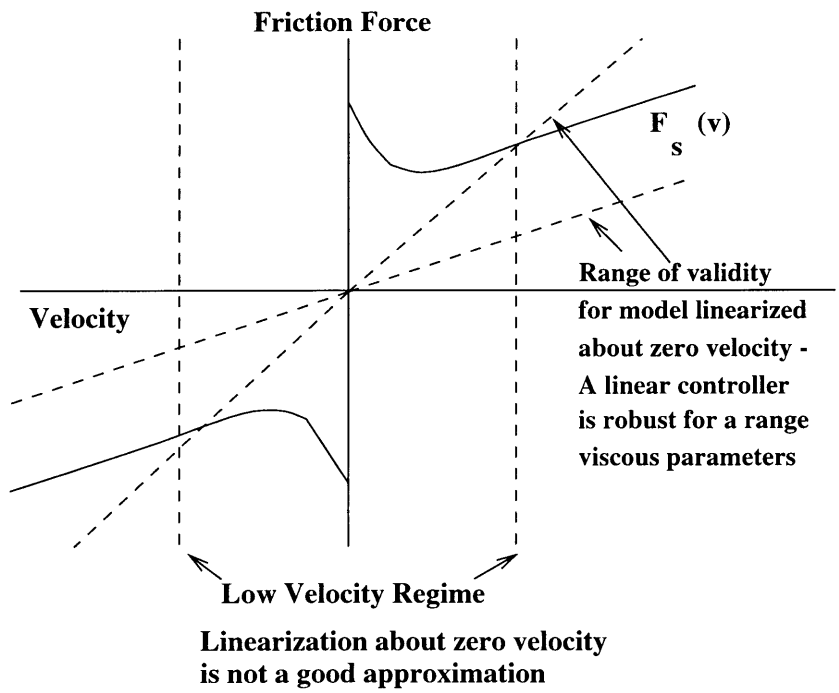

Figure 2-6: A linear controller uses a linearized model of the friction force. However, friction is a nonlinear function of velocity as well as internal contact surface dynamics. The linearization range is only valid for higher velocities. Consequently, any controller which neglects the nonlinear and dynamic effects of friction will have tracking problems for trajectories which spend significant portions of time in the low velocity regime.

thesis, we will return to this baseline study of three tasks. In this section, we present the three tasks to illustrate the problems due to friction for linear control system and the potential of nonlinear adaptive control in reducing these problems. In the next chapter, we design and adaptive nonlinear friction compensator and we return to the three baseline tasks to illustrate that although the method has potential to improve tracking performance, stability of the adaptive algorithm must be addressed. Finally in chapter 5, we show that for the three tasks, the solution presented in chapter 4, which makes use of persistent excitation in the input trajectory, can improve tracking performance using a stable algorithm.

The linear controller for the baseline study is a P.I.D. controller

$$u_L = \ddot{x}_d + k_v(\dot{x}_d - \dot{x}) + k_p(x_d - x) + k_i\left(\int (x_d(\tau) - x(\tau)d\tau\right) \tag{2.17}$$

where the gains, $k_i = 4$, $k_d = 6$, $k_p = 3$, from [4] are used. This gives a low bandwidth (1 rad/sec) controller which will exhibit control problems at low velocities.

The first type of task is a low constant velocity tracking task, i.e. a ramp in position, which can experience stick-slip. Even though the velocity is not zero, we see that at low velocities, stick slip can cause undesirable tracking errors in a simple tracking tasks. The second task is characterized by repeated zero velocity crossings. We use a low velocity sinusoid for this task. This type of task can experience large tracking errors (on the order of the task) because the mass can stay stuck. Low velocity tasks such as these are used in machine tools and robots under position control. Pick and place maneuvers can be affected by friction in low velocity regimes. An example of a task with repeated zero velocity crossings is multiple degree of freedom robots in which one degree of freedom is held steady by small oscillations about zero [2]. The third task is a regulation task, in which the presence of friction can result in hunting about the set point. We use a unit step response for this task. Regulation tasks are necessary in precision pointing applications. In addition, to illustrating the inadequacies of using linear control for these tasks, the first and third tasks verify that the friction model presented earlier in this chapter exhibits the undesirable stick slip limit cycling observed by many researchers [2].

P.I.D. Control for Low Velocity Task 1- A Constant Velocity Task

In the first task, the desired trajectory consists of a constant low velocity trajectory, which is a ramp in position. The velocity is .02 m/sec which is 20 times the Stribeck parameter, a value which the simulations show is low enough to exhibit a stick slip limit cycle and high enough to exhibit nonlinearities in the response. Figure 2-7 shows a set of simulation results for this task using the linear controller. Instead of the desired smooth position ramp, the actual position of the mass alternates between stick, a period of no motion, and slip, a period in which the mass quickly overshoots the

desired trajectory. The amplitude of the tracking errors is at least five centimeters. The control force and the magnitude of the friction force are also plotted and show the reason for the stick slip behavior. At low control force levels, the friction matches the control force, exhibiting the rising static friction behavior discussed earlier. Eventually, for this steady velocity condition, at values near the static friction force of 1.5 N, the friction force can no longer match the control force. As the friction force drops suddenly, the difference between the control and the friction force acts as an impulse to the mass and it quickly slips forward. The control terms are reduced as the mass overshoots the desired position and this causes the mass to stick and the limit cycle to begin again.

P.I.D Control for Low Velocity Task 2- A Task with Repeated Zero Velocity Crossings

Because the zero velocity region is the most problematic, we shall show in the second task that a trajectory with more frequent zero velocity crossings may exhibit more tracking errors problems. In this section, we will see that it is possible to construct a low velocity trajectory with zero velocity crossings in which the mass stays stuck. For a low velocity trajectory with repeated velocity crossings, if the velocity changes sign before breakaway occurs, then the mass can stay stuck. The tracking error is relatively large, on the order of the task, because breakaway conditions are never reached. Simulations for a sinusoid of with a desired position of $x_d = .05sin.5t$ are presented in figure 2-8. This corresponds to a velocity level that is twenty-five times the Stribeck parameter. Because the friction force nearly always balances the control force, the mass essentially stays in stick consequently the tracking errors are on the order of magnitude of the desired task, which is five centimeters in position. Note that this simulation was made with high enough sampling frequency, and hence the behavior is a result of the friction physics and not due to sampling. The figure also shows that due to the lag between the velocity and the friction force, a hysteresis

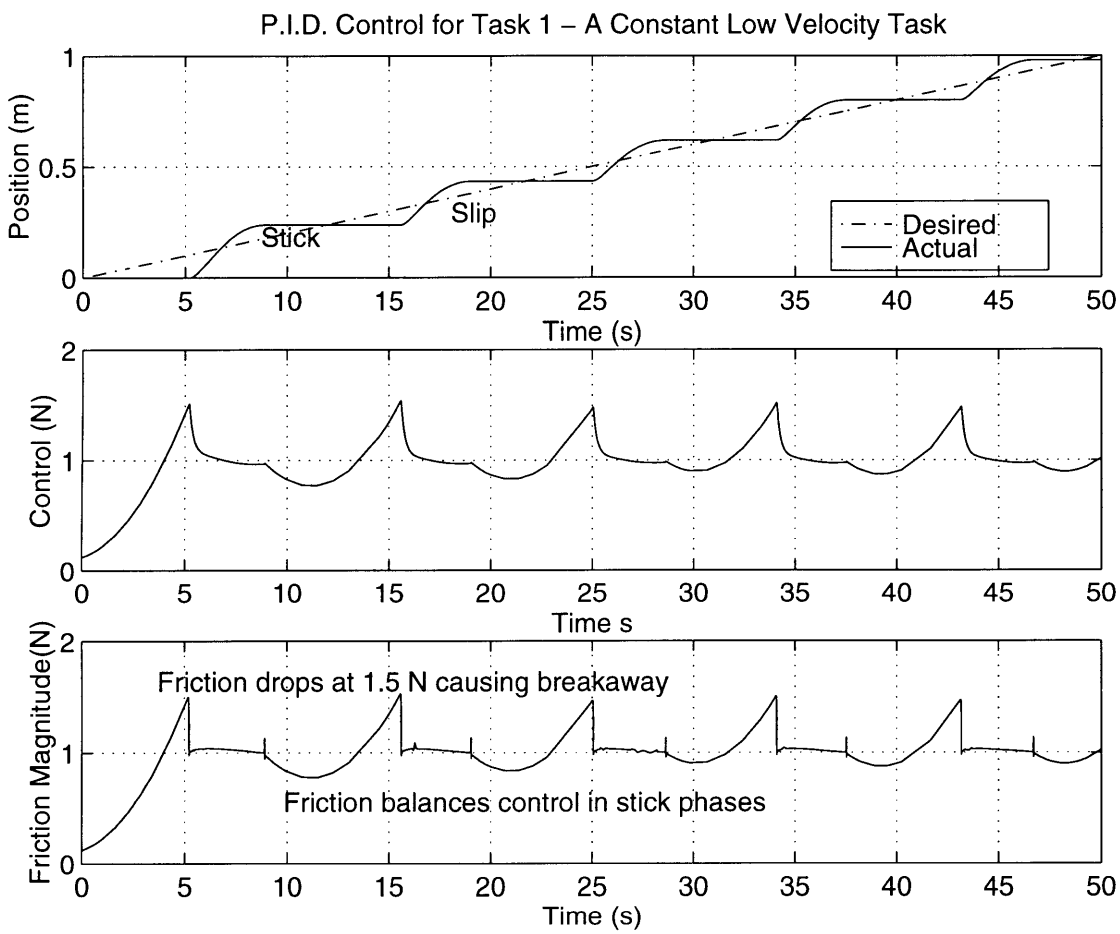

Figure 2-7: A constant low velocity tracking task under linear control exhibits a stick slip limit cycle with jumps causing tracking errors of at least 5 cm. Initially the friction force balances the low applied force level (rising static friction). Breakaway is reached at approximately 1.5 N for this steady velocity condition. As the friction force drops suddenly, the overall force acts as an impulse response and the mass quickly slips forward, overshooting the desired position. As the mass slows down, the friction force again balances the control force and the limit cycle begins again. This simulation shows that friction can cause tracking errors and undesirable limit cycling in a standard linear control scheme.

loop is present. The shape of the hysteresis loop is qualitatively different from that in figure 2-5. This is due to the effects of stick. In [9], behavior near stick was observed and noted, but the study focused on capturing the behavior of the hysteresis loops when stick was not such as the plots in figure 2-5.

P.I.D Control for Low Velocity Task 3 - A Regulation Task

The third control task is a regulation task which is a unit step response. The stick slip limit cycle it exhibits is sometimes called hunting in the literature. The simulation results are shown in figure 2-9 . Instead of reaching zero steady state error as a P.I.D controller should, the mass gets stuck at zero velocity. The amplitude of the peak tracking errors after the transients have died away is about six and a half centimeters. The integral terms in the controller builds up during stick times until the friction force no longer balances the control force and causes the mass to breakaway. As in the position ramp in task 1, the sudden change in forces cause the mass to slip quickly, and overshoot the desired position, and get stuck again beginning the limit cycle again.

For a step response, it is the integral action in the controller which causes the limit cycle. As observed in the behavior of systems with friction, a P.D. controller for this system does not exhibit hunting about a set point [22].

2.3.2 The Potential of Adaptive Nonlinear Friction Compensation

Nonlinear adaptive control has the potential to reduce the problems associated with control of systems with friction. In this section, we present simulation examples for the baseline low velocity control tasks for two different types of nonlinear controllers

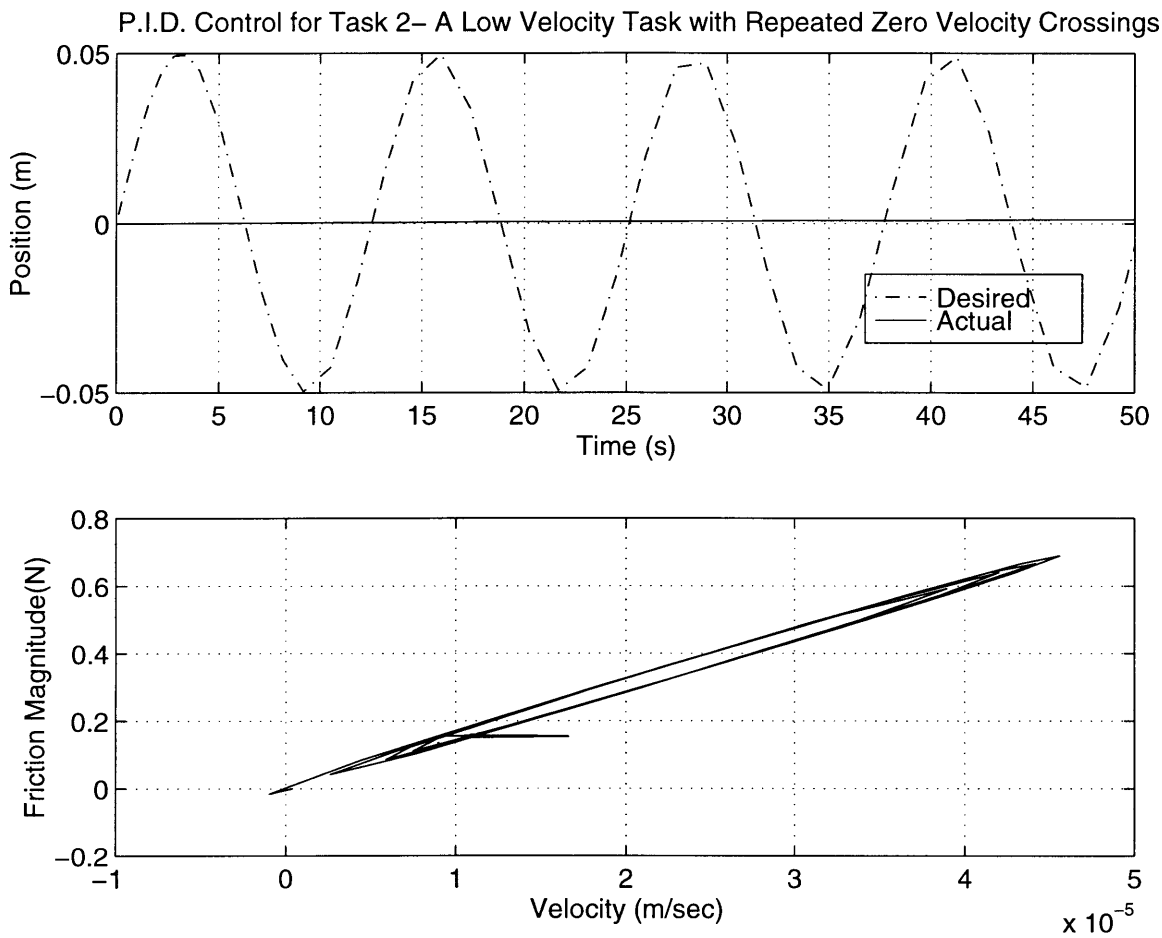

Figure 2-8: This plot shows that the tracking errors for a linear control system with friction can be relatively large, on the order of the task itself. For this simulation, the mass hardly moves at all and essentially remains in stick because the friction force is nearly always balances the control force. The lag between the velocity and friction force creates a hysteresis loop.

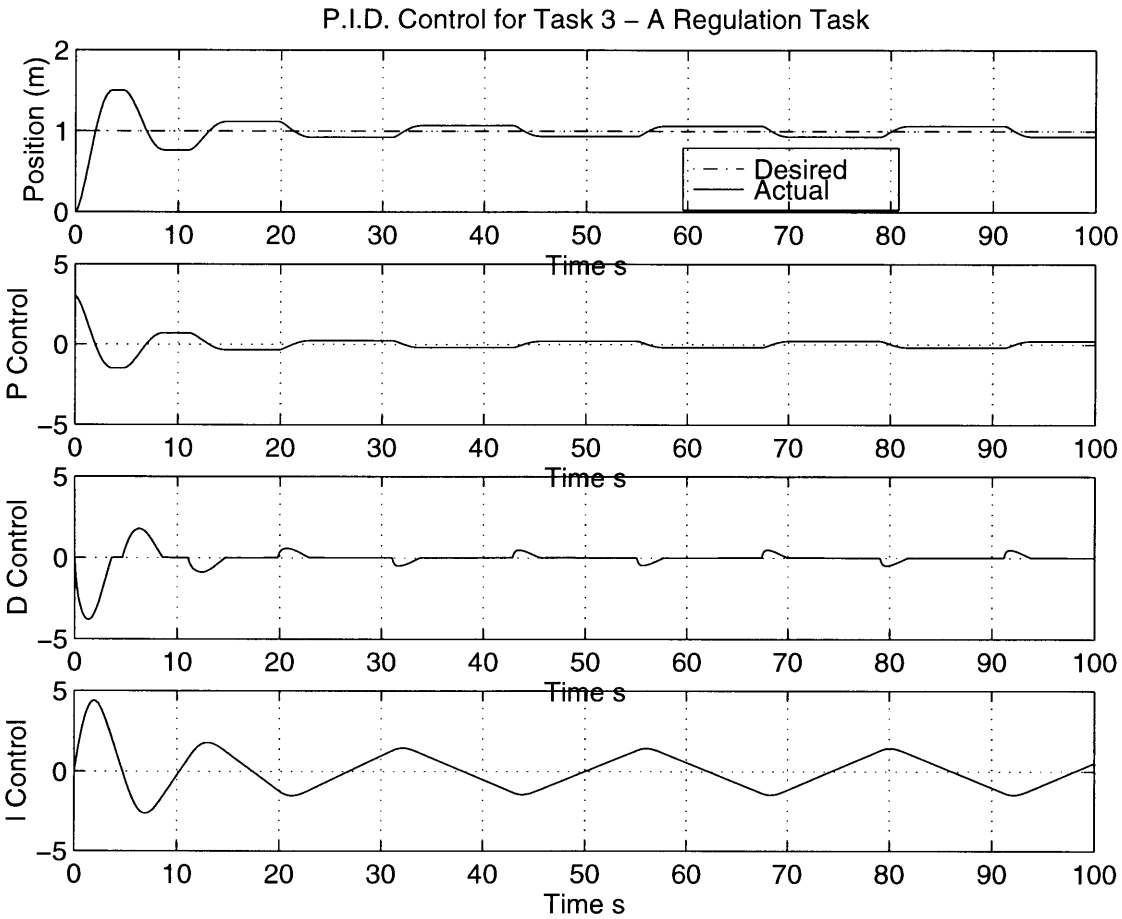

Figure 2-9: In a regulation task, the integral terms in a P.I.D. controller build up when the mass is in stick, eventually causing the mass to breakaway and slip. This stick slip limit cycle is called hunting about a set point. The tracking errors in steady state have an amplitude of about 6.5 centimeters.

with detuning in the parameters. The first is an estimator for the static friction force. Although there is tracking performance improvement compared to the linear controller in the previous section, the improvement for this controller is shown to be is sensitive to parameter detuning. The second type of nonlinear controller uses an approach that is similar to that in [4]. The tracking is substantially improved even with parameter detuning; however, the stability requirements for this type of controller are very restrictive and satisfying them requires a large bandwidth linear controller. Not satisfying may mean that the performance improvement is not very robust to modelling uncertainties. The third controller is included to show the potential of a nonlinear adaptive friction compensator.

Potential of Nonlinear Control

The first simulation is for a controller in which the friction compensation is for the static friction force, $F_s(v)$. However, three of the linearly occurring parameters, b_v α_0, and α_1 are detuned by minus ten or plus fifty percent. The friction estimate is

$$\hat{F} = \hat{b}_v v + \hat{\alpha}_0 sat(v) + \hat{\alpha}_1 e^{-(v/v_0)^2} sign(v) \tag{2.18}$$

and the control law consists of the linear control law in the previous section in equation (2.17) and the friction force estimate as follows

$$u = u_L + \hat{F} \tag{2.19}$$

The tracking performance is improved compared to the results of the linear controller in the previous section; however, the performance improvement is sensitive to how well the parameters are known as shown in figure 2-10. For the simulations in which the parameters are detuned by minus ten percent, stick slip limit cycles observed in the previous section are eliminated in the ramp and the step response tasks. In the

sinusoidal tasks, the error is 2 centimeters, which is a substantial improvement over the linear controller in which the mass stayed stuck. For the simulations in which the parameters are detuned by plus fifty percent, the tracking error levels are about twenty centimeters for all three tasks, and this is worse than the linear controller in the previous sections where the tracking errors were about five or six centimeters for all three tasks.

Potential of Nonlinear Control

The second type of nonlinear controller is designed similarly to the techniques in [4]. It consists of an estimator for the internal friction state, z, and the linear control, u_L, in equation (2.17) as shown below,

$$\begin{aligned} \dot{\hat{z}} &= v - \hat{\sigma}_0 \frac{h(v)z}{\hat{\alpha}_0 + \hat{\alpha}_1 e^{-(v/v_0)^2}} + k(x_d - x) \\ \hat{F} &= \hat{\sigma}_0 \hat{z} + \hat{\sigma}_1 \dot{\hat{z}} + \hat{\alpha}_2 v \\ u &= u_L + \hat{F} \end{aligned} \tag{2.20}$$

where we used an observer $k = 10$ with the baseline linear controller in the previous section. With perfect parameter estimates, the overall system reduces to the following

$$\begin{aligned} e &= -\frac{\sigma_1 s + \sigma_0}{s^2 + k_v s + k_p + \frac{k_i}{s}} \tilde{z} \\ \dot{\tilde{z}} &= -\frac{h(v)}{g(v)} \tilde{z} - ke \end{aligned} \tag{2.21}$$

where $\tilde{z} = z - \hat{z}$ is the estimation error for the internal friction state, z, and e is the position tracking error.

As discussed in [4], stability arguments for this type of controller are based on satisfying SPR requirements. The requirements for this system would require very large bandwidths because the dynamics in the friction model are fast. The zero in the

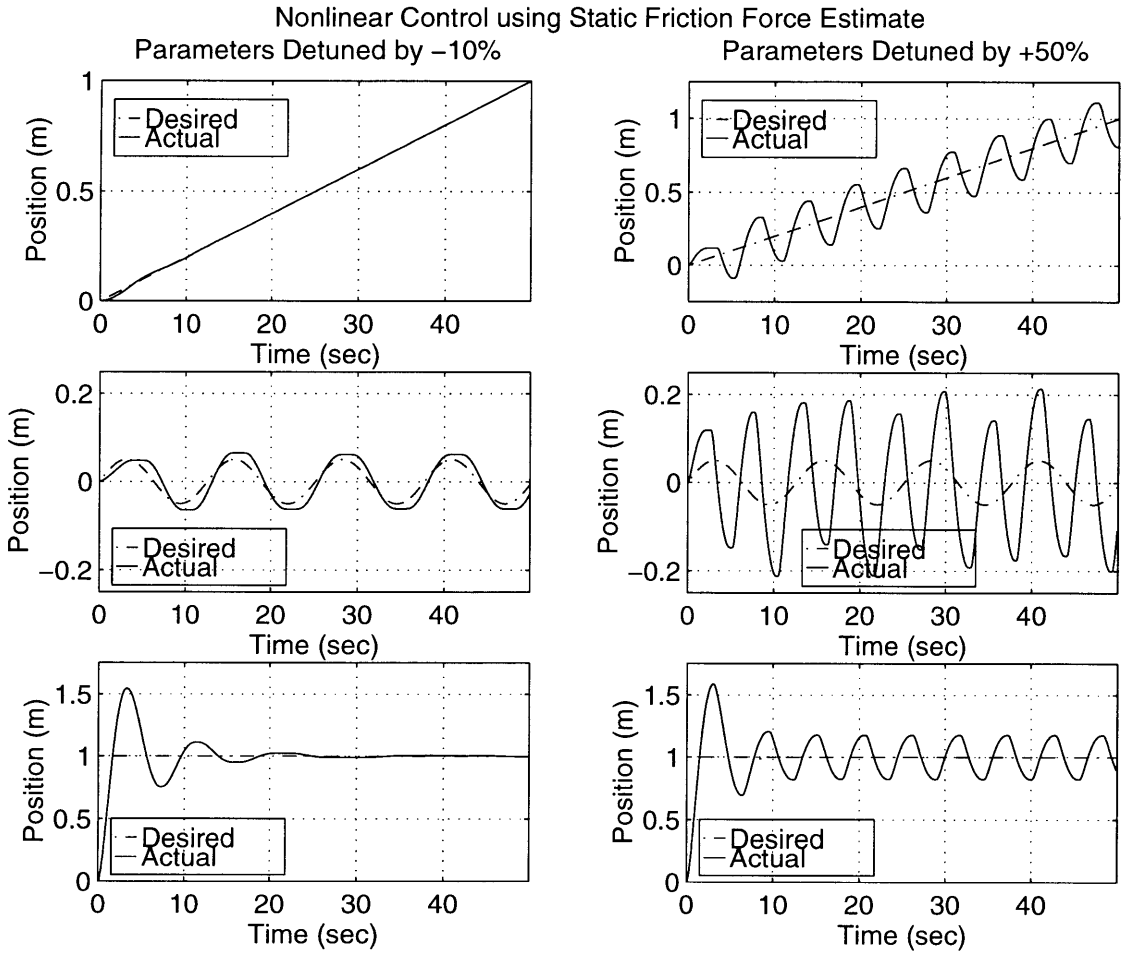

Figure 2-10: A nonlinear friction compensator using a static friction force estimate. Tracking performance is improved but is sensitive to how well the parameters are known

above transfer function, $\frac{\sigma_0}{\sigma_1}$ occurs at 50 Hz. So the bandwidth of the linear control portion of the system would have to be greatly increased from its value of less than 1 Hz in order to meet these SPR requirements. This is undesirable because of the problems associated with high gain control including robustness issues and large control inputs.

The controller was simulated without satisfying the restrictive stability requirements, which may be overly conservative, in order to show that nonlinear control does have potential to improve tracking even with parameter detuning. All of the linearly-occurring parameters were increased by fifty percent.

The results in figure 2-11 show that the stick slip limit cycle is eliminated in both the ramp and the step responses. However, due to the detuning, there is an oscillation of about a half a centimeter about the desired ramp position. Similarly, the sinusoid response has tracking errors of about 10 percent or about a half of a centimeter and the step response has tracking errors of about one percent or about 1 centimeter.

These simulations shows that both types of nonlinear control have the potential to improve these tracking problems due to friction. However, performance can be sensitive to parameter detuning. Furthermore, developing a nonlinear compensation with lower bandwidth stability requirements would be beneficial.

Potential of Adaptation

The introduction of adaptation can desensitize a nonlinear friction compensator to parameter detuning, but stability of the overall system, which includes the parameter estimates, must be addressed. To illustrate the effect of adaptation, the next simulation, shown in figure 2-12, consists of a nonlinear friction compensation using perfect parameter estimates. Due to the modelling uncertainty, perfect estimation of parameters is not possible but the simulation serves to illustrate the potential of

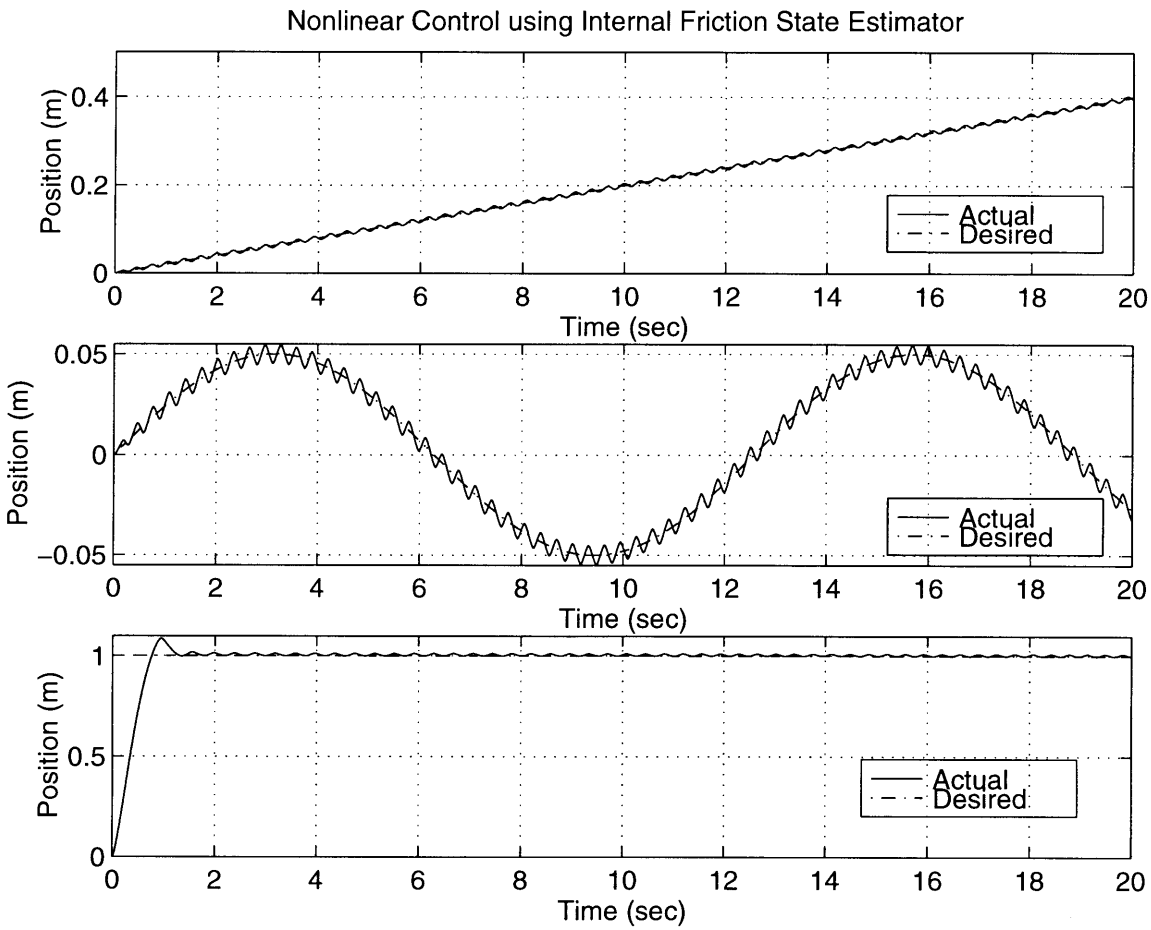

Figure 2-11: A nonlinear friction compensator based on an estimator for the internal friction state, z has the potential to improve tracking performance. Stick slip is eliminated in the ramp. The sinusoidal trajectory does not stay in stick as in the linear controller and the problem of hunting about a set point is eliminated for the step. The parameters were detuned by fifty percent. Small tracking errors of about ten percent for the sinusoid and one percent for the step response are present. The ramp response has about a half a centimeter error. The stability requirement for this type of controller are restrictive and would require large bandwidths

adaptive nonlinear compensation. Tracking problems associated with the effects of friction are not seen at all in these simulations. The ramp response does not exhibit a stick slip limit cycle. The sinusoidal response does not get stuck or stay in stick. And hunting is eliminated in the step response.

2.4 Chapter Summary

In this chapter, we discussed the underlying physical processes of friction and how they can cause the tracking problems in low velocity tasks in control applications. We presented a model recently published by [4] that captures more of the important problematic friction effects, including Stribeck effect and hysteresis effects than friction model in earlier friction compensation work. We also discussed alternative modelling techniques that will be useful for the study robustness issues in later chapters. We showed that linear control methods are inadequate to deal with the problems due to friction and we introduced a baseline study of three representative low velocity tasks that we will return to throughout the thesis. These include a constant low velocity task, which exhibits a stick slip limit cycle under linear control, a task with repeated zero velocity crossings, which stays stuck and barely moves at all under linear control, and a regulation task, which exhibits hunting about a set point under linear control with integral terms. Finally we showed that nonlinear and nonlinear adaptive control have the potential to eliminate these problems, but considerations must be made regarding modelling uncertainty, stability requirements and robustness.

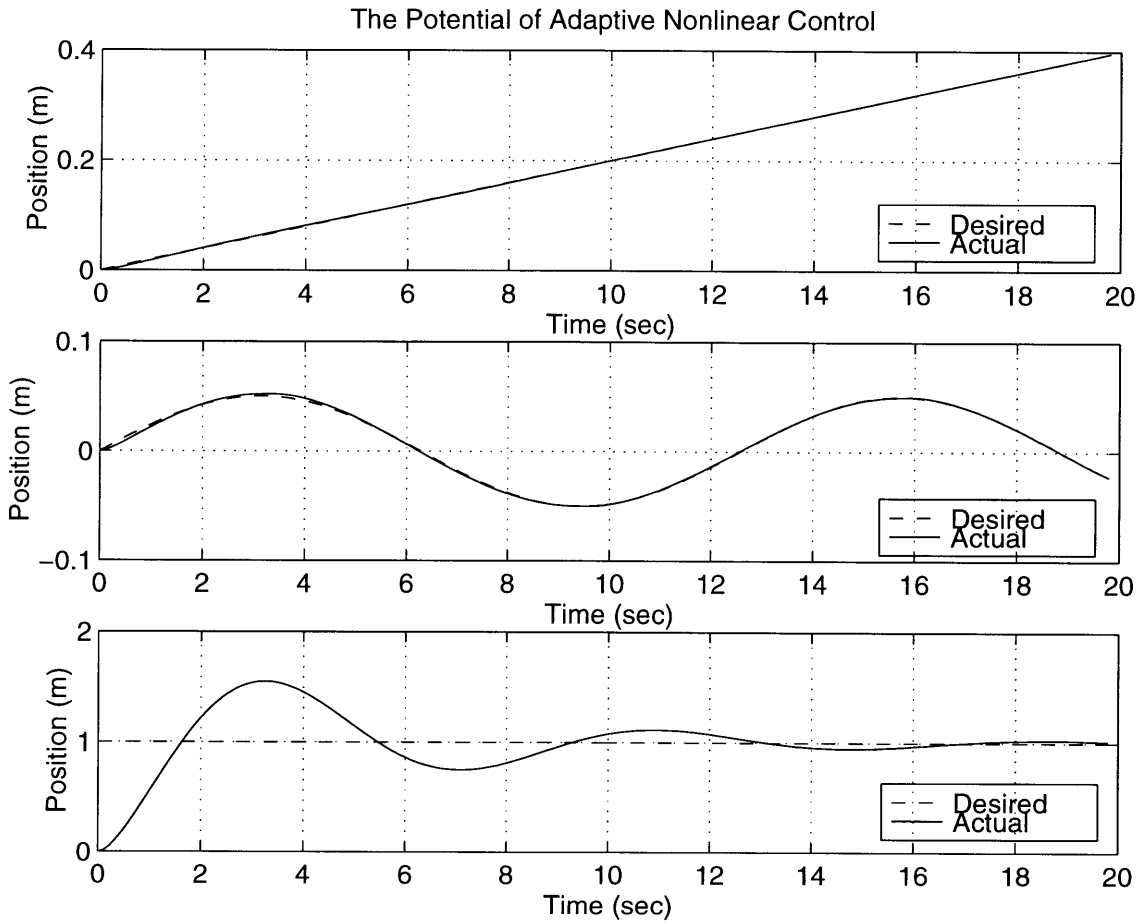

Figure 2-12: A nonlinear adaptive controller has potential to improve the tracking problems caused by friction in low velocity tasks. In this simulation, the friction force parameters are estimated with no errors. Although this situation is not realistically possible, it serves to verify the potential of nonlinear adaptive compensation. The tracking problems associated with a linear controller are completely eliminated. Stick slip effects are eliminated from the ramp and step responses. The sinusoidal response does not stay in stick.

Chapter 3

An Adaptive Nonlinear Compensator Design

In this chapter we motivate and design an adaptive nonlinear friction compensator for a position control system with the friction model discussed in the previous chapter. The design objective is a friction force estimator that will cancel out the effects of friction. Because of the uncertainty in the model, both in the internal friction state, z, which has nonlinear dynamics, as well as in the parameters of the system, it is not possible to estimate all of the features of the friction force. So we modify the design objective to estimate a part of the friction force and make sure the overall system design is robust to the unestimated part of the friction force. We choose to estimate the components of the friction force representing the static, Coulomb and viscous components. And this choice makes the unestimated part of the friction equal to perturbations in the friction model due to dynamics. We show that these perturbations are 'small' in the sense that they consist of bounded terms and terms which grow linearly with velocity.

We introduce error models and formulate the design objective in terms of an error model stability problem. The choice of the parameter adaptive laws are motivated by keeping the effects of the friction estimation error 'small' in a sense, which is equivalent to keeping the effects of the parameter errors in the system 'small'.

We identify the friction compensation algorithm as a special case of a new type of error model. We discuss how stability of the error model is non-trivial problem which must be addressed in order for the adaptive algorithm to behave in a stable fashion. We describe how disturbances in the system can cause an instability mechanism by which the parameters grow unbounded. We introduce the concept of persistently exciting inputs to address the stability issue, and make adaptive algorithm robust to model perturbations. Finally, we present simulations for the friction compensator that verify that the dynamic perturbations in the friction model can make the adaptive nonlinear compensation scheme unstable if there insufficient persistent excitation in the inputs.

In the next chapter, we explore the new error model and develop conditions for boundedness of the solutions.

3.1 Design Objective

Figure 3-1 shows a block diagram of a friction compensation scheme. The plant consists of the inertia with dynamic nonlinear friction modelled in the previous chapter. The friction depends on the internal friction state, z, the velocity, v, and a set of parameters. The friction compensator consists of two main components- a linear controller and a friction estimator. The purpose of the friction estimator is to cancel out the undesirable effects of friction that cause the problems discussed in the previous chapter -tracking errors and undesirable limit cycles in low velocity conditions. Sup-

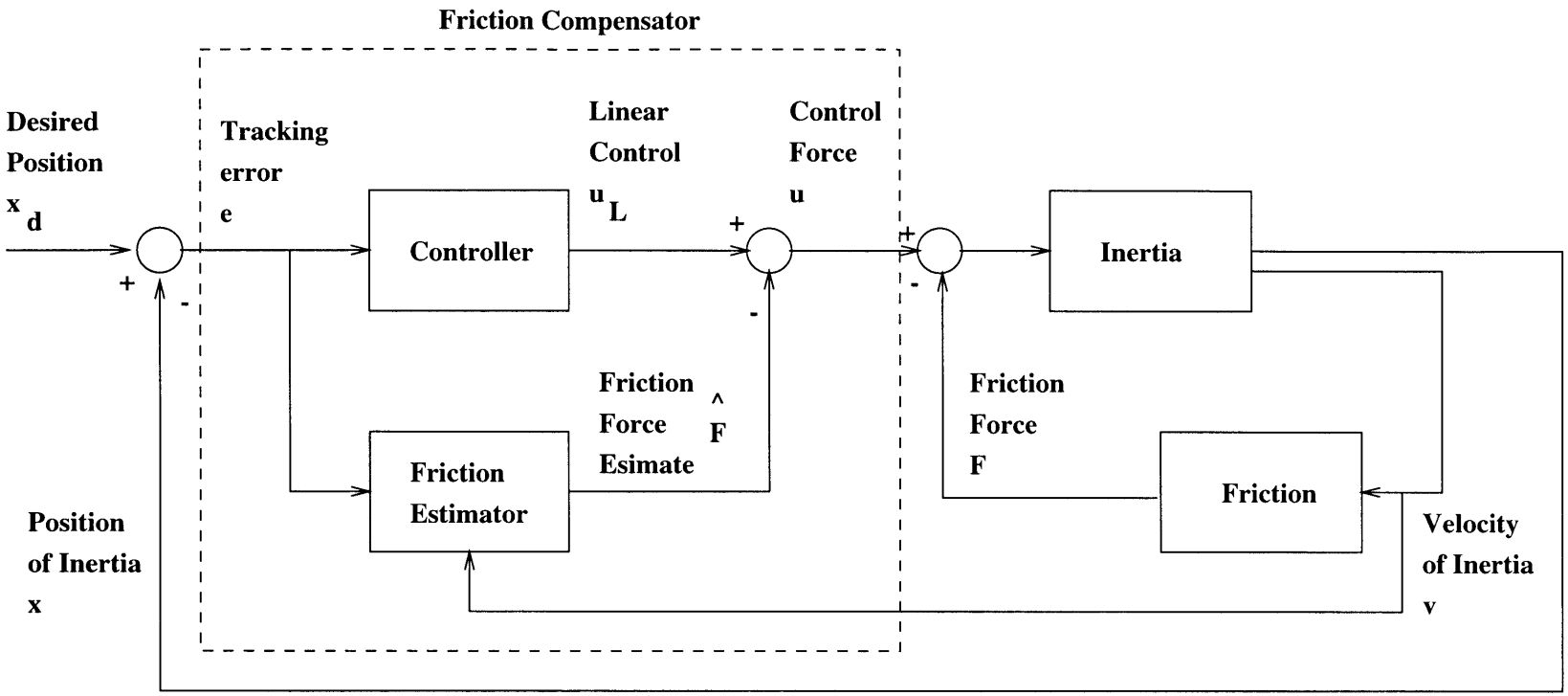

Figure 3-1: Friction Compensation Scheme- A position control system for a mass with friction. The friction force is a nonlinear dynamic model with velocity as an input. The internal state of the friction model is not measurable and the parameters are poorly known. A friction compensator consists of a linear controller and a friction estimate. When the friction estimate balances the friction force, the overall system reduces to a linear system, eliminating the problematic tracking problems due to friction.

pose we could make the friction force estimate, $\hat{F}$, exactly equal to the friction force F. Then the overall system in figure 3-1 would be a linear controller and inertia, and standard linear techniques could be applied without exhibiting the problematic behavior caused by dynamic nonlinear friction effects. Ideally then, the design goal is to make the friction estimate approach the actual friction force so that the tracking error will be acceptable. That is,

$$\text{For good tracking, make } \hat{F} \rightarrow F$$

This goal is not achievable at this time because it is difficult to exactly match the friction estimate to the actual friction force. In addition to being a function of the velocity, which is measurable, the friction force is also a function of internal friction state, z, which is unknown and unmeasurable, as well as the parameters which typically are poorly known. Estimating both the state and the parameters is difficult because a dynamic state estimate for the internal friction state, z, would require some knowledge of the unknown parameters, while a parameter estimator for all of the parameters requires knowledge of the internal state, z.

Although we can not match the friction force exactly, friction compensation techniques may still be useful and we may still be able to improve tracking performance if we can make the friction estimate 'close' to the actual friction force in some sense. The design must also be robust to the differences between the friction estimate and the actual friction force. In the next section, we design a friction compensator that is motivated by this goal.

3.2 Design of Adaptive Nonlinear Friction Compensator

In this section we design the specific components for the friction compensation scheme described in figure 3-1. These components consist of a linear controller and a friction estimator. We make two main design choices about the friction estimator. The first is the structure of the friction estimator. The second is the choice of the parameter adaptive law.

As stated previously, it is difficult to estimate both the internal friction state, z, and the full set of parameters, so the structure of the friction compensator can not be a certainty equivalence type design which consists of all of the parameters and the state variables which make up the friction force. Motivated by the design objective of keeping the difference between the friction force and the estimated friction force small, we structure the friction force into two parts, a part that we will estimate, F_{est}, and a part that will remain unestimated, F_{unest}, would should be chosen to be 'small'. This is shown in figure 3-2. The friction force consists of two parts and the goal of the friction compensator is to make the differences between $\hat{F}$ approach F_{est} 'small' and to make the overall system robust to the uncertainties represented by F_{unest}. We now re-phrase the design objective stated in the previous section.

For good tracking,
choose $F = F_{est} + F_{unest}$ so that F_{unest} is 'small'
and make $\hat{F} \rightarrow F_{est}$

In order to meet this modified design objective, we will choose to estimate the static part of the friction force, $F_{est} = F_s$. We have discussed in the previous chapter that the dynamic effects in the model are perturbations of the static force. In this section we will support this choice and quantify the size of the unestimated part of the friction

force.

The second main design choice for the friction estimator is the parameter adaptive law. The static friction force, presented in chapter 2 in equation (2.1), is a function of linearly-occurring parameters. The parameter adaptive law is an on-line algorithm for dynamically varying the parameter estimates so that the effect of the differences between the estimated force and static friction force $\hat{F} \rightarrow F_s$ are also 'small'. In this section, we will also state the choice of parameter update law and introduce the concept of an error model. The motivation for the particular choice of parameter update law is postponed until the next section where it is explained by reconsidering the design objective as an equivalent error model stability problem.

Thus in this section we present an adaptive nonlinear friction compensator, which consists of a linear control law and a friction estimator that is motivated by the objective of cancelling the undesirable effects of friction. The design is characterized by two primary design choices, the structure of the estimator, which is discussed in this section and the choice of parameter update laws, which is discussed in the next section in the context of error models.

Note that there are alternatives to how to choose the friction force estimate. For example in the last section of the previous chapter (2.3.2), two nonlinear compensators were described briefly. The first is like this design but without the parameter estimation. The second uses an estimator for the internal friction state, z, and assumes known parameters. The performance and stability robustness of these other types of designs can also be thought of in terms how much error there is in the friction force estimate and how that error affects the stability of the overall system. The method designed here is distinguished from these by its motivation, which is for stable adaptation without the use of high control gains. Although the analysis in chapter 4 suggests that some bandwidth restrictions are required, the simulations in chapter 5 show that these restrictions are moderate and performance is improved with the low

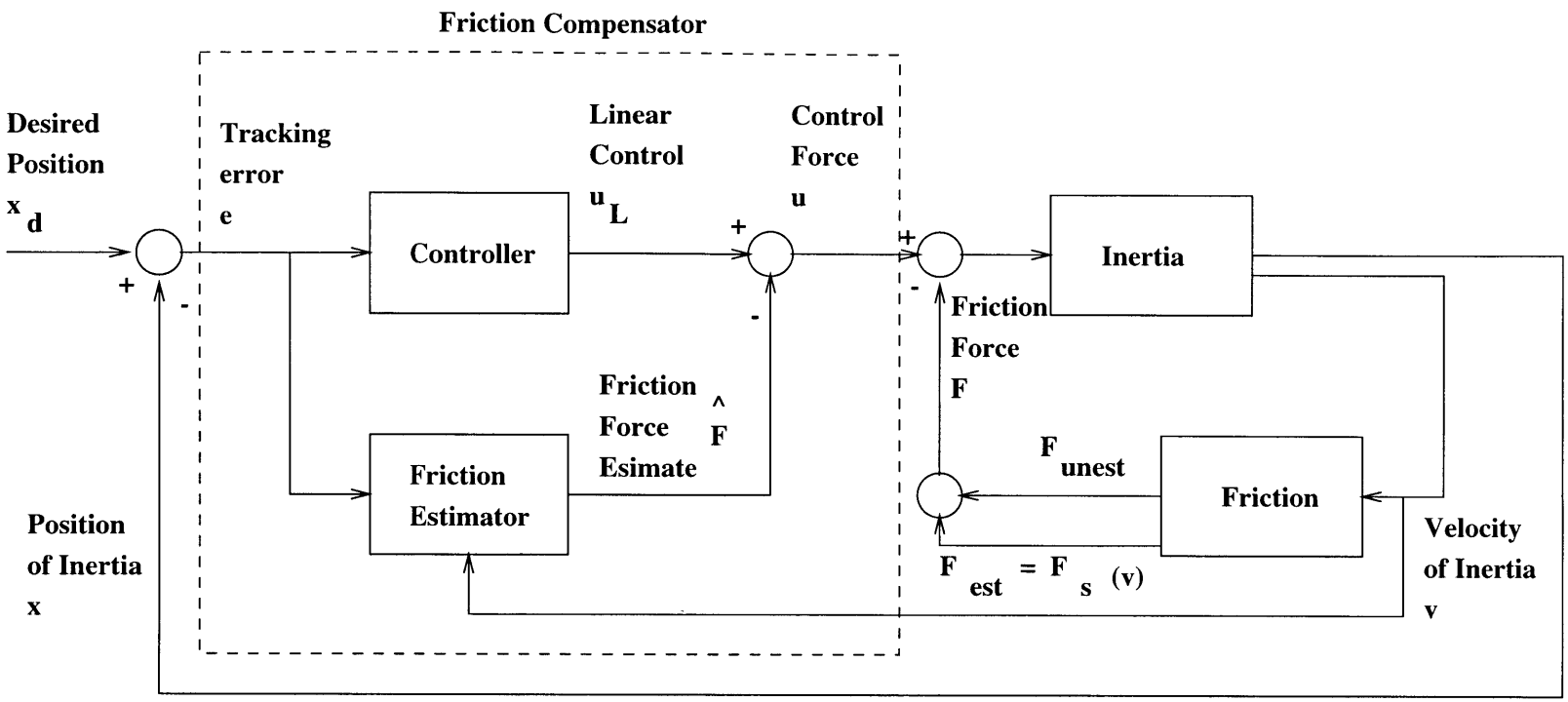

Figure 3-2: The friction force estimator is unable to estimate all of the features of the friction force. So instead, the compensation scheme estimates the static part of the friction force, $F_{est} = F_s(v)$. The unestimated part of the friction force, F_{unest} is due to dynamic model perturbations which should be small in some sense.

bandwidth controller.

3.2.1 Linear Controller

Define a tracking error vector, e, in terms of the difference between the plant position, x, and a desired reference position, x_d.

$$e = \begin{bmatrix} \int(x_d(\tau) - x(\tau))d\tau & x_d - x & \dot{x}_d - \dot{x} \end{bmatrix}^T \tag{3.1}$$

We also define the linear control term, u_L, that consists of a feedforward term, $\ddot{x}_d$, a linear P.I.D term,

$$u_L = \ddot{x}_d + k_v(\dot{x}_d - \dot{x}) + k_p(x_d - x) + k_i\left(\int(x_d(\tau) - x(\tau)d\tau\right) \tag{3.2}$$

Throughout this study the desired trajectory states, x_d, $\dot{x}_d$ and $\ddot{x}_d$ are assumed to be bounded.

3.2.2 Friction Estimator

The Choice of Friction Estimator Structure

The static friction force, which we discussed in chapter 2, can be characterized by a vector of linearly-occurring parameters, $\theta = \begin{bmatrix} b_v & \alpha_0 & \alpha_1 \end{bmatrix}^T$, multiplied by the vector, $\omega(v)$, where

$$\omega(v)^T = \begin{bmatrix} v & \text{sat}(v) & \text{sat }(v)e^{-(\frac{v}{v_0})^2} \end{bmatrix}^T \tag{3.3}$$

Recall in the previous chapter that these parameters had the interpretation of the viscous friction constant, Coulomb friction constant, and the difference between static and Coulomb friction constants, respectively. Defining $\hat{\theta}$ as vector estimated parameter estimates

$$\hat{\theta}^T = \begin{bmatrix} \hat{b}_v & \hat{\alpha}_0 & \hat{\alpha}_1 \end{bmatrix} \tag{3.4}$$

Then the structure of our friction estimator is given by

$$\hat{F} = \hat{\theta}^T \omega(v) \tag{3.5}$$

Notice that the vector $\omega(v)$, which we will refer to as the regression vector for the friction compensator design, is measurable because the velocity is measurable. In adaptive control, the regression vector is the function of known system variables that is used to generate the adaptive laws, and in upcoming sections we will define a parameter adaptive law for the friction compensator in terms of this vector and we will motivate our choice.

Before moving on to the choice of parameter adaptation, we first support our choice of the structure of the friction estimator. Consider the unestimated part of the friction force, F_{unest}, which is the difference between the actual friction force and the friction force at steady velocity. In appendix (B), we quantify this difference as a function of the difference between the internal friction state, z, and its value at steady velocity, z_s, which is defined in chapter 2 equation (2.7). We define this value as the error ϵ

$$\epsilon = z - z_s \tag{3.6}$$

Figure 3-3 shows the static friction force and a shaded region that represents the maximum bound on the region that in which the unestimated part of the friction force could lie. The perturbation of the static friction vs. velocity curve is caused

by the dynamic effects of the internal friction state and is bounded by a region around the static friction curve that grows linearly with velocity. In appendix (B)

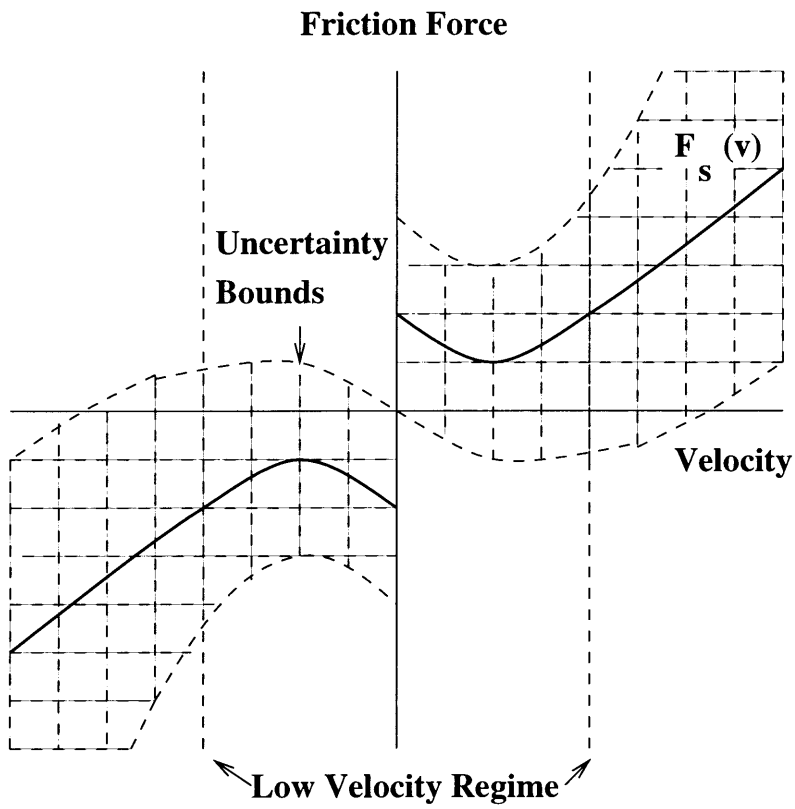

Figure 3-3: The unestimated part of the friction force is due to perturbations in the static model caused by dynamic effects. The maximum size of these perturbations is shown by the shaded region.

the unestimated part of the friction force is shown to be 'small' in the sense that it is scaled by the error, ϵ, which should be small. Because the internal friction state, z, is bounded, a fact that was shown in the previous chapter, this error is also bounded. Assuming upper and lower bounds on the parameters that are not estimated, the appendix shows that unestimated part of the friction force can be written as the sum of a bounded function and a Lipschitz bounded function, which is a function bounded by linear growth constraints. The linear growth of the perturbation with velocity is due to the fact that the internal friction dynamics become faster as the velocity is increased.

By designing a compensator that will be robust to the model perturbations represented by the shaded region, then the range of acceptable performance will include the low velocity region. In chapter 2, the range of acceptable performance for a linear controller, shown in figure 2-6, does not include the low velocity region.

The Choice of Parameter Adaptive Laws

Define a vector of parameter errors, $\tilde{\theta}$, as the difference between the actual parameters and the parameter estimates, i.e.

$$\tilde{\theta} = \theta - \hat{\theta} \tag{3.7}$$

The overall friction compensator in figure 3-2 can be reduced the system which relates tracking error, e, parameter error, $\tilde{\theta}$, and model perturbations, F_{unest}. This system is described by the error equation below and depicted in figure 3-4. In the figure, the dynamics of the error equation are stable and one of the inputs to the system is the vector of parameter errors, $\tilde{\theta}$ multiplied by the regression vector, $\omega(v)$. Note that it is a vector which consists of functions which are first and third quadrant functions of the velocity. In the next chapter, we will show how we can exploit properties of this class of systems. The other input to the system is F_{unest} which is the unestimated part of the friction force. Using the notation in appendix, (B), we break this down into a bounded plus a Lipschitz bounded components. The error equation below describes the overall system,

$$\dot{e} = Ae - b\omega^T(v(t))\tilde{\theta} + bF_{unest} \tag{3.8}$$

where A is a stable matrix given by the P.I.D gains

$$
\begin{aligned}
A &= \begin{bmatrix} 0 & 1 & 0 \\ 0 & 0 & 1 \\ -k_i & -k_d & -k_p \end{bmatrix} \\
b^T &= \begin{bmatrix} 0 & 0 & 1 \end{bmatrix}
\end{aligned} \tag{3.9}
$$

The following parameter adaptive law, also denoted in the figure, will be chosen

$$
\dot{\tilde{\theta}} = \omega(v) b^T P e \tag{3.10}
$$

where $P = P^T > 0$ is a positive definite matrix associated with a Lyapunov equation for the stable matrix A.

The overall system of the error equation and the parameter update law is called an error model system. Consider the design objective in terms of the behavior of the error model system. We want the tracking error to behave as if the friction were not present. In terms of the error equation, this means that our goal would be reached if the unestimated part of the friction force, F_{unest}, and the parameter error, $\tilde{\theta}$, were zero because then the effects of friction would be cancelled out and the tracking error equation would be that of a stable linear system. Although, we can not achieve this goal perfectly, the presence of the stable linear part of overall error system implies that if we can keep the effects of these terms small then the tracking error system can be dominated by desirable dynamics. By the structure of the estimator, we have attempted to make F_{unest} 'small' in the sense that is scaled by the error ϵ. The choice of adaptation laws is motivated by the desire to keep the effects of $\tilde{\theta}$ 'small', and we will discuss this in the next section. .

To understand the motivation for the choice of the parameter adaptive law, in the next

section, we will re-cast our original design goal as an error model stability problem. We will also see that the friction compensation algorithm results in a new type of error model, the analysis of which is the subject of the next chapter.

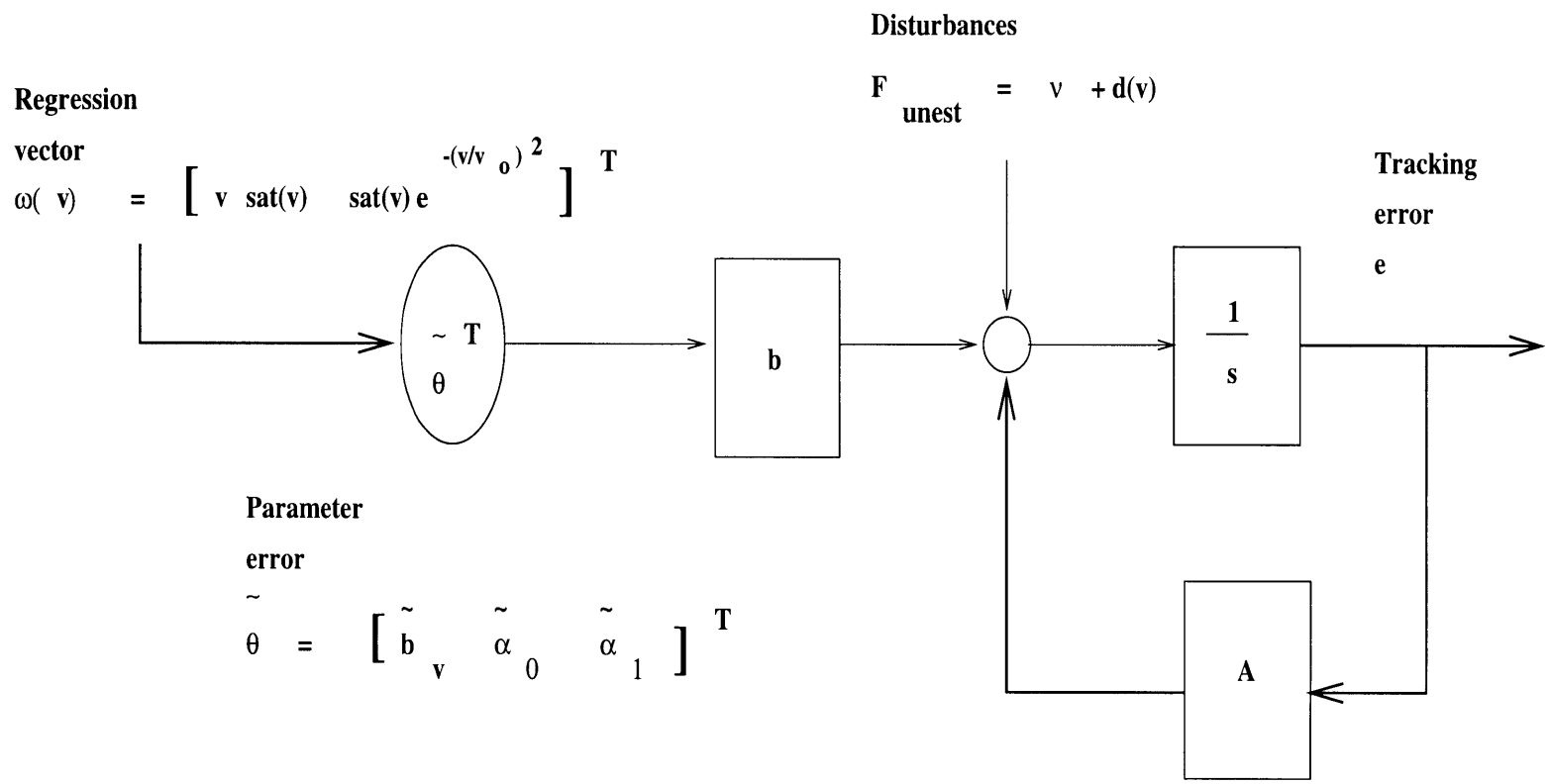

Figure 3-4: The overall block diagram can be reduced to an error equation with stable dynamics. The inputs are due to the parameter estimation error and the unestimated part of the friction force, which are dynamic perturbations in the model. Adaptation laws are motivated by keeping the effects of $\tilde{\theta}$ small. Bounds on the dynamic perturbations are known. The design goal is to allow stable dynamics to dominate the system.

3.3 An Error Model Approach to the Design

In this section, we reformulate the design objective in terms of the error model stability problem. We examine why stability issues for the nonlinear error model system are not immediately obvious, motivating the analysis in chapter 4. Finally, we generalize the features of the friction error model system to define a new type of error model. In the next section, we will discuss the use of persistent excitation in robust adaptation and we verify by simulation, that stability of the error model is indeed a problematic issue by presenting simulations in which the parameter errors can grow unbounded. This further motivates the development of the conditions in chapter 4 under which this instability mechanism can be prevented.

First consider more specifically what the design objective means in terms of the error model system. The unestimated part of the friction, F_{unest}, a model perturbation consisting of bounded as well as Lipschitz bounded terms, acts as a disturbance to the error model system. The compensator was designed so that F_{unest} is small, but we must also ensure that the overall system performance, in particular the error model stability is robust to this disturbance.

The difference between the estimated friction force and the static friction force is as follows

$$F - F_s = \tilde{\theta}^T \omega(v) \tag{3.11}$$

Ideally, the effect of these differences on the overall system would be eliminated if the parameter estimates, were updated in a way such that the parameter error, $\tilde{\theta}$, converged to zero. Additionally, another possible way that these effects would be eliminated is if the parameter error vector converged to a null space of the regression vector. Parameter convergence to values that are not the true values, which may happen if the inputs are not persistently exciting, is not uncommon in linear adaptive

control. Thus the effects of parameter error are 'small' when either the parameter estimates reach the true values or the parameters converge to in such a way that the parameter errors multiplied by the regression vector is zero.

The results of the next chapter indicate that similarly to the linear adaptive control problem, the presence of disturbances in the system prohibits uniform asymptotic stability of the error model system, which would imply perfect estimation of the parameters. Instead, we will find conditions under which the parameters estimates and the tracking errors remain bounded.

More specifically, we can rephrase the friction compensation design objective as follows

For good tracking, make the difference $\hat{F} - F_s$ small by making the effects of the parameter error, $\tilde{\theta}$, 'small' and make the error model system robust to the model perturbations represented by F_{unest}

The results in chapter 4 will show tracking and parameter errors can remain bounded if the input is sufficiently persistently exciting. The size of the bounds depend in part on the size of the bounds for the disturbance term, F_{unest}.

3.3.1 Why Stability of the Error Model is a Problem

In this section we show why the stability of the error model system discussed above is a problem which must be addressed in order for the friction compensator to perform reasonably.

The most natural step to investigate stability would be to define a scalar positive definite function, $V(q(t))$, of the system errors and to try to use Lyapunov techniques

to make the derivative negative. Define

$$\begin{aligned} V(q(t)) &= q^T q \\ &= e^T P e + \tilde{\theta}^T \tilde{\theta} \end{aligned} \tag{3.12}$$

where $q \in \Re^6$ is defined as $q^T = \begin{bmatrix} \sqrt{P}e^T & \tilde{\theta}^T \end{bmatrix}$ and $P = P^T$ is the associated positive definite matrix satisfying the Lyapunov equation $Q = Q^T > 0 = -(PA + A^T P)$. The derivative of V along a trajectory of the tracking error equation is as follows

$$\dot{V} = -e^T Q e + 2e^T P b F_{unest} + 2\tilde{\theta}^T \left(\dot{\tilde{\theta}} - \omega(v) b^T P e \right) \tag{3.13}$$

The motivation for the adaptive laws becomes clear by examining this equation. The adaptive laws are chosen to eliminate terms in the derivative of V which may be positive. Because the terms multiplying the parameter error, $\tilde{\theta}$, in the above equation could be positive, a choice of the parameter adaptive laws is made that will cancel those terms. This choice makes the derivative of V along a trajectory as follows

$$\dot{V} = -e^T Q e + 2e^T P b F_{unest} \tag{3.14}$$

However, due to the presence of the disturbance terms represented by the unestimated part of the friction model, which may be positive or negative, we can not completely eliminate terms which could be positive and thus we can not guarantee that the derivative of V is negative definite or even negative semi-definite.

Alternative techniques could be used to address the stability issues of this system. One approach would be to try to incorporate knowledge of the sign of the unestimated part of the friction force and choose the adaptive law accordingly. When the unestimated force is actually zero; however, this approach may lead to bounded tracking and parameter errors.

There are two types of robust adaptive approaches that have been successfully employed for linear adaptive control in the presence of bounded disturbances. These are adaptive law modifications such as dead zones, σ or e modification. In these approaches, when the disturbances are zero, the system may not have zero tracking errors. We applied these methods to this problem as well with some additional assumptions on the disturbances, but this study will not focus on those approaches.

The other robust adaptive approach, which is the focus of this thesis, is the use of persistent exciting inputs. The idea in using p.e. is to make the tracking errors can periodically large enough so that the function V decreases more than it increases on an interval. This is the approach in the next chapter.

Using the notation in appendix (B) the unestimated part of the friction force consists of bounded and a Lipschitz bounded function. Consider the case when the first term of the above equation is the least negative and the second term is the most positive. The resulting bound for the derivative of V along a trajectory is presented below

$$\dot{V} \leq -\lambda'_Q ||e||^2 + 2\lambda_{P_{max}} \nu'_{max} ||e|| \tag{3.15}$$

where

$$\begin{aligned} \lambda'_Q &= \lambda_{Q_{min}} - 2\lambda_{P_{max}} b_{max} d_{max} \\ \nu'_{max} &= b_{max}(\nu_{max} + d_{max} v_{d_{max}}) \end{aligned} \tag{3.16}$$

and $\lambda_{Q_{min}}$ is defined as the minimum eigenvalue of Q, $\lambda_{P_{max}}$ is defined as the maximum eigenvalue of P, and b_{max} is defined as the maximum element of the vector b.

Due to the presence of disturbance terms, the function V will not work as a Lyapunov function because for small values of $||e||$, V can increase. This shows that the stability problem of this error model system is not immediately obvious. For small tracking errors, the parameter errors could grow unbounded.

A reasonable question is that if small tracking errors can be obtained, why does it matter if the parameter errors become large? The answer is that it is important to have bounded parameter estimates because as changes occur in the input trajectory, large parameter estimates could cause large transients in the tracking error. So in order for the friction compensation design to work reasonably well, the parameter errors must remain bounded.

3.3.2 A New Type of Error Model

In this section, we define a general error model system below which will be analyzed in chapter 4. The friction compensation error model system is a special case of this type of system. In the equations below, e is an nth order vector of tracking errors representing the difference between the desired state, x_d and the actual state, x. And $\tilde{\theta} \in \Re^m$ is a vector of parameter errors.

$$\begin{aligned} \dot{e} &= Ae - b\omega^T(v(t))\tilde{\theta} + b(\nu + d(x)) \\ \dot{\tilde{\theta}} &= \omega(v(t))b^T Pe \end{aligned} \tag{3.17}$$

where A is a stable matrix and where the term ν is a bounded function of the state and $d(v)$ is a Lipschitz bounded function of the jth component of the state, v, and consequently the error, e, i.e.

$$\begin{aligned} \nu &\leq \nu_{max} \\ d(x) &\leq d_{max}|v| \\ &\leq d_{max}(v_{d_{max}} + ||e||) \end{aligned} \tag{3.18}$$

For error model under consideration, the regression vector is comprised of continuous first and third quadrant functions of the jth state element, v. In addition, one of the

functions in the regression vector is the state element v itself. The other functions may be nonlinear.

$$\omega(v(t)) = \begin{bmatrix} v(t) & f_2(v(t)) \cdot & \cdot & \cdot & f_m(v(t)) \end{bmatrix}^T \tag{3.19}$$

As in the previous section for the friction system, we define a positive definite function of the system errors, V, and derive its derivative along a trajectory as below. We will use these expressions in the next chapter and include them here as part of the characterization of the new error model for completeness.

$$\begin{aligned} V(q(t)) &= q^T q \\ &= e^T P e + \tilde{\theta}^T \tilde{\theta} \end{aligned} \tag{3.20}$$

where $q \in \Re^m$ is defined as $q^T = \begin{bmatrix} \sqrt{P} e^T & \tilde{\theta}^T \end{bmatrix}$ and $P = P^T$ is the associated positive definite matrix satisfying the Lyapunov equation $Q = Q^T > 0 = -(PA + A^T P)$.

The derivative of V along a trajectory of the tracking error equation can be bounded as follows,

$$\dot{V} \leq -\lambda'_Q ||e||^2 + 2\lambda_{P_{max}} \nu'_{max} ||e|| \tag{3.21}$$

where

$$\begin{aligned} \lambda'_Q &= \lambda_{Q_{min}} - 2\lambda_{P_{max}} b_{max} d_{max} \\ \nu'_{max} &= b_{max}(\nu_{max} + d_{max} v_{d_{max}}) \end{aligned} \tag{3.22}$$

and $\lambda_{Q_{min}}$ is defined as the minimum eigenvalue of Q, $\lambda_{P_{max}}$ is defined as the maximum eigenvalue of P, and b_{max} is defined as the maximum element of the vector b.

Comparison with Other Error Models

Next we show how the error model differs from previous work [16, 17]. The system studied in [16] is like the error model presented above, however, it has no disturbance term and instead of the term $\omega(v(t))$, the regression vector, is a bounded function of time. The system studied in [17] has a bounded disturbance term and where our system has $\omega(v(t))$ containing a bounded nonlinear functions of state element, v, the system in [17] has $\omega(x(t))$ as a linear function of state vector, x. Thus the error model we study in equation (3.17) is a natural extension of these results but differs from them in two respects. The first difference is that the regression vector $\omega(v)$, can contain nonlinear functions of an element of the plant state. The second difference is that the term, $\nu + d(v)$, which we will consider as a disturbance term in the error model, is not a bounded function as in [17], but it contains a bounded function as well as a Lipschitz bounded function of state.

Although our error model is an extension of the other error models, we should expect to be able to derive a similar boundedness result. This is because the nonlinearity in the regression vector is 'nice' in the sense that it could be scaled, 'stretched', continuously deformed to look like a linear function. Additionally, the second difference, which is the addition to the error model of a Lipschitz bounded function, should not interfere with a error model boundedness result because similar to linear control, we can take care of this type of perturbation by having high enough bandwidth. Although, in keeping with the original motivation for the friction compensation approach, we want to avoid using higher bandwidth control. The size of the Lipschitz disturbance will determine the required bandwidth. The next chapter deals specifically with the stability analysis of the new error model.

The new error model is similar to that considered in [11] in that both contain a nonlinear regression vector that is a function of an output. The stability proof there is based on a Lyapunov type argument in which terms are added to the control law

to counter the effect of the growing nonlinearities. Here we consider an additional unknown disturbance term.

3.3.3 The Role of Persistent Excitation for Robust Adaptation

In this section we motivate the use of persistent excitation as a tool for solving our error model problem. We briefly overview the history of its use in adaptive control. Then we define persistent excitation and show some examples. Finally, we show by simulations that with inputs that have insufficient persistent excitation, the adaptive algorithm we designed may result in unbounded parameter estimates.

Persistent excitation was used in adaptive control in the linear adaptive control parameter convergence problem. If persistent excitation was present and no disturbances were present, then adaptive structures could be adopted such that the parameter errors converged to zero ([20], [19]). The idea was that if the input dynamics excited all the dynamic modes of the system, then the parameter error could not converge to a null space of the regression vector.

Adaptive control of linear systems with bounded disturbances was studied in the 1980's. It was discovered that in the presence of bounded disturbances, the parameter errors could become unbounded [23]. In the error model in this study, the model perturbation acts as a disturbance and the parameters can become unbounded as shown in the simulations which follow. To address these issues, researchers developed the field of robust linear adaptive control using either adaptive law modifications or persistent excitation techniques.

In the presence of bounded disturbances, the work of [17] showed that the linear adaptive control problem is has bounded solutions if the level of persistent excitation

is high enough. When the input is sufficiently persistently exciting, then the tracking error periodically becomes large enough to prevent the instability mechanism we discussed above- i.e. a situation where the tracking error stays small, but the parameter errors grow without bound. Critical in the proof was the fact that the regression vector in the linear adaptive control problem is a linear function of the state. The regression vector in our error model does not have this feature; however, in the next chapter, we will see how the first and third quadrant property can be used to argue a similar boundedness result.

Persistent excitation is defined as follows.

DEFINITION 3.3.1 *Persistent Excitation*

A bounded vector $\omega : R^+ \rightarrow \Re^n$ *is persistently exciting (p.e.) with degree* ϵ_0 *if positive constants* T_{0_P}, δ_0, *and* ϵ_0 *exist such that there is a subinterval* $\begin{bmatrix} t_2 & t_2 + \delta_0 \end{bmatrix}$ *of any interval* $\begin{bmatrix} t_i & t_i + T_{0_P} \end{bmatrix}$ *such that*

$$\left| \int_{t_2}^{t_2+\delta_0} \omega^T(\tau) r d\tau \right| \geq \epsilon_0 T_{0_P}$$

for all $t_i \geq t_0$ *and any unit vector* $r \in \Re^n$

We use the terms p.e. degree and p.e. level interchangeably for the term ϵ_0. We also refer frequently to the term, δ_0, as the p.e. subinterval width. And sometimes we refer to the term T_{0_P} as the p.e. interval.

EXAMPLE 3.3.1 $\omega(t) = \begin{bmatrix} sin(\Omega t) & cos(\Omega t) \end{bmatrix}^T$ *is p.e. in* $\Re^2$

EXAMPLE 3.3.2 $\omega(t) = \begin{bmatrix} sin(\Omega t) & sin(\Omega t) & sin(\Omega t + \phi) \end{bmatrix}^T$, *where* ϕ *is a constant phase difference, is not p.e. in* $\Re^3$

Instability and Lack of Sufficient Persistent Excitation

In this section, we show specifically that when the inputs have insufficient persistent excitation, then this error model can be unstable. We return to the three baseline tasks in the previous chapter- a low velocity position ramp, a low velocity tracking task with zero velocity crossings and a step input. The main result of the next chapter will be to develop persistent excitation conditions on the input trajectory that will guarantee the stability of the error model. The purpose of the examples in this section is to show that without this result, the adaptive friction compensation algorithm can result in an unstable error model. By applying the adaptive compensation algorithm to the simulation examples presented in chapter 3, we show that with insufficient persistent excitation conditions on the input trajectory, the parameter estimates can grow without bound, thus making the error model unstable. We include one more task which is also a sinusoid to show that some input trajectories naturally have enough persistent excitation in the input so that the algorithm improves tracking performance with bounded parameter estimates. This is significant because many of the types of tasks for which nonlinear dynamic friction effects are problematic include trajectories with repeated zero velocity crossings. For example pick and place maneuvers have repeated zero velocity crossings. These types of trajectories have some level of persistent excitation occurring naturally.

Adaptive Nonlinear Friction Compensation with Insufficient P.E. for Low Velocity Task 1- A Constant Velocity Task

In this section, we examine the first task in the baseline study using the friction compensator designed in this chapter. The desired input trajectory for the first task is a position ramp with a low velocity of .02m/sec.

Simulation results are shown in figure 3-5. Initially, up until about 25 seconds, the

tracking error is low. In fact, if we compare this plot to the corresponding plot without friction compensation in chapter 2, we find that the algorithm is initially successful. In chapter 2, stick starts at 5 seconds (figure 2-7) but here that is delayed. However, once stick is reached, the friction compensation algorithm with insufficient p.e. inputs does not recover. The mass stays stuck resulting in errors which become worse than with no friction compensation.

The parameter estimates are shown in the next plot in the simulation set in figure 3-5. Two of which are growing. Without the persistent excitation conditions we will develop in the next chapter, the error is not p.e. in every direction. In this case, the parameter update laws, which depend on the error, cause the parameter errors can grow large in a particular direction. Because the parameter estimates are used to compute an estimated friction force, the difference between the actual friction force and the estimated friction force, which is initially a small difference eventually grows large as is shown in the figure.

The overall forces on the mass consist of the control force, which consists of the linear terms and the friction estimate, and the friction force. The mass gets stuck because the growing terms in the friction force estimate balance the growing terms in the P.I.D. portion of the control force. The overall force becomes small and the mass stays stuck. Misapplied, the friction compensation algorithm can actually worsen performance.

Friction Compensation with Insufficient P.E. for Low Velocity Task 2- A Task with Repeated Zero Velocity Crossings

The next set of simulations is for the second task in the baseline study, which is the low velocity sinusoid. The desired position is $x_d = .05sin(t/2)$. Figure 3-6 is a plot of the desired and actual trajectories. Up until about 27 seconds, the trajectories track fairly well, with the mass getting stuck first at ten seconds, then for a little longer at

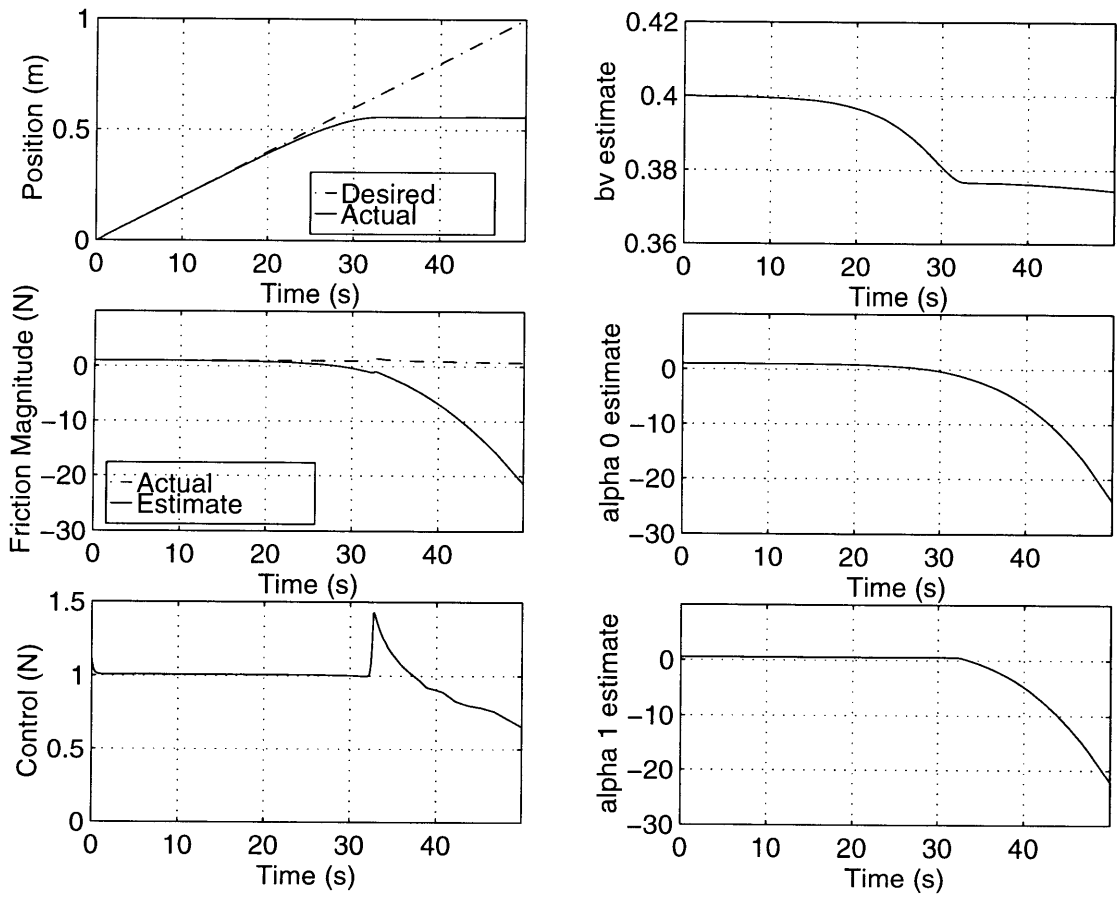

Figure 3-5: Initially the friction compensation scheme with insufficient p.e. is successful at eliminating the stick slip limit cycle observed in a linear controller for a desired trajectory of a position ramp. However, the tracking error is stabilizing and because it does not have richness in all directions, two of the parameters start to grow large. This causes the estimated friction force to grow and this is balanced by components of the control force. The overall forces on the mass become small and the mass gets stuck.

fifteen seconds, then for longer at 22 seconds. Finally the mass gets stuck and stays stuck at about 27 seconds.

The figure also shows the parameter estimates, α_2, the viscous parameter, as well as α_0 and α_1. The parameter α_2 is stabilizing at a value above .39. Similarly, to the first task, the other parameters; however, start to grow large causing the error in the estimated friction force to grow large.

The final plot for this simulation set is the control force. The control force consists of the linear parts of the controller as well as the estimated friction force. When the estimated friction force grows, the linear terms in the control grow as well so that in this simulation, the overall control force does not grow and balances the actual friction force causing the mass to eventually remain stuck.

We can compare this set of simulations to the corresponding set of simulations in chapter 2 (figure 2-8). We see that without the required p.e. conditions, the friction compensation controller initially improves tracking for about 27 seconds. Eventually, however the mass becomes stuck and the tracking errors stay within the bounds of the desired trajectory.

Although this trajectory does lead to an unstable error model, the results of this simulation lead to the speculation that some trajectories, with frequent zero crossings, could naturally have enough persistent excitation to satisfy the input conditions. This is important because many types of tasks where friction is a problem do have frequent zero crossings, for example, pick and place manuevers. We will see that our speculation is correct by showing a trajectory with enough excitation naturally occurring to get a stable algorithm. This simulation will be presented later in this section.

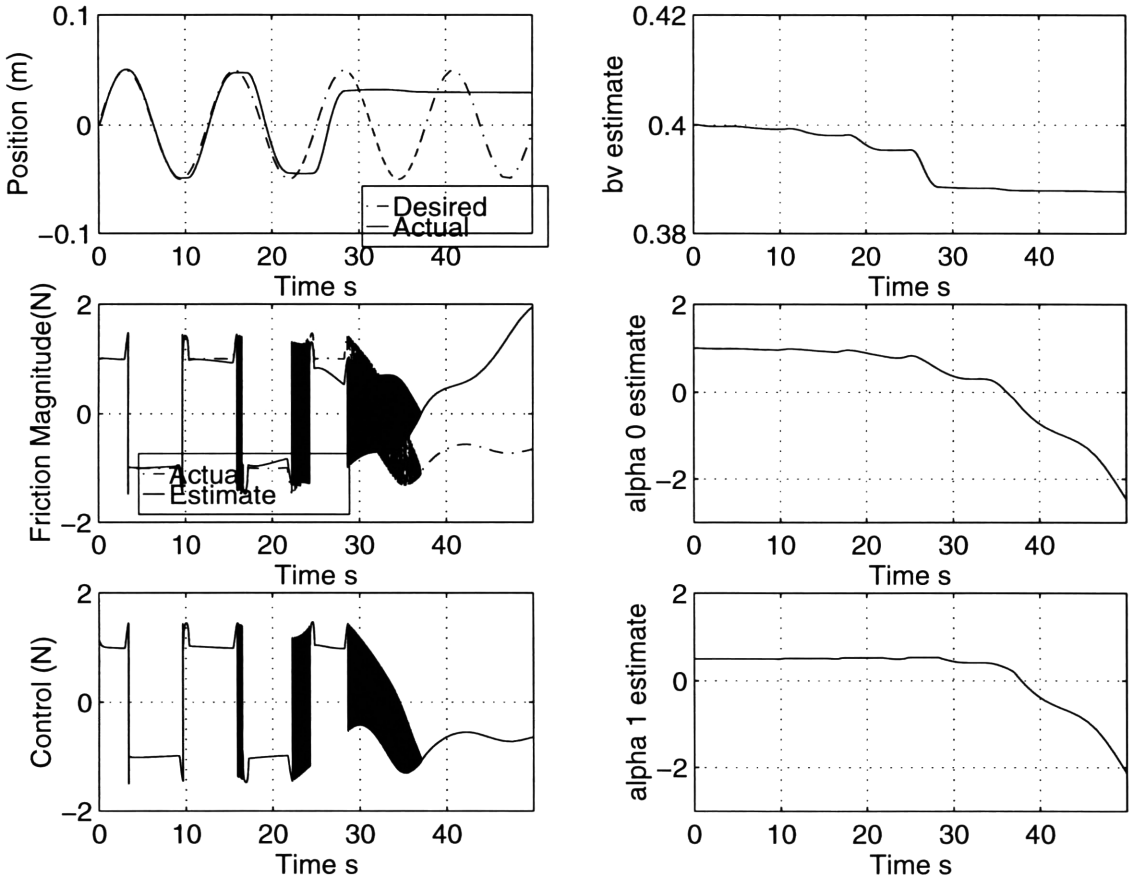

Figure 3-6: Initially, the friction compensator with insufficient p.e. in the input tracks the desired sinusoidal trajectory. The mass gets stuck for progressively longer times as the parameter estimates start to grow. The presence of disturbances or modelling uncertainties can cause the parameter estimates can grow in a particular direction when the tracking error is not excited in every direction.

Adaptive Nonlinear Friction Compensation with Insufficient P.E.- A Regulation Task

The next set of simulations show a unit step response when the friction compensation is used without the required p.e. input conditions. Figure 3-7 shows the desired trajectory, which is a unit step, as well as the actual trajectories. The actual trajectory has a constant steady state error of about 10 percent which equals ten centimeters. This is larger than the 6.5 centimeter steady state hunting oscillation in the linear control system in figure 2-9. At approximately 3 seconds, the mass becomes stuck and the tracking error stays constant.

The results of this simulation are similar to the results of the previous two low velocity tasks. The adaptation on the parameter estimates can not effectively reduce the tracking problems in the system. The growth of some of the parameter estimates causes the estimated force to grow and the force error to grow. The overall control force eventually matches the actual friction force causing stick. The parameter errors for α_0 and α_1 continue to grow, while the parameter estimate for α_2, the viscous parameter reaches a steady value.

A Low Velocity Task with Repeated Zero Velocity Crossings that Naturally has Sufficient P.E.

In this section, we present a higher frequency sinusoid, $x_d = .05sin(t)$. The simulation results support the previous speculation that some trajectories have enough P.E. naturally occurring so that the friction compensation algorithm performs well. Figure 3-8 shows the desired and actual positions and low tracking error. The mass does not get stuck. The parameter estimates remain fairly steady, and the error in the estimated friction force is not growing.

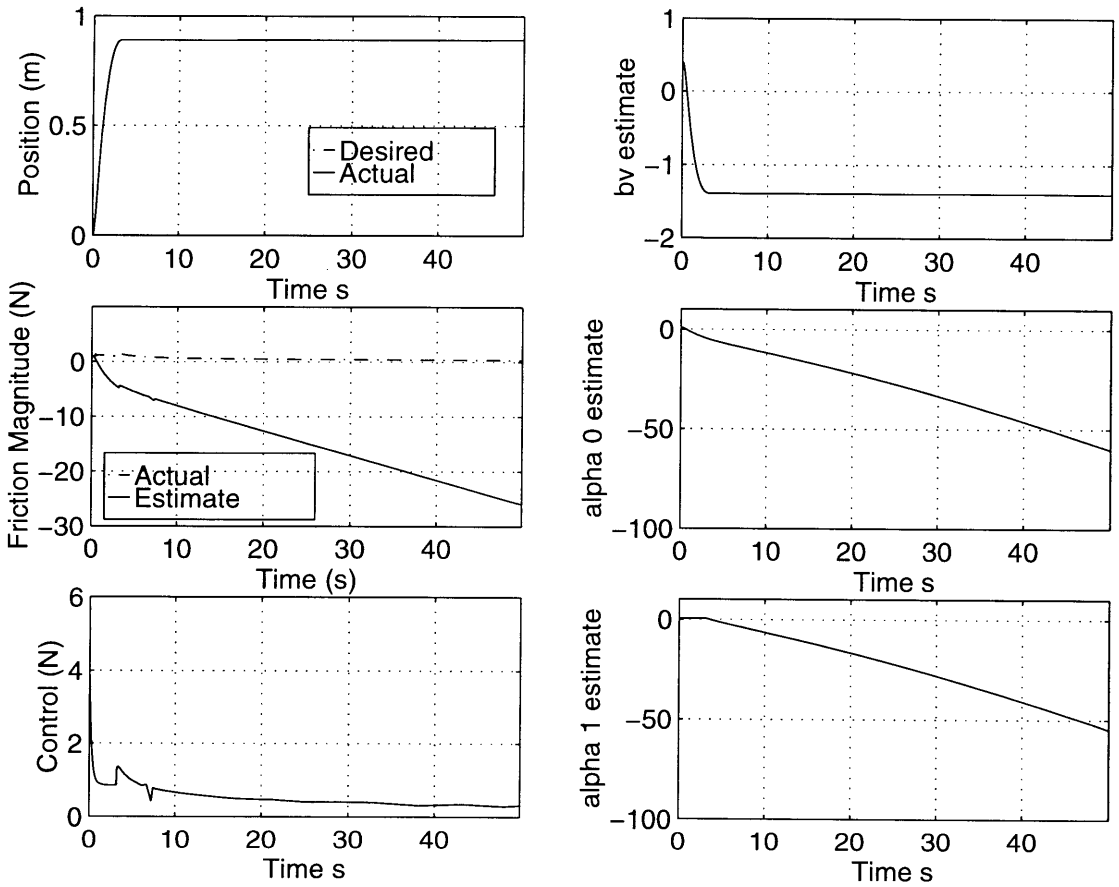

Figure 3-7: The adaptive nonlinear friction compensator with insufficient p.e. gets stuck with errors of about ten percent. The instability mechanism occurs because the tracking error does not have dynamics in every direction. Some of the parameter errors start to grow.

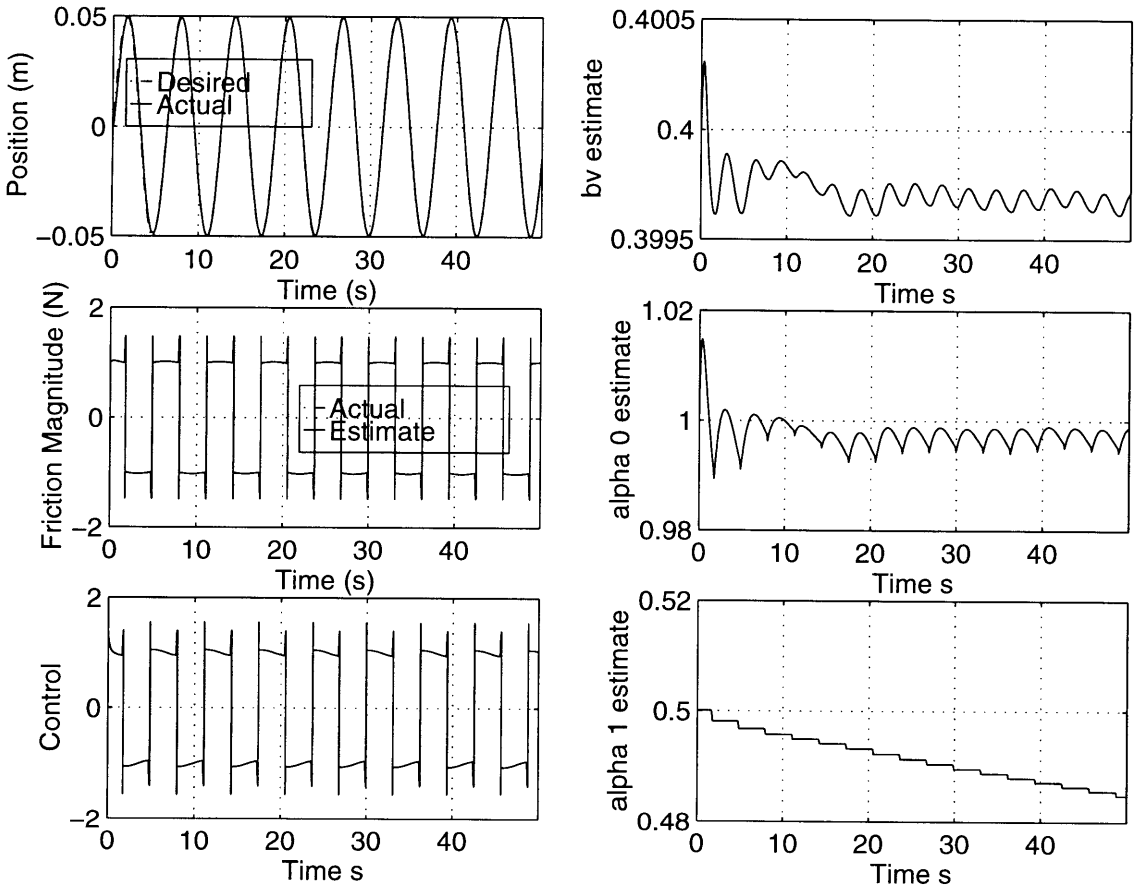

Figure 3-8: Tasks with repeated velocity tasks have some amount of p.e. occurring naturally. In this simulation the amount of naturally occurring p.e. is sufficient for tracking errors to stay low and parameter errors not to grow unreasonably large.

3.4 Chapter Summary

In this chapter, we designed an adaptive nonlinear compensator to address the tracking problems due to friction that were presented in chapter 2. The design is based on compensating for the static, Coulomb and viscous components of the friction force while remaining robust to dynamic perturbations. We show these perturbations are 'small' in the sense that they consist of bounded terms and Lipschitz bounded terms which grow linearly with velocity and these terms are scaled by the difference between the internal friction state and its steady value.

We showed how the design objective can be viewed equivalently as an error model stability problem for a new type of error model characterized by a regression vector with first and third quadrant functions with bounded or Lipschitz bounded disturbances. We described how the presence of disturbances can cause an instability mechanism in which the tracking errors stay small but the parameter errors grow unbounded. We introduced persistent excitation as a tool for addressing this problem. We verified that dynamic model perturbations which act as disturbances can cause adaptive nonlinear friction compensator with insufficient p.e. in the input to become unstable.

In the next chapter, we present a solution to the stability issues by using inputs which are sufficiently persistently exciting.

Chapter 4

Stability of the Adaptive Controller

In this chapter, we use persistent excitation in the input trajectory as an approach to proving conditions for boundedness of solutions for the new error model discussed in the previous chapter in section (3.3.1) and shown in section (3.3.3).

First, we give an idea of why the proof works and an overview of the chapter.

Consider the error model equations from equation (3.17), which are reprinted below.

$$\begin{aligned} \dot{e} &= Ae - b\omega^T(v(t))\tilde{\theta} + b(\nu + d(x)) \\ \dot{\tilde{\theta}} &= \omega(v(t))b^T Pe \end{aligned} \tag{4.1}$$

We defined a positive definite function of the errors, V, and we saw the derivative of V is negative at large tracking errors but positive at small tracking errors (equation (3.21)).

The error model system has a similar structure to that studied in [16]. That result stated that if $\omega(v)$ is p.e., then the above system is uniformly asymptotically stable if

the disturbances are zero (which will be defined as the 'unforced' error model system). We will consider two cases. For the first case, the regression vector, $\omega(v)$, satisfies a p.e. condition on an interval, and we will be able to show that implies V decreases if the initial condition is large enough.

In the second case, $\omega(v)$ does not satisfy a p.e. condition on an interval. And we let the input have enough persistent excitation so that the desired regression vector does satisfy the p.e. condition on the interval. Because the regression vector consists of first and third quadrant functions that are essentially scaled versions of linear functions, we will be able to establish conditions such that this implies there must be a tracking error. Thus, the type of regression vector allows us to conclude that a measure of errors in the regression vector implies a measure of errors in tracking. Persistent excitation in the input trajectory can prevent the instability mechanism in this case by guaranteeing that the tracking error periodically becomes large enough to allow V to decrease.

We will show that if the input to the control system is p.e. over a small enough subinterval and with a high enough degree, and if the bandwidth of the linear part of the compensator is high enough compared to the Lipschitz bounded disturbances, then error model presented in an earlier chapter has bounded solutions. This means that the tracking error is bounded and the control algorithm results in bounded parameter estimates. A second theorem, which is important to make the friction compensation method implementable and useful for a control designer, shows that if the Lipschitz disturbances are small enough, an algorithm exists which will converge to p.e. conditions that satisfy the requirements for the friction compensation system and the error model solution bounds can be computed.

First, we present three sections of preliminary results about the error model system under investigation. In the first preliminary section, properties about continuous first and third quadrant functions which make up the regression vector are examined.

Quantifying the minimum size of the tracking error in terms of the error in the regression vector will be a key feature used in the main stability to quantify the decrease in V on a the p.e. subinterval. The second section contains results about the error model, and third section contains bounds on an interval for the state and the associated function V. In the fourth and fifth sections, the main theorem is presented and proved. Finally in the sixth section, a second theorem is presented about the computing the solution bounds and the conditions required for stability for the friction compensation system.

4.1 Preliminaries: Properties About First and Third Quadrant Continuous Functions

In this section, we are going to establish useful properties for the type functions that make up the regression vector. These functions consist of first and third quadrant continuous functions which may or may not be nonlinear. The first section deals with scalar first and third quadrant functions, and the second section deals with a vector of first and third quadrant functions. Under certain conditions, the features of these functions allow us to relate measure of the error in the regression vector to a minimum measure of the tracking error. Finally, in the third section, we discuss the set of conditions which are required to apply the first two properties and we present a useful property that will be used in the the proof of theorem (4.4.1).

4.1.1 A Property about First and Third Quadrant Continuous Functions

A first and third quadrant continuous functions is essentially a scaled version of the signal. If we integrate over a small enough interval, then we will show how the integral of the signal and the integral of the function of the signal can be related in size by a scaling factor which we will call k. We will do this by choosing the subinterval width, δ_0, small enough so that $v(\tau)$ does not change sign for $\tau \in \left[\begin{array}{cc} t_2 & t_2 + \delta_0 \end{array} \right]$, and then by choosing the scaling factor, k, small enough so that the two integrals in equation (4.5) have similar minimum magnitudes. We will choose a small positive constant, v_c, and choose the subinterval width small enough so that $|v|$ does not reach this value. This idea is shown in figure 4-1 and stated more formally in the property below.

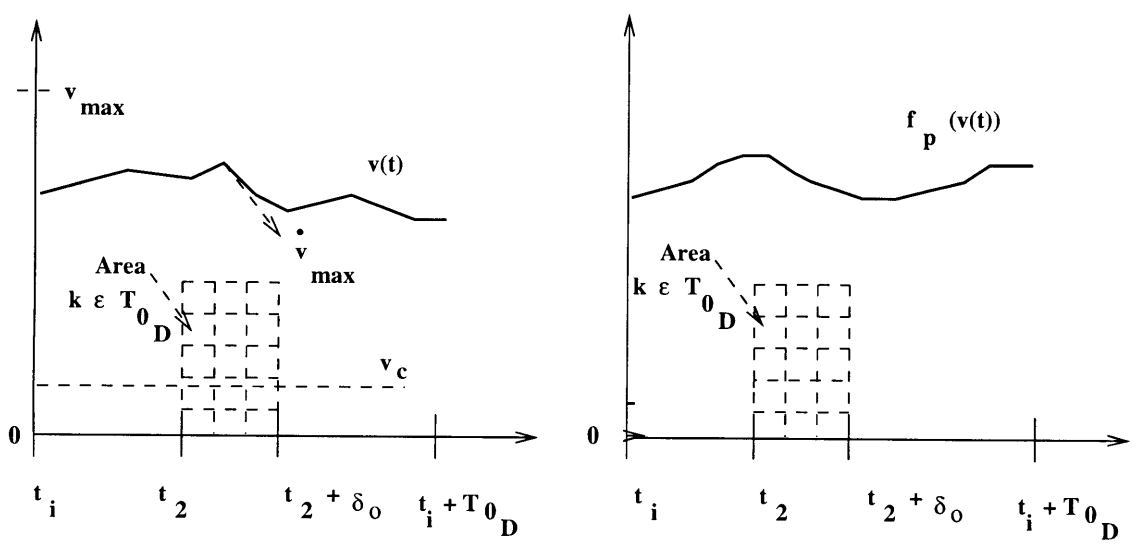

Figure 4-1: Given an upper bound on the rate of change of v over the interval, $\dot{v}_{max}$, the subinterval width, δ_0, can be chosen small enough so that $|v|$ does not reach zero in the subinterval. The scaling factor, k, can be chosen small enough so that the integral of the two signals over the subinterval are related in size.

PROPERTY 4.1.1 *Let $v : \Re^1 \rightarrow \Re^1$ be a continuous differentiable function and $f_p : \Re^1 \rightarrow \Re^1$ be a continuous first and third quadrant function, i.e.*

$$\begin{aligned} f_p(0) &= 0 \\ f_p(v) &> 0 \qquad if\ v > 0 \\ f_p(v) &< 0 \qquad if\ v < 0 \end{aligned}$$

Assume the following,

(i.) Upper bounds for $|v(t)|$ and $|\dot{v}(t)|$, on the subinterval $t \in \left[\ t_2 \quad t_2 + \delta_0\ \right]$ are as follows,

$$\begin{aligned} |v(t)| &\leq v_{max} \qquad for\ t \in \left[\ t_2 \quad t_2 + \delta_0\ \right] \\ |\dot{v}(t)| &\leq \dot{v}_{max} \qquad for\ t \in \left[\ t_2 \quad t_2 + \delta_0\ \right] \end{aligned} \tag{4.2}$$

(ii.) The subinterval width, δ_0, is small enough so that,

$$\delta_0 < \left(\frac{\frac{k\epsilon_0 T_{0_D}}{\delta_0} - v_c}{\dot{v}_{max}} \right) \tag{4.3}$$

(iii.) The scaling factor, k, is small enough so that,

$$0 < k < 1$$

$$max_{p=2,..m} \left(\frac{1}{f_{p_{min}} \left[\ -v_{max} \quad -v_c\ \right] \cup \left[\ v_c \quad v_{max}\ \right]} k\epsilon_0 T_{0_D} \right) \leq \delta_0 \tag{4.4}$$

Then

$$\textit{If} \quad \left| \int_{t_2}^{t_2+\delta_0} v(\tau)d\tau \right| \geq k\epsilon_0 T_{0_D} \ \textit{then} \quad \left| \int_{t_2}^{t_2+\delta_0} f_p(v(\tau))d\tau \right| \geq k\epsilon_0 T_{0_D} \tag{4.5}$$

The proof, detailed in appendix (C), proceeds in three parts. First, we show that the given conditions imply that the signal must be at least a threshold magnitude, $v_T = \frac{k\epsilon_0 T_{0_D}}{\delta_0}$, somewhere on the interval. Second, using an upper bound of the maximum rate of change of v on the interval, we choose δ_0 small enough to ensure that $v(\tau)$ does not reach zero in the subinterval; instead, $v(\tau)$ is in a closed, bounded set $\begin{bmatrix} -v_{max} & -v_c \end{bmatrix} \cup \begin{bmatrix} v_c & v_{max} \end{bmatrix}$. Third, we compute the minimum value for the integral of the first and third quadrant nonlinear function, f_p, over this interval and choose the scaling factor, k, small enough to satisfy the desired property. The notation used above is defined in appendix (C).

This property allows us to think of the first and third quadrant function as a scaled version of the signal and relate a measure of the signal and a measure of the function. In the next section, we examine a similar result for a vector of first and third quadrant functions.

4.1.2 A Property About a Vector of First and Third Quadrant Continuous Functions

In this section, we are going to establish the main property that will allow us to deal with possible nonlinearity in the regression vector. We would like to think of the regression vector, $\omega(v)$, projected onto any direction, as a scaled version of the signal v. This condition is going to be useful will allow us to relate a measure of the error in the regression vector to a minimum measure of the tracking error.

The next lemma implies that under given assumed conditions, an error in the regression vector implies an error in tracking.

LEMMA 4.1.1 *Given that the regression vector, $\omega : \Re^1 \rightarrow \Re^m$, is a vector of scalar continuous first and third quadrant functions,*

$$\omega(v(t)) = \begin{bmatrix} f_1(v(t)) & \cdot & \cdot & \cdot & f_m(v(t)) \end{bmatrix}^T \tag{4.6}$$

where $f_1(v(t)) = v(t)$. Assume the following,

(i.) Upper bounds for jth element of the state vector, v, and its derivative, $\dot{v}$, and the jth element of the desired state vector, v_d, and its derivative, $\dot{v}_d$, are as follows,

$$\begin{aligned} |v(t)| &\leq v_{max} && \text{for } t \in \begin{bmatrix} t_2 & t_2 + \delta_0 \end{bmatrix} \\ |\dot{v}(t)| &\leq \dot{v}_{max} && \text{for } t \in \begin{bmatrix} t_2 + t_2 + \delta_0 \end{bmatrix} \\ |v_d(t)| &\leq v_{d_{max}} && \text{for } t \in \begin{bmatrix} t_2 & t_2 + \delta_0 \end{bmatrix} \\ |\dot{v}_d(t)| &\leq a_{d_{max}} && \text{for } t \in \begin{bmatrix} t_2 + t_2 + \delta_0 \end{bmatrix} \end{aligned} \tag{4.7}$$

(ii.) For each of the component functions of the regression vector, $f_p(v(t))$, the subinterval width, δ_0, and scaling factor, k, are chosen small enough to meet the conditions of property (4.1.1)

$$\begin{aligned} \delta_0 &< \left(\frac{\frac{k\epsilon_0 T_{0_D}}{\delta_0} - v_c}{\dot{v}_{max}} \right) \\ 0 &< k < 1 \end{aligned} \tag{4.8}$$

$$max_{p=2,..m}\left(\frac{1}{f_{p_{min}\left[\begin{array}{cc} -v_{max} & -v_c \end{array}\right]\cup\left[\begin{array}{cc} v_c & v_{max} \end{array}\right]}}k\epsilon_0 T_{0_D}\right) \leq \delta_0 \quad (4.9)$$

(iii.) *The subinterval width, δ_0 is small enough so that*

$$\delta_0 < \left(\frac{\frac{\epsilon_0 T_{0_D}}{\delta_0} - v_c}{a_{d_{max}}}\right) \quad (4.10)$$

(iv.) *There is an error in the regression vector such that,*

The desired regression vector satisfies the following p.e condition. On subinterval $\left[\begin{array}{cc} t_2 & t_2+\delta_0 \end{array}\right]$

$$\left|\int_{t_2}^{t_2+\delta_0} \omega^T(v_d((\tau))rd\tau\right| \geq \epsilon_0 T_{0_D} \quad (4.11)$$

for any unit vector $r \in \Re^m$.

The regression vector does not satisfy a specified p.e. condition. Instead, on subinterval $\left[\begin{array}{cc} t_2 & t_2+\delta_0 \end{array}\right]$, *the regression vector, $\omega(v(\tau))$, satisfies the following condition,*

$$\left|\int_{t_2}^{t_2+\delta_0} \omega^T(v((\tau))rd\tau\right| \leq k\epsilon_0 T_{0_D} \quad (4.12)$$

for some unit vector $r \in \Re^m$.

These together imply that the tracking error does satisfy a p.e. condition, and a measure of the error in the regression vector is

$$\epsilon_0 T_{0_D}(1-k) \leq \left|\int_{t_2}^{t_2+\delta_0} \left(\omega^T(v_d(\tau)) - \omega^T(v(\tau))\right) rd\tau\right| \quad (4.13)$$

for any unit vector r in $\Re^m$.

(v.) ϵ_0 *is chosen large enough so that*

$$0 < \epsilon_0 T_{0_D}(1 - k - k_{eff}) \tag{4.14}$$

where $0 \leq k_{eff} < 1$ *exists and is defined as an upper bound for a measure of the differences between the component functions of the vector,* $\omega(v(t))$*, such that*

$$\frac{1}{\epsilon_0 T_{0_D}} \left| \int_{t_2}^{t_2+\delta_0} \sum_{p=2}^{p=m} r_p \left(f_p(v(\tau)) - f_p(v_d(\tau)) \right) d\tau \right| \leq k_{eff} \tag{4.15}$$

for the following

$$\begin{aligned} v &\in \left[-v_{max} \quad -v_c \right] \cup \left[v_c \quad v_{max} \right] \\ v_d &\in \left[-v_{d_{max}} \quad -v_c \right] \cup \left[v_c \quad v_{d_{max}} \right] \end{aligned} \tag{4.16}$$

Then a positive lower bound for a measure of the jth *element of the tracking error vector is*

$$0 < \epsilon_0 T_{0_D}(1 - k - k_{eff}) \leq \left| \int_{t_2}^{t_2+\delta_0} (v_d(\tau) - v(\tau))\, d\tau \right| \tag{4.17}$$

Conditions (i.) and (ii.) are the conditions that are required to apply property (4.1.1) which ensures that the jth element of the state does not change sign over the subinterval and that the component functions of the regression vector have integral measures that can be scaled appropriately. Condition (iii.) is an additional upper bound on the p.e. subinterval. This condition together with the assumed p.e. condition on the desired regression vector in condition (iv.) ensures that the jth element of the desired state element, v_d, also does not change sign over the subinterval. In condition (iv.) the desired regression vector is 'large' in the sense that it satisfies a p.e. con-

dition over the subinterval. The actual regression vector is 'small' in the sense that it does not satisfy a smaller specified p.e. condition. Hence, there is an error in the regression vector. Condition (v.) ensures that the corresponding minimum measure of the tracking error will have a positive lower bound by scaling the p.e. level on the desired regression vector, ϵ_0, large enough. This is important because, as we saw in section (3.3.1), when the tracking error is large enough the positive definite function of errors, V, can decrease, and this idea will used in to prove the main stability theorem (4.5).

Consider conditions (ii.), (iii.), and (v.) on the p.e. subinterval width, δ_0, scaling factor, k, and the p.e. level, ϵ_0. Another variable, T_{0_D}, is also used in these conditions, and it will be defined in the next section (4.2) and it will represent the interval length over which we argue that V decreases in the main stability proof. These conditions are going to be of importance in both the design and the performance of the system. They are important to the design because they determine the p.e. conditions that the desired input trajectory must satisfy. Additionally, they are important to the performance because they determine the largeness of the measure of the tracking error that will be used in the main stability proof to make V decrease. Notice that the conditions are interdependent and therefore, it is not initially obvious how a control designer can make these choices. In the last section of this chapter, an algorithm is presented to show how the conditions and bounds can be computed if the Lipschitz disturbances are small enough.

An idea of the proof of lemma (4.1.1), which is detailed in the appendix (D), is presented here. First consider the simpler case when r is the pth standard unit basis vector and f_p is the pth component of the regression vector. A depiction of a possible situation that meets the conditions of the lemma for this case is shown in figure 4-2. By condition (iv.), both the desired state element, $v_d(t)$ and the function $f_p(v_d(t))$ satisfy the p.e. condition and are 'large' over the subinterval because the area under the respective curves at least equal to $\epsilon_0 T_{0_D}$. By condition (v.), $f_p(v)$, is 'small' over

the subinterval, because it has a smaller area under the curve, which is less than $k\epsilon_0 T_{0_D}$ where, $k < 1$. Property (4.1.1) was designed so that the only way condition (v.) can be true is if v also is 'small' over the subinterval and therefore has an area of at most $k\epsilon_0 T_{0_D}$. This means that over the subinterval, there is a difference between the state element, v, and the desired state element, v_d, hence there is a tracking error over the subinterval. Furthermore, we can quantify this measure of the tracking error and it is at least

$$0 < \epsilon_0 T_{0_D}(1-k) \leq \left| \int_{t_2}^{t_2+\delta_0} (v_d(\tau) - v(\tau))\, d\tau \right| \tag{4.18}$$

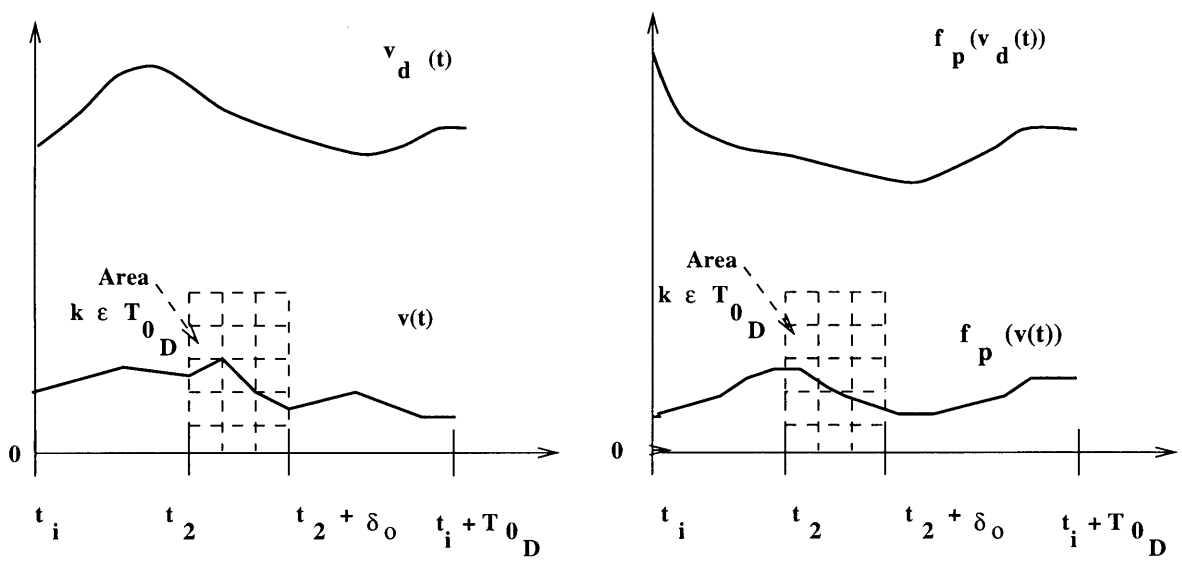

Figure 4-2: If the function $f_p(v)$ is 'small' over the subinterval in the sense that the area under the curve is less than $k\epsilon_0 T_{0_D}$ for $k < 1$, then property (4.1.1) implies that v must also be 'small' over the subinterval. Under assumed conditions that both the desired state element v_d, and the function, $f_p(v_d)$, are 'large' over subinterval in the sense that area under their respective curves over the subinterval is bigger than or equal $\epsilon_0 T_{0_D}$, a difference in the scalar function, $f_p(v) - f(v_d)$, over the subinterval implies a tracking error over the subinterval.

When r is a general unit vector, the situation is more complicated. Consider the

measure of the error in the regression vector that we are using,

$$\left| \int_{t_2}^{t_2+\delta_0} r_1(v - v_d) + \sum_{2}^{m} \left(f_p(v) - f_p(v_d)\right) d\tau \right| = \left| \int_{t_2}^{t_2+\delta_0} \left(\omega^T(v_d(\tau)) - \omega^T(v(\tau))\right) r d\tau \right|$$

In particular, consider the term in summation on the left-hand side of the above equation. The more the functions change over the interval, the more they contribute to this measure of the error in the regression vector, but not necessarily to the measure of the tracking error itself. For example, suppose one of the component functions is the signum function, $f_p(v) = sign(v)$, if v and v_d both have the same sign in the interval, then this term contributes nothing to the measure of the error in the regression vector. Suppose that one of the component functions is the signum function multiplied by a decaying exponential, $f_p(v) = sign(v)e^{-(v/v_0)^2}$, if the decay rate is large, the term on the left hand side of the above equation could be contributing a lot to the error in the regression vector even when the actual tracking error is small. Note that in the friction system the component functions behave like these functions because v_c appropriately small.

The amount that these functions can contribute to the error in the regression vector is bounded in the lemma by the term involving k_{eff}. So k_{eff} is essentially a measure of complexity in the regression vector. Functions which are highly nonlinear can increase the value of k_{eff}. Functions which are linear with a high slope can also increase the value of k_{eff}.

REMARK 4.1.1 It is advantageous for the designer to use the tightest bound as possible. A smaller value of k_{eff} implies a smaller level of p.e. is required to satisfy the conditions of the lemma.

REMARK 4.1.2 A reasonable question is why the restriction to first and third quadrant functions (or second and fourth quadrant functions which are similar)? Consider

Lipschitz or locally Lipschitz functions, which are functions satisfy a Lipschitz condition

$$||f_l(v) - f(v_d)|| \leq L||v - v_d|| \tag{4.19}$$

either globally or locally, respectively, for some $L > 0$ called the Lipschitz constant. Due to this scaling characteristic, a condition such as property (4.1.1), for a scalar Lipschitz function could be derived. For a vector of Lipschitz functions, however, it would be more complicated to derive a result such as lemma (4.1.1). We need a minimum measure of the tracking error. The measure that we need, a positive lower bound for

$$\left| \int_{t_2}^{t_2+\delta_0} (v_d(\tau) - v(\tau))\, d\tau \right| \tag{4.20}$$

is sign-dependent. Because the absolute value function is outside the integral in this measure, if the regression vector were composed of Lipschitz functions, an error in the regression vector could imply a measure of the tracking error that is zero, while we need a positive lower bound. Extensions to this type of regression vector may be possible by considering the location of zeros of the component functions.

4.1.3 A Property About the Conditions Required to Apply First and Third Quadrant Function Properties

In this section, we discuss the conditions (ii.), (iii.) and (v.) in lemma (4.1.1) because these become important in the stability theorem (4.4.1). Conditions (ii.) and (iii.) on the smallness of the p.e. subinterval, δ_0 and the scaling factor, k are also required in the stability theorem, and they become condition (iii.) in theorem (4.4.1). Additionally, the minimum measure of the tracking error, which is measured by condition

(v.) of lemma (4.1.1), is required by condition (ii.) in theorem (4.4.1) to be large compared to the disturbances in the system.

In this section, first we introduce an alternative notation to measure the minimum tracking error over a subinterval that will be useful in the proof of the main stability theorem in the upcoming sections.

Then we present a useful property about the conditions required in the main stability theorem on p.e. level, ϵ_0, p.e. subinterval width, δ_0, and scaling factor, k. This property says that if the conditions are satisfied for a given set of upper bounds on the state variables of interest, then the conditions are also satisfied for a set of lower upper bounds, and this is useful in the main stability proof in section (4.5) to argue that the required conditions are satisfied for every interval.

Condition (v.) in lemma (4.1.1) is a minimum measure of the tracking error. In the stability theorem (4.4.1), we will require that this minimum measure of the tracking error is large compared to the disturbances in the system.

$$\epsilon_0(1 - k - k_{eff}) > \gamma' \nu'_{max} \tag{4.21}$$

Define δ and δ_{eff} so that

$$\begin{aligned} 1 - k &= \frac{\gamma' \nu'_{max}}{\gamma' \nu'_{max} + \delta} \\ 1 - k - k_{eff} &= \frac{\gamma' \nu'_{max}}{\gamma' \nu'_{max} + \delta + \delta_{eff}} \end{aligned} \tag{4.22}$$

Then an equivalent representation of the requirement on the p.e. level in equation (4.21) is as follows

$$\epsilon_0 > \gamma' \nu'_{max} + \delta + \delta_{eff} \tag{4.23}$$

Next we prove a useful property is about the conditions on p.e. level, ϵ_0, p.e. subinterval width, δ_0, and scaling factor, k. Both these conditions depend on the upper bounds for the jth element of the state and desired state, v and v_d, respectively, and their derivatives. This property says that if these conditions are chosen for a set of upper bounds for these variables, then these conditions are also satisfied for a set of lower upper bounds for these variables.

Suppose we are given an a set of lower upper bounds,

$$\begin{aligned} v_{max_{I_{i_P}}} &\leq v_{max} \\ \dot{v}_{max_{I_{i_P}}} &\leq \dot{v}_{max} \end{aligned} \tag{4.24}$$

Define $k_{eff_{I_{i_P}}}$ as an upper bound for a measure of the differences between the component functions of the vector, $\omega(v(t))$, using the alternative upper bounds, as follows

$$\frac{1}{\epsilon_0 T_{0_D}} \left| \int_{t_2}^{t_2+\delta_0} \sum_{p=2}^{p=m} r_p \left(f_p(v(\tau)) - f_p(v_d(\tau)) \right) d\tau \right| \leq k_{eff_{I_{i_P}}} \tag{4.25}$$

for the following

$$\begin{aligned} v &\in \left[-v_{max_{I_{i_P}}} \quad -v_c \right] \cup \left[v_c \quad v_{max_{I_{i_P}}} \right] \\ v_d &\in \left[-v_{d_{max}} \quad -v_c \right] \cup \left[v_c \quad v_{d_{max}} \right] \end{aligned} \tag{4.26}$$

Also define $\delta_{eff_{I_{i_P}}}$

$$1 - k - k_{eff_{I_{i_P}}} = \frac{\gamma' \nu'_{max}}{\gamma' \nu'_{max} + \delta + \delta_{eff_{I_{i_P}}}} \tag{4.27}$$

Because we are defining $k_{eff_{I_{i_P}}}$ over a subset of the interval used to define k_{eff}, then

$$k_{eff_{I_{i_P}}} \leq k_{eff} \tag{4.28}$$

LEMMA 4.1.2 *Given a set a lower upper bounds*

$$\begin{aligned} v_{max_{I_{i_P}}} &\leq v_{max} \\ \dot{v}_{max_{I_{i_P}}} &\leq \dot{v}_{max} \end{aligned} \tag{4.29}$$

If the conditions on p.e. level, ϵ_0, p.e. subinterval width, δ_0, and scaling factor, k, hold as follows for the upper bounds v_{max} and $\dot{v}_{max}$,

(i.) The p.e. level, ϵ_0, is large enough so that

$$\epsilon_0 > \gamma' \nu'_{max} + \delta + \delta_{eff} > 0 \tag{4.30}$$

(ii.) The p.e. subinterval width, δ_0 is small enough so that

$$\delta_0 \quad < \quad min\left(\frac{\frac{\epsilon_0 T_{0_D}}{\delta_0} - v_c}{a_{d_{max}}}, \frac{\frac{k\epsilon_0 T_{0_D}}{\delta_0} - v_c}{\dot{v}_{max}}\right) \tag{4.31}$$

(iii.) The scaling factor, k, is small enough so that

$$0 < k < 1$$

$$max_{p=2,..m}\left(\frac{1}{f_{p_{min}}\begin{bmatrix} -v_{max} & -v_c \end{bmatrix} \cup \begin{bmatrix} v_c & v_{max} \end{bmatrix}} k\epsilon_0 T_{0_D}\right) \leq \delta_0 \tag{4.32}$$

Then these conditions also hold for the lower upper bounds, $v_{max_{I_{i_P}}}$ and $\dot{v}_{max_{I_{i_P}}}$, as follows

(i'.)

$$\epsilon_0 > \gamma' \nu'_{max} + \delta + \delta_{eff_{I_{i_P}}} \tag{4.33}$$

(ii'.)

$$\delta_0 \;\; < \;\; min \left(\frac{\frac{\epsilon_0 T_{0_D}}{\delta_0} - v_c}{a_{d_{max}}}, \frac{\frac{k\epsilon_0 T_{0_D}}{\delta_0} - v_c}{\dot{v}_{max_{I_{i_P}}}} \right) \tag{4.34}$$

(iii.')

$$0 < k < 1$$

$$max_{p=2,..m} \left(\frac{1}{f_p{}_{min} \left[\; -v_{max_{I_{i_P}}} \quad -v_c \; \right] \cup \left[\; v_c \quad v_{max_{I_{i_P}}} \; \right]} k\epsilon_0 T_{0_D} \right) \leq \delta_0 \tag{4.35}$$

The proof is in appendix (E).

4.2 Preliminaries: Properties About the 'Unforced' Error Model System

In this section, we establish properties pertaining to the study of the error model without the disturbance terms, $\nu + d(v)$, which we will call the 'unforced' error model system. In order to study the way the error model evolves with the disturbances, it will be useful to use the same techniques as in [16] to establish facts about the growth of the 'unforced' error model system.

Define the 'unforced' system in equation (4.36) below. Let previous definitions hold for associated system variables A, b P, and Q.

$$\begin{aligned} \dot{e}_u &= Ae_u - b\omega(v(t))^T\tilde{\theta}_u \\ \dot{\tilde{\theta}}_u &= \omega(v(t))b^T Pe_u \end{aligned} \tag{4.36}$$

where the velocity, $v(t)$, is a solution based on the 'forced' system in equation (3.17). Define

$$q_u = \begin{bmatrix} \sqrt{P}e_u & \tilde{\theta}_u \end{bmatrix}^T \tag{4.37}$$

Define $V_u(q(t), t)$ as a positive definite function of the system errors for the 'unforced' error model system.

$$V_u(q_u(t), t) = q_u^T q_u = e_u^T Pe_u + \tilde{\theta}_u^T \tilde{\theta}_u \tag{4.38}$$

Then the derivative along a trajectory is negative semidefinite.

$$\dot{V}_u(q_u(t), t) \leq -\lambda_{Q_{min}} ||e_u||^2 \tag{4.39}$$

This system is similar to the system studied in [16] (equation (4.36)), where it is shown if $\omega(v(t))$ is persistently exciting, which means that it is bounded as well as that it satisfies an integral p.e. condition on every interval, then the system in (4.36) is uniformly asymptotically stable. Notice that in our problem, however, we cannot assume that $\omega(v(t))$ is bounded because it is a function of $v(t)$ for the forced system and we have not yet proved that $v(t)$ for the forced system is bounded.

We can use the techniques in [16] for the unforced system to construct conditions so that if $\omega(v(t))$ satisfies a p.e. condition on a specified interval $I_{i_P} = \begin{bmatrix} t_i & t_i + T_{0_P} \end{bmatrix}$,

then on an interval, $I_{i_D} = \left[\begin{array}{cc} t_i & t_i + T_{0_D} \end{array} \right]$, the function, V_u, decreases such that

$$V_u(q_u(t_i + T_{0_D})) \leq cV_u(q_u(t_i)) \tag{4.40}$$

for some $0 < c < 1$. This is stated in the following property and used in the proof theorem (4.4.1) in section (4.5) to study the evolution of the 'forced' system.

It will be useful to work with the given p.e. level condition in terms of either T_{0_P} or T_{0_D}, so define ϵ_0' so that

$$\epsilon_0 T_{0_D} = \epsilon_0' T_{0_P} \tag{4.41}$$

PROPERTY 4.2.1 *Let the 'unforced' error model system and the function $V_u(q_u(t), t)$ be defined as above in equations (4.36), (4.37), (4.38). Given positive constants T_{0_P}, δ_0, k and ϵ_0'. If*

(i.) *$\omega(v(t))$ satisfies the following p.e. condition on an interval $\left[\begin{array}{cc} t_i & t_i + T_{0_P} \end{array} \right]$: There is a subinterval $\left[\begin{array}{cc} t_2 & t_2 + \delta_0 \end{array} \right]$*

$$\int_{t_2}^{t_2+\delta_0} \omega(v(\tau))^T r d\tau \geq k\epsilon_0' T_{0_P} \tag{4.42}$$

for any unit vector $r \in \Re^m$.

(ii.) *An upper bound on $||v(t)||$ is known for $t \in \left[\begin{array}{cc} t_i & t_i + T_{0_P} \end{array} \right]$*

$$||v(t)|| \leq v_{max_{I_{i_P}}} \text{ for } \qquad t \in \left[\begin{array}{cc} t_i & t_i + T_{0_P} \end{array} \right] \tag{4.43}$$

(iii.) *An initial bound on V_u such that*

$$||V_u(q_u(t_i), t_i)|| \leq \epsilon_1 \tag{4.44}$$

Then an interval $\left[\begin{array}{cc} t_i & t_i + T_{0_D} \end{array}\right]$ *can be constructed such that* V_u *decreases such that for some* $0 < c < 1$,

$$V_u(q_u(t_i + T_{0_D})) \leq cV_u(q_u(t_i)) \tag{4.45}$$

The proof of this property uses the results and method in [16] and is included in the appendix (F).

The size of the interval length, T_{0_D}, over which V_u decreases by at least the amount c is an important quantity. In the stability proof for the forced system in section (4.5), the presence of the Lipschitz disturbances require constraint on c and T_{0_D} as follows

$$c' = ce^{k_2 T_{0_D}} < 1 \tag{4.46}$$

where $k_2 \geq 0$ depends on the bound for the Lipschitz disturbances (see case 1 of the proof in section (4.5)). If there are no Lipschitz disturbances, then $k_2 = 0$.

For the stability proof of theorem (4.4.1), we must guarantee that values of T_{0_D} and c exist such that the constraint is satisfied given any level of disturbances. The existence of values that will satisfy the constraint is the subject of the following lemma.

LEMMA 4.2.1 *If the following p.e. assumption on the desired regression vector is satisfied*

$\omega(v_d)$ *satisfies a persistent excitation condition on any interval* $\left[\begin{array}{cc} t_i & t_i + T_{0_P} \end{array}\right]$, *i.e. on a subinterval* $\left[\begin{array}{cc} t_2 & t_2 + \delta_0 \end{array}\right]$

$$\left| \int_{t_2}^{t_2+\delta_0} \omega^T(v_d((\tau))rd\tau \right| \geq \epsilon_0' T_{0_P} \tag{4.47}$$

for any unit vector $r \in \Re^m$ *for* $\epsilon_0' > 0$. *Then for any* $k_2 \geq 0$, *then* c *and* T_{0_D} *exist*

such that

$$\begin{aligned} 0 < c &< 1 \\ V_u(q_u(t_i + T_{0_D})) &\leq cV_u(q_u(t_i)) \end{aligned} \tag{4.48}$$

subject to the constraint $c' = ce^{k_2 T_{0_D}} < 1$.

By corollary (4.5.1) this lemma is true because the 'unforced' error model system is uniformly asymptotically stable.

Calculating a value for T_{0_D} is of interest for our problem for several reasons. First, conditions (ii.) and (iii.) on the p.e. subinterval and scaling factor in lemma 4.1.1 are in terms of T_{0_D}. These requirements become condition (iii.) in theorem (4.4.1). Additionally, the requirement on p.e. level in condition (ii.) of theorem (4.4.1) also depends on T_{0_D} because the definition for k_{eff} in equation (4.15) depends on T_{0_D}. In addition to the conditions of theorem (4.4.1), the bounds on the error model solutions are a function of the interval width, T_{0_D}, as well as the c', as well as the level of disturbances in the system (see equations (4.80) and (4.103)) in the proof in section (4.5).

In order to compute the conditions of the stability theorem or the bounds on the error model solution, a control designer must know a either a value of T_{0_D} or an appropriate bound for T_{0_D}. Notice that when k_2 becomes zero, the constraint equation is automatically satisfied. For small enough levels of Lipschitz disturbances, k_2, the value of T_{0_D} can be computed and this is the subject of the next lemma.

LEMMA 4.2.2 *For a small Lipschitz disturbances,* k_2^*, *defined in the lemma proof, values for* c *and* T_{0_D}, *which satisfy the conditions of property (4.2.1) and the constraint in equation (4.46), can be computed.*

The proof is in appendix (F).

4.3 Preliminaries: Properties Bounding the Error Model State and the Function, V, on an Interval

Most of the properties developed in the preliminary sections of this chapter have required a bound on the state variables over a time interval. In this section, we develop these bounds as well as a growth rate bound on the positive definite function of the errors, V. The first property is the an upper bound maximum growth of the function V on a closed time interval, and it will be used in the main stability proof to compare the maximum increase of V on a time interval to the minimum decrease of V on a time interval. It will also be used to derive the second property, which are the upper bounds for the state on a closed interval in terms of the value of the function V at the beginning of the interval.

4.3.1 A Property About the Maximum Increase in V on an Interval

Property 4.3.1 *Define $V(q(t))$ as the positive definite function of tracking and parameter errors for the error model system in (3.17) as*

$$V(q(t)) \;=\; q^T q = e^T P e + \tilde{\theta}^T \tilde{\theta} \tag{4.49}$$

where $P = P^T > 0$ is the solution to the Lyapunov equation for $Q > 0$ and $Q = -(PA + A^T P)$ and $q \in \Re^6$ is defined as $q^T = \begin{bmatrix} \sqrt{P}e^T & \tilde{\theta}^T \end{bmatrix}$ Then the derivative of

V along trajectories of the error model system is

$$\dot{V} \leq -\lambda'_Q||e||^2 + 2\lambda_{P_{max}}\nu'_{max}||e|| \tag{4.50}$$

The maximum increase in V over an time interval $I_{int} = \begin{bmatrix} t_i & t_i + T_{int} \end{bmatrix}$ is

$$V(q(t_i + T_{int})) - V(q(t_i)) = \frac{\gamma'^2\nu'^2_{max}}{4}\lambda'_Q T_{int} \tag{4.51}$$

where

$$\gamma' = \frac{2\lambda_{P_{max}}}{\lambda'_Q} \tag{4.52}$$

Because the derivative of V has a maximum positive value, for a time interval of fixed length, the function V can increase by a limited amount. The details are of the proof of this property are presented appendix (G).

4.3.2 A Property About Upper Bounds for States and State Derivatives on an Interval

The regression vector is a function of the state element, v. The following property contains bounds for this state element as well as its derivative and the regression vector on a time interval in terms of the value of the function V at the beginning of a time interval.

Property 4.3.2 *Let $I_{int} = [t_i + T_{int}]$. Let v be the jth element of the state vector of the error model system defined in (3.17). The maximum magnitudes of the state element $v(t)$ and derivative of state element $\dot{v}(t)$ for $t \in I_{int}$ exist. Additionally, the*

maximum of $||\omega(v(t))||$ *for* $t \in I_{int}$ *exists. If we define,*

$$v_{max_{I_{int}}} = max(|v(t)|) \qquad for\ t \in I_{int} \tag{4.53}$$

$$\dot{v}_{max_{I_{int}}} = max(|\dot{v}(t)|) \qquad for\ t \in I_{int} \tag{4.54}$$

$$\tag{4.55}$$

then an upper bound for $v_{max_{I_{int}}}$ *is*

$$v_{max_{I_{int}}} \leq \frac{1}{\lambda_{P_{min}}}\sqrt{V(q(t_i)) + \frac{\gamma'^2\nu'^2_{max}}{4}\lambda'_Q T_{int}} + v_{d_{max}} \tag{4.56}$$

and we can denote an upper bound for $||\omega(v(t)||$ *as*

$$||\omega(v(t))|| \leq \omega_{max_{I_{int}}} \tag{4.57}$$

And an upper bound for $\dot{v}_{max_{I_{int}}}$ *is*

$$\begin{aligned}\dot{v}_{max_{I_{int}}} \leq\ & a_{d_{max}} \\ & + (A_{max} + b_{max}d_{max})\frac{1}{\lambda_{P_{min}}}\sqrt{V(q(t_i)) + \frac{\gamma'^2\nu'^2_{max}}{4}\lambda'_Q T_{int}} \\ & + b_{max}\omega_{max_{I_{int}}}\sqrt{V(q(t_i)) + \frac{\gamma'^2\nu'^2_{max}}{4}\lambda'_Q T_{int}} \\ & + \nu'_{max}\end{aligned} \tag{4.58}$$

On an interval, the function, V, can only grow by a limited amount. The fact that V is defined in terms of the tracking and parameter errors implies that bounds for these errors may be obtained in terms of the bounds for the function, V. Using the bounds for the state on an interval, then bounds for the regression vector on the interval can be obtained. The dynamic error model equation can be used to determine bounds for the state derivative on the interval. Details are in appendix (G).

4.4 Robust Adaptive Approach - Use of P.E. Inputs

In this section, we state the main stability theorem, which is proved in the next section. The use of sufficient persistent excitation in the input will prevent the instability mechanisms presented in the previous chapter in which the parameter estimates became unbounded at low tracking errors.

In the theorem statement below, it is assumed that the desired input trajectory satisfies a p.e. condition on every interval. Then three additional conditions are required. First, condition (i.), is a bandwidth constraint. It requires that the linear portion of the controller is fast enough compared to the level of Lipschitz disturbances in the system. Second, condition (ii.) requires that the level of p.e. in the input is large enough compared to the level of disturbances in the system, represented by $\gamma'\nu'_{max}$, and an additional term, δ_{eff}, which depends on the features of regression vector. Finally, condition (iii.) is a condition on the smallness of the p.e. subinterval, δ_0 and the scaling factor, k. We need this condition to satisfy the assumptions of lemma (4.1.1).

We will address issues related to the computability of these conditions in the final section of this chapter.

Theorem 4.4.1 *Given the error model system in section (3.3.2),*

$$\begin{aligned} \dot{e} &= Ae - b\omega^T(v)\tilde{\theta} + b(\nu + d(x)) \\ \dot{\tilde{\theta}} &= \omega(v)b^T Pe \end{aligned} \tag{4.59}$$

where A is a stable matrix, $\tilde{\theta} \in \Re^m$, is a vector of parameter errors and $e = x_d - x$ is the tracking error vector for a dynamic system in which $x \in \Re^n$ and $x_d \in \Re^n$ are the state vector and the desired state vector, respectively. And v and v_d denote the jth

element of the state and desired state vectors respectively.

The regression vector, $\omega(v) : \Re^1 \rightarrow \Re^m$*, is a vector function in which* $f_1(v(t)) = v(t)$ *and the other elements,* $f_p(v(t))$ *for* $p = 2, ..m$*, are first and third quadrant continuous functions of the* j*th element of the state,* v*, i.e.*

$$\omega(v(t)) = \left[\begin{array}{cccc} f_1(v(t)) & \cdot & \cdot & \cdot \quad f_m(v(t)) \end{array} \right]^T \tag{4.60}$$

The disturbance term, $\nu + d(x)$*, can be bounded such that*

$$|\nu + d(x)| \quad \leq \quad \nu'_{max} + d_{max}||e|| \tag{4.61}$$

Assume the following p.e. condition on the desired input trajectory,

$\omega(v_d)$ *satisfies a persistent excitation condition on any interval* $\left[\begin{array}{cc} t_i & t_i + T_{0_P} \end{array} \right]$*, i.e. on a subinterval* $\left[\begin{array}{cc} t_2 & t_2 + \delta_0 \end{array} \right]$*,*

$$\left| \int_{t_2}^{t_2+\delta_0} \omega^T(v_d((\tau))rd\tau \right| \geq \epsilon'_0 T_{0_P} \tag{4.62}$$

for any unit vector $r \in \Re^m$*.*

Also assume bounds on the initial errors and on the desired trajectory as in equations (4.69) and (4.71), respectively, which are defined in the notation below.

If the following conditions,

(i.) A*,* P *and* Q *are chosen so that* $\lambda'_Q > 0$*.*

(ii.) The p.e. degree, ϵ_0*, is large enough so that*

$$\epsilon_0 > \gamma' \nu'_{max} + \delta + \delta_{eff} > 0 \tag{4.63}$$

(iii.) The p.e. subinterval width, δ_0, and a scaling factor, $0 < k < 1$, are small enough to satisfy the following

$$
\begin{aligned}
0 &< k < 1 \\
0 &< max_{p=2,..m}\left(\frac{1}{f_{p_{min}}\left[\begin{array}{cc} -v_{max} & -v_c \end{array}\right]\cup\left[\begin{array}{cc} v_c & v_{max} \end{array}\right]} k\epsilon_0 T_{0_D}\right) \leq \delta_0 \\
\delta_0 &< min\left(\frac{\frac{\epsilon_0 T_{0_D}}{\delta_0} - v_c}{a_{d_{max}}}, \frac{\frac{k\epsilon_0 T_{0_D}}{\delta_0} - v_c}{\dot{v}_{max}}\right)
\end{aligned}
\tag{4.64}
$$

hold, where the notation has been defined in the preliminaries and remaining notations are defined in the proof. Then, the error model system has bounded solutions.

NOTATION

$$V(q(t)) = e^T P e + \tilde{\theta}^T \tilde{\theta} \tag{4.65}$$

where $q^T = \left[\begin{array}{cc} \sqrt{P}e^T & \tilde{\theta}^T \end{array}\right]$, and $P = P^T > 0$ is the associated positive definite matrix satisfying the Lyapunov equation for $Q = Q^T = -(PA + A^T P)$.

$$\lambda_{P_{min}} e^T e \leq e^T P e \leq \lambda_{P_{max}} e^T e \tag{4.66}$$

We derived in chapter 3 that the derivative of V for this error model satisfies the following,

$$\dot{V} \leq -\lambda'_Q ||e||^2 + 2\lambda_{P_{max}} \nu'_{max} ||e|| \tag{4.67}$$

Define $\gamma' = \frac{2\lambda_{P_{max}}}{\lambda'_Q}$, A_{max} as the maximum eigenvalue of A.

Let

$$
\begin{aligned}
I_{i_P} &= \begin{bmatrix} t_i & t_i + T_{0_P} \end{bmatrix} \\
I_{i_D} &= \begin{bmatrix} t_i & t_i + T_{0_D} \end{bmatrix}
\end{aligned} \tag{4.68}
$$

And let $T_{0_P} = T(\epsilon_1, \delta_s)$, be defined as in the proof of property (4.2.1). This is so that the interval, I_{i_D}, on which we will argue that V decreases is at least as large as the p.e. interval, I_{i_P}. Let $0 < c < 1$, and T_{0_D} be a decrease level and an interval width, respectively, that satisfies property (4.2.1) such that the positive definite function of the errors for the 'unforced' system decreases by at least c over interval I_{i_D}. Furthermore, let c and T_{0_D} be such that the constraint in equation (4.78) later in the proof is satisfied. These values exist by lemma (4.2.1).

Let an initial bound on the tracking and parameter errors be such that

$$V(q(t_0)) \leq \epsilon_1 \tag{4.69}$$

Let the bounds on the jth element of the desired trajectory and its derivative be denoted

$$v_{d_{max}} = max(v_d(t)) \qquad \text{for } t \geq 0 \tag{4.70}$$

$$a_{d_{max}} = max(\dot{v}_d(t)) \qquad \text{for } t \geq 0 \tag{4.71}$$

4.5 Proof of Theorem

Before proceeding, we discuss strategy briefly here and outline the steps in the proof. The strategy is to make the positive definite function of the system errors, V, decrease more than it increases on every interval.

First we establish conditions under which V will decrease on the ith interval I_{i_D}. As in [17], we consider two possible cases that encompass all possibilities. The first case is if regression vector $\omega(v)$ satisfies a specified p.e. condition on the interval $\begin{bmatrix} t_i & t_i + T_{0_P} \end{bmatrix}$. In this case, the results of [16] indicate the useful property that solutions of the 'unforced' error model system, which is the system without the disturbance term, decrease over an interval $\begin{bmatrix} t_i & t_i + T_{0_D} \end{bmatrix}$. We analyze the additional effect of the disturbance terms and are able to conclude that if the initial condition is large enough V decreases on the interval $\begin{bmatrix} t_i & t_i + T_{0_D} \end{bmatrix}$. In this case when the regression vector satisfies a p.e. condition, a difference in our problem and that of [17] is the fact that the disturbance has an additional Lipschitz bounded term, $d(x)$.

The second case is if the regression vector $\omega(v)$ does not satisfy the specified p.e. condition on the interval $\begin{bmatrix} t_i & t_i + T_{0_P} \end{bmatrix}$. Under the assumption given in the theorem, the desired regression vector, $\omega(v_d)$, does satisfy a larger p.e. condition. Because there is an error in the regression vector, then if the additional conditions of lemma (4.1.1) apply, we can exploit the first and third quadrant properties of the regression vector and establish a measure of the tracking error. This measure of the tracking error enables us to find the minimum decrease of V over the p.e. subinterval. By ensuring that this decrease is larger than the maximum increase of V over the rest of the interval of I_{i_D}, we can ensure conditions by which V must decrease over the given interval I_{i_D}. Note however, that the conditions of the lemma as well as the measure of the tracking error are both in terms of bounds for v and $\dot{v}$ on the interval.

By considering these two possible cases on the ith interval, we can conclude under certain conditions, which are interval-dependent, then V decreases more than it increases on the interval.

The next step is to ensure that the required conditions are met on every interval. Assuming conditions that will satisfy the requirements on the first interval, we proceed by induction to show that the conditions chosen will also satisfy the requirements for

every subsequent interval, ensuring boundedness of the solutions. An algorithm in the next section is presented to show that conditions can be chosen to satisfy the conditions for the first interval if the Lipschitz disturbances are small enough.

Next we proceed to the proof of the theorem.

4.5.1 Establish Sufficient Conditions for V to Decrease on ith Interval I_{i_D}

Case 1: $\omega(v)$ satisfies a p.e. condition

Suppose there is a subinterval $\left[\begin{array}{cc} t_2 & t_2+\delta_0 \end{array}\right]$ of $\left[\begin{array}{cc} t_i & t_i+T_{0_P} \end{array}\right]$, such that

$$\left| \int_{t_2}^{t_2+\delta_0} \omega^T(v(\tau))r d\tau \right| \geq k\epsilon_0 T_{0_D} \tag{4.72}$$

for any unit vector $r \in \Re^m$. This case, in which the regression vector $\omega(v)$ satisfies the specified p.e. condition on interval I_{i_P}, is called Case 1. Consider the error model system given in the theorem in equation (4.59) as a forced system, with the disturbance, $\nu + d(x)$ acting as a forcing input. In the preliminaries, we studied the error model system without the effect of these disturbances. We can apply the Bellman-Gronwall inequality to obtain an upper bound for $V(q(t_i + T_{0_D}))$. Let $q_u(t)$ denote the solution to the unforced system, then $q(t)$, the solution to the forced system, satisfies the following inequality.

$$q(t) \;\leq\; q_u(t) + \int_{t_i}^{t_i+t} \sqrt{P}b(\nu + d(v(\tau)))d\tau \tag{4.73}$$

$$||q(t_i + T_{0_D})|| \leq ||q_u(t)|| + \int_{t_i}^{t_i+T_{0_D}} \lambda_{P_{max}} b_{max}(\nu'_{max} + d_{max}||q(\tau)||)d\tau \tag{4.74}$$

We apply the Bellman-Gronwall lemma and obtain

$$||q(t_i + T_{0_D})|| \leq (c||q(t_i)|| + \lambda_{P_{max}} b_{max} \nu'_{max} T_{0_D})\, e^{\lambda_{P_{max}} b_{max} d_{max} T_{0_D}} \tag{4.75}$$

Define

$$k_1 = \lambda_{P_{max}} b_{max} T_{0_D} e^{k_2 T_{0_D}} \tag{4.76}$$

$$k_2 = \lambda_{P_{max}} b_{max} d_{max} \tag{4.77}$$

$$c' = c e^{k_2 T_{0_D}} \tag{4.78}$$

By lemma (4.2.1), we can choose c small enough so that $c' < 1$,

$$||q(t_i + T_{0_D})|| \leq c'||q(t_i)|| + k_1 \nu'_{max} \tag{4.79}$$

Define c'_1 as

$$c'_1 = k_1 \nu'_{max}/(1 - c') \tag{4.80}$$

As long as $\epsilon_1 > c_1'^2$ then

$$V(q(t_i + T_{0_D})) < V(q(t_i)) \;\text{ if }\; V(q(t_i)) > c_1'^2 \tag{4.81}$$

CASE 2: $\omega(v)$ DOES NOT SATISFY A P.E. CONDITION

Suppose on any subinterval $\begin{bmatrix} t_2 & t_2 + \delta_0 \end{bmatrix}$ of $\begin{bmatrix} t_i & t_i + T_{0_P} \end{bmatrix}$, there is some unit vector, $r \in \Re^m$, such that

$$\left| \int_{t_2}^{t_2+\delta_0} \omega^T(v(\tau))r d\tau \right| < k\epsilon_0 T_{0_D} \tag{4.82}$$

This case, in which the regression vector $\omega(v)$ does not satisfy the p.e. condition on the interval I_{i_P} is called Case 2.

Under the assumption given in the theorem, the desired regression vector, $\omega(v_d)$, does satisfy a larger p.e. condition. We proceed in four steps to establish conditions under which V will decrease on the interval I_{i_D}.

STEP 1: ESTABLISH CONDITIONS UNDER WHICH WE CAN APPLY LEMMA (4.1.1) TO OBTAIN A MEASURE OF THE TRACKING ERROR OVER THE SUBINTERVAL $\left[\begin{array}{cc} t_2 & t_2+\delta_0 \end{array}\right]$

Let upper bounds for the jth state element, v, and its derivative be denoted as follows

$$|v(t)| \leq v_{max_{I_{i_P}}} \text{ for } t \in I_{i_P} \tag{4.83}$$

$$|\dot{v}(t)| \leq \dot{v}_{max_{I_{i_P}}} \text{ for } t \in I_{i_P} \tag{4.84}$$

The assumptions of lemma (4.1.1) will be satisfied, if the following condition holds for the interval I_{i_P},

$$0 < k < 1$$

$$max_{p=2,..m}\left(\frac{1}{f_{p_{min}\left[\begin{array}{cc} -v_{max_{I_{i_P}}} & -v_c \end{array}\right]\cup\left[\begin{array}{cc} v_c & v_{max_{I_{i_P}}} \end{array}\right]}} k\epsilon_0 T_{0_D}\right) \leq \delta_0$$

$$\delta_0 < min\left(\frac{\frac{\epsilon_0 T_{0_D}}{\delta_0} - v_c}{a_{d_{max}}}, \frac{\frac{k\epsilon_0 T_{0_D}}{\delta_0} - v_c}{\dot{v}_{max_{I_{i_P}}}}\right) \tag{4.85}$$

If the above conditions hold, then by lemma (4.1.1) a measure of the tracking error on the subinterval, $\left[\begin{array}{cc} t_2 & t_2+\delta_0 \end{array}\right]$, is

$$0 < \epsilon_0 T_{0_D}\left(1 - k - k_{eff_{I_{i_P}}}\right) \leq \left|\int_{t_2}^{t_2+\delta_0} (v_d(\tau) - v(\tau))d\tau\right| \tag{4.86}$$

where $k_{eff_{I_{i_P}}}$ was defined in the preliminaries in equation (4.25) as an upper bound for the following

$$\frac{1}{\epsilon_0 T_{0_D}}\left|\int_{t_2}^{t_2+\delta_0}\sum_{p=2}^{p=m} r_p\left(f_p(v(\tau)) - f_p(v_d(\tau))\right)d\tau\right| \leq k_{eff_{I_{i_P}}} \tag{4.87}$$

The tracking error on the subinterval is proportional to the level of p.e., ϵ_0, in the input trajectory.

Notice that the conditions under which we can apply the lemma as well as the measure of the tracking error are interval-dependent because they depend on the bounds on the interval of the jth state element and its derivative, $v_{max_{I_{i_P}}}$ and $\dot{v}_{max_{I_{i_P}}}$. They also depend on the interval width, T_{0_D}, and the p.e. level, ϵ_0.

STEP 2: USING THE MEASURE OF TRACKING ERROR ON THE SUBINTERVAL $\left[\begin{array}{cc} t_2 & t_2+\delta_0 \end{array}\right]$, CALCULATE THE MINIMUM DECREASE OF V ON THE SUBINTERVAL

The derivative of V along system trajectories satisfies the following,

$$\dot{V} \leq -\lambda'_Q||e||^2 + 2\lambda_{P_{max}}\nu'_{max}||e|| \tag{4.88}$$

The minimum decrease in V over $\begin{bmatrix} t_2 & t_2+\delta_0 \end{bmatrix}$ is

$$V(q(t_2)) - V(q(t_2+\delta_0)) \geq \lambda'_Q \int_{t_2}^{t_2+\delta_0} ||e(\tau)||^2 d\tau - 2\lambda_{P_{max}}\nu'_{max} \int_{t_2}^{t_2+\delta_0} ||e(\tau)||d\tau \quad (4.89)$$

By the Cauchy-Schwartz inequality, we have

$$V(q(t_2)) - V(q(t_2+\delta_0)) \geq$$

$$\frac{\lambda'_Q}{\delta_0} \int_{t_2}^{t_2+\delta_0} ||e(\tau)||d\tau \left(\int_{t_2}^{t_2+\delta_0} ||e(\tau)||d\tau - 2\frac{\lambda_{P_{max}}}{\lambda'_Q}\nu'_{max}\delta_0 \right) \quad (4.90)$$

And by equation (4.86), the minimum decrease of V on the subinterval is

$$V(q(t_2)) - V(q(t_2+\delta_0)) \geq$$

$$\frac{\lambda'_Q}{\delta_0}(1-k-k_{eff_{I_{i_P}}})\epsilon_0 T_{0_D} \left((1-k-k_{eff_{I_{i_P}}})\epsilon_0 T_{0_D} - 2\frac{\lambda_{P_{max}}}{\lambda'_Q}\nu'_{max}\delta_0 \right) \quad (4.91)$$

Notice that the tracking error over the subinterval and hence the minimum decrease in V on the subinterval is larger when the level of p.e. in the input trajectory, ϵ_0, is larger.

STEP 3: FIND THE MAXIMUM INCREASE OF V OVER THE REST OF INTERVAL I_{i_D}

Using property (4.3.1) derived in the preliminaries, the maximum increase on the rest of the interval I_{i_D} is

$$V(q(t_i+T_{0_D})) - V(q(t_i)) \;=\; \frac{\gamma'^2\nu'^2_{max}}{4}\lambda'_Q(T_{0_D}-\delta_0) \quad (4.92)$$

STEP 4: SPECIFY CONDITIONS ON THE P.E. LEVEL SO THAT V DECREASES MORE THAN IT INCREASE ON I_{i_D}

Define $\delta_{eff_{I_{i_P}}}$ so that

$$1 - k - k_{eff_{I_{i_P}}} = \frac{\gamma' \nu'_{max}}{\gamma' \nu'_{max} + \delta + \delta_{eff_{I_{i_P}}}} \tag{4.93}$$

In addition to the other conditions established in this case 2 condition, if the p.e. level, ϵ_0 satisfies the following,

$$\epsilon_0 > \gamma' \nu'_{max} + \delta + \delta_{eff_{I_{i_P}}} \tag{4.94}$$

Then the minimum decrease in V over $\begin{bmatrix} t_2 & t_2 + \delta_0 \end{bmatrix}$ will be

$$V(q(t_2)) - V(q(t_2 + \delta_0)) \;\geq\; \lambda'_Q \frac{T_{0_D}}{\delta_0} (\gamma' \nu'_{max})^2 (T_{0_D} - \delta_0) \tag{4.95}$$

which is greater than the maximum increase in V over the time period $T_{0_D} - \delta_0$ in equation(4.92).

Summarize Conditions to Make V Decrease on Interval I_{i_D}

On interval subinterval I_{i_P} of I_{i_D}, either Case 1 applies and $\omega(v)$ satisfies the p.e. condition in equation (4.72) or Case 2 applies and $\omega(v)$ does not satisfy the p.e. condition in equation (4.72).

If case 1. applies, then we conclude that if $V(q(t_i)) > c_1'^2$, then $V(q(t_i + T_{0_D})) < V(q(t_i))$, i.e. V decreases on interval I_{i_D}. If $V(q(t_i)) \leq c_1'^2$, then using the maximum increase of V over a time interval T_{0_D}, we obtain, $V(q(t_i + T_{0_D})) \leq c_1'^2 + (1/4)(\gamma' \nu'_{max})^2 \lambda'_Q T_{0_D}$.

If case 2. applies and the condition on p.e. level in equation (4.94) holds and the conditions on p.e. subinterval width, δ_0 and scaling factor, k in equation (4.85) hold, then V decreases on I_{i_D}.

Since we have examined the only two possibilities for interval I_{i_D}, we conclude that if the conditions in equations (4.94) and (4.85) hold for interval I_{i_P}, then if $V(q(t_i)) > c_1'^2$, then $V(q(t_i+T_{0_D})) < V(q(t_i))$. If $V(q(t_i)) \leq c_1'^2$, then using the maximum increase of V over a time interval T_{0_D}, we obtain, $V(q(t_i+T_{0_D})) \leq c_1'^2 + (1/4)(\gamma'\nu'_{max})^2\lambda'_Q T_{0_D}$.

4.5.2 Choose Conditions to Make V Decrease First Interval and on Every Subsequent Intervals, Ensuring Bounded Solutions

Define

$$\epsilon_1' = max(\epsilon_1, c_1'^2 + (1/4)(\gamma'\nu'_{max})^2\lambda'_Q T_{0_D}) \tag{4.96}$$

Define

$$\begin{aligned} v_{max} &= \frac{1}{\lambda_{P_{min}}}\sqrt{\epsilon_1' + \frac{\gamma'^2\nu'^2_{max}}{4}\lambda'_Q T_{0_P}} + v_{d_{max}} \\ \dot{v}_{max} &= a_{d_{max}} \\ &\quad + (A_{max} + b_{max}d_{max})\frac{1}{\lambda_{P_{min}}}\sqrt{\epsilon_1' + \frac{\gamma'^2\nu'^2_{max}}{4}\lambda'_Q T_{0_P}} \\ &\quad + b_{max}\omega_{max_{I_{1_P}}}\sqrt{\epsilon_1' + \frac{\gamma'^2\nu'^2_{max}}{4}\lambda'_Q T_{0_P}} \\ &\quad + \nu'_{max} \end{aligned} \tag{4.97}$$

where the bound on the regression vector, $\omega_{max_{I_{i_P}}} = max(||\omega(v(t))||)$ exists because it is a continuous function defined on the compact set $t \in I_{i_P}$ for which $v \in \left[\ -v_{max}, v_{max}\ \right]$.

Assume that conditions (ii.) and (iii.) in the theorem statement hold. From condition

(ii.) The p.e. level, ϵ_0, satisfies the following,

$$\epsilon_0 > \gamma' \nu'_{max} + \delta + \delta_{eff} > 0 \tag{4.98}$$

where δ_{eff} is defined using the definitions in equations (4.87) and (4.22). And from condition (iii.) the p.e. subinterval, δ_0 and the scaling factor, k, satisfy the following

$$0 < k < 1$$

$$max_{p=2,..m} \left(\frac{1}{f_{p_{min}} \begin{bmatrix} -v_{max} & -v_c \end{bmatrix} \cup \begin{bmatrix} v_c & v_{max} \end{bmatrix}} k\epsilon_0 T_{0_D} \right) \leq \delta_0$$

$$\delta_0 < min \left(\frac{\frac{\epsilon_0 T_{0_D}}{\delta_0} - v_c}{a_{d_{max}}}, \frac{\frac{k\epsilon_0 T_{0_D}}{\delta_0} - v_c}{\dot{v}_{max}} \right) \tag{4.99}$$

Because $V(q(t_0)) \leq \epsilon_1 \leq \epsilon'_1$, by applying the results of property (4.3.2). in which bounds where determined for the state and derivative in terms of the function V, we have

$$\begin{aligned} v_{max_{I_{1_P}}} &\leq v_{max} \\ \dot{v}_{max_{I_{1_P}}} &\leq \dot{v}_{max} \end{aligned} \tag{4.100}$$

We apply lemma (4.1.2), which says that if the conditions hold for one set of upper bounds they also hold for a set of lower upper bounds; and we conclude that the conditions in equations (4.94) and (4.85) hold for interval I_{1_P}. By the results in the previous section, we can conclude for interval I_{1_D}, if $V(q(t_0)) > c_1'^2$, then $V(q(t_0 + T_{0_D})) < V(q(t_0))$. If $V(q(t_0)) \leq c_1'^2$, then $V(q(t_0 + T_{0_D})) \leq c_1'^2 + (1/4)(\gamma' \nu'_{max})^2 \lambda'_Q T_{0_D}$.

Now we proceed by induction to show that we can conclude a similar result for every

subsequent interval. Suppose that

$$
\begin{aligned}
v_{max_{I_{i_P}}} &\leq v_{max} \\
\dot{v}_{max_{I_{i_P}}} &\leq \dot{v}_{max}
\end{aligned}
\tag{4.101}
$$

Then lemma (4.1.2) again applies and we conclude that the conditions in equations (4.94) and (4.85) hold for interval I_{i_P}. Therefore for interval I_{i_D}, if $V(q(t_i)) > c_1'^2$, then $V(q(t_i + T_{0_D})) < V(q(t_i))$. If $V(q(t_i)) \leq c_1'^2$, then $V(q(t_i + T_{0_D})) \leq c_1'^2 + (1/4)(\gamma'\nu'_{max})^2\lambda'_Q T_{0_D}$

Furthermore because $V(q(t_i + T_{0_D})) \leq \epsilon'_1$,

$$
\begin{aligned}
v_{max_{I_{i+1_P}}} &\leq v_{max} \\
\dot{v}_{max_{I_{i+1_P}}} &\leq \dot{v}_{max}
\end{aligned}
\tag{4.102}
$$

Therefore, for $t \geq t_0$,

$$
V(q(t)) \leq c_1'^2 + (1/4)(\gamma'\nu'_{max})^2\lambda'_Q T_{0_D} \qquad \text{for } t \geq t_0 \tag{4.103}
$$

END OF PROOF

COROLLARY 4.5.1 *Given the p.e. assumption on the desired regression vector in theorem (4.4.1) equation, (4.62), if there are no disturbances in the system,* $\nu + d(v) = 0$, *then the error model defined in equation (4.59), which is the 'unforced' error model, is uniformly asymptotically stable.*

PROOF OF COROLLARY

If the disturbances are zero, in the analysis above, then $c'_1 = 0$. Uniform asymptotic stability follows.

Note that because in this case $k_2 = 0$, then the pair $0 < c < 1$ and T_{0_D} can be chosen to satisfy property (4.2.1). This result does not require lemma (4.2.2). Additionally, in case 2, since V does not increase at all, any amount of decrease in V will suffice and this happens as long as $\epsilon_0 > 0$.

REMARK 4.5.1 THE THEOREM CONDITION ON BANDWIDTH AND LIPSCHITZ DISTURBANCE LEVEL The first condition in the theorem, which mandates that $\lambda'_Q > 0$ is essentially a minimum bandwidth constraint. For a given level of d_{max}, the Lipschitz disturbance bound, the constraints on A, P and Q are equivalent to a bandwidth constraint for the linear portion of the adaptive compensator system. Note that because friction compensation was motivated by achieving performance with lower bandwidth control, this condition has direct impact on how well this goal can be achieved.

REMARK 4.5.2 THE THEOREM CONDITION ON INPUT P.E. DEGREE The second condition in the theorem requires that the input degree of p.e. in the system, ϵ_0 is large enough compared to the sum, $\gamma'\nu'_{max} + \delta + \delta_{eff}$. This term increases if the level of disturbances in the system is higher and it also depends on characteristics of the functions which make up the regression vector.

REMARK 4.5.3 THE THEOREM CONDITION ON P.E. SUBINTERVAL WIDTH, δ_0, AND SCALING FACTOR, k. The third condition of the theorem is due to the fact that we wanted to apply lemma (4.1.1) so that an error in the regression vector and over the subinterval implies a tracking error over the subinterval. In order to do this, we chose the p.e. subinterval width, δ_0 small enough so that v and v_d would not change sign in the subinterval $\begin{bmatrix} t_2 & t_2 + \delta_0 \end{bmatrix}$. We also chose scaling factor, k, small enough so the the integral of the signal, v, and the integral of the first and third quadrant function of the signal both have a similar magnitude.

REMARK 4.5.4 RECOVERY OF RESULT FOR LINEAR ADAPTIVE PROBLEM WITH BOUNDED DISTURBANCES Suppose the regression vector consisted of just the linear

part $\omega(v) = v$, then $\delta_{eff} = 0$ and the second condition in the theorem is no longer required, making δ just an arbitrary positive constant. We recover the result of [17].

REMARK 4.5.5 EXTENDING RESULT TO MORE GENERAL ERROR MODELS Note that in [17] the regression vector could also be a linear function of other state variables. It would be interesting to try to extend our result similarly and to let the regression vector contain terms that are functions of the other state variables. This is not a trivial problem, however, because the nature of above proof was to let a measure of the regression vector imply a measure of an element of the tracking error vector. When we let the regression vector be a function of other variables, the analysis method must be adjusted or changed to accommodate this fact.

Similarly, in the friction problem, our basic result holds for a unitary or a known mass. If we wanted to extend the result to make the mass an unknown parameter, it is not hard to show that the regression vector would contain a term related to the acceleration of the desired trajectory, $\ddot{x}_d$. The analysis is harder for this case.

4.6 COMPUTING THEOREM CONDITIONS AND BOUNDS FOR THE FRICTION SYSTEM

In this section, we discuss the conditions in theorem (4.4.1). Because conditions (ii.) and (iii.) depend on each other, it is not obvious how to choose a p.e. level, ϵ_0, p.e. subinterval width, δ_0, and scaling factor, k, that will meet the requirements of the stability theorem. In this section, we show how choices can be made for these variables that will satisfy conditions (ii.) and (iii.) of theorem (4.4.1).

Consider condition (ii.) in theorem (4.4.1), which is a requirement on the p.e. level, ϵ_0, and as discussed in section (4.1.3), the requirement on the p.e. level can be

equivalently written as

$$\epsilon_0(1 - k - k_{eff}) > \gamma' \nu'_{max} \tag{4.104}$$

This shows that the p.e. level, ϵ_0, depends on the scaling factor, k, which is part of condition (iii.)

Next consider condition (iii.) in theorem (4.4.1). These are conditions on the smallness of the p.e. subinterval width, δ_0, and the scaling factor, k. However, they also depend on the p.e. level, ϵ_0. Additionally, they are also implicit conditions. The upper bound condition on the p.e. subinterval width, δ_0, depends on the scaling factor, k. And the condition on the smallness of the scaling factor, k, depends on the p.e subinterval width, δ_0. Furthermore, the requirements in condition (iii.) depend on the interval, T_{0_D}, which is the length of the interval, I_{i_D}. Issues about the interdependence of these conditions are resolved in the following theorem.

THEOREM 4.6.1 *Given the error model system for the friction system, assumptions and notation defined in the previous theorem. Assume the following*

(i.) The Lipschitz disturbances are small enough so that

$$\begin{aligned} k_2 &\leq k_2^* \\ \lambda'_Q &> 0 \end{aligned} \tag{4.105}$$

where k_2^* is derived in lemma (4.2.2) and $\lambda'_Q = \lambda_{Q_{min}} - 2k_2$ is defined chapter 3 equation (3.22).

An iterative algorithm exists to compute the input p.e. level, ϵ_0, the p.e. subinterval width, δ_0, and the scaling factor, k, which converges to values that satisfy the conditions (ii.) and (iii.) in the previous theorem (equations (4.63) and (4.64)).

Furthermore, the bound on the error model solutions can calculated in terms of the apriori information.

PROOF

For the first part of the theorem to show that the conditions exist, we define an algorithm which proceeds in 4 steps. In step 1, we set up the initial variables of interest of the problem and calculate bounds for v_{max} and $\dot{v}_{max}$. We also choose, δ_0, the p.e. subinterval width which will satisfy condition (iii.) and can be decoupled from the choices for p.e. level, ϵ_0 and scaling factor k using the results in appendix (H). In step 2, we set up the beginning of an iteration process for the level of input p.e., ϵ_0, that is needed. In step 3, based on a given p.e. level, we choose the scaling factor k small enough to satisfy condition (iii.) in the theorem (4.64). In step 4, we check whether the p.e. level that was chosen in step 2 is high enough to meet condition (ii.) in the theorem (4.63). If it is not we return to increase the degree of p.e. and return to step 2.

Finally, we show why the overall iteration process in steps 2-4 converges to a values of the p.e. level, p.e. subinterval width, and scaling factor that will satisfy the conditions (ii.) and (iii.) in theorem (4.4.1)

The following notation will be used,

$$I_{v_c,v_{max}} = \begin{bmatrix} -v_{max} & v_c \end{bmatrix} \cup \begin{bmatrix} v_c & v_{max} \end{bmatrix} \tag{4.106}$$

The value for v_c will be assumed to be zero at first and will be chosen at the end of the algorithm. For the friction system, v_c, can be chosen arbitrarily small and calculations can be made independent of the value of v_c. This is because the first and third quadrant nonlinearities in the regression vector for the friction problem have a magnitude near 1 at values near zero. Recall these functions were $sat(v)$ and

$sat(v)e^{-(v/v_0)^2}$. Note that we can choose the cutoff term in the saturation function (which is called v_c in definition in equation (2.5)) to be the same as the small positive value, v_c, that we are choosing so that v and v_d do not change sign in the p.e. subinterval. So we can always choose v_c so that $f_{p_{minI_{v_c,v_{max}}}}$ is independent of v_c.

STEP 1. INITIAL ASSUMPTIONS

Let $T_{0_P} = T(\epsilon_1, \delta_s)$ which is defined in the proof of property (4.2.1). Using the value for T_{0_P}, calculate the upper bounds for v and $\dot{v}$, (v_{max} and $\dot{v}_{max}$, respectively) using equation (4.97).

The results in appendix (H) show the upper bound on the p.e. subinterval width, δ_0, in condition iii. of theorem (4.4.1) can be decoupled from the equations for p.e. level, ϵ_0 and scaling factor, k. From equation (H.7), choose δ_0 to satisfy

$$\delta_0 < \frac{1}{\dot{v}_{max}} f_{p_{minI_{v_c,v_{max}}}} \tag{4.107}$$

STEP 2. ITERATION FOR P.E. DEGREE IN THEOREM CONDITION (II)

Choose an input p.e. level, ϵ_0, for this pass through steps 2-4 as follows.

If this is the first pass of the iteration procedure choose $\delta_{pass_1} > 0$ as a small arbitary positive constant.

$$\epsilon_0 > \gamma' \nu'_{max} + \delta_{pass_1} \tag{4.108}$$

If this is not the first pass through the iteration procedure and it is the *ith* pass for

$i \geq 2$, increase the p.e. degree by choosing

$$\epsilon_0 > \gamma' \nu'_{max} + \delta_{pass_i} \tag{4.109}$$

such that $\delta_{pass_i} > \delta_{pass_{i-1}}$

Compute k_{eff} using the choice in step 1 for δ_0, using the above lower bound on ϵ_0, and using T_{0_D} calculated from lemma (4.2.2) in equation (4.15), which is restated below,

$$\frac{1}{\epsilon_0 T_{0_D}} \left| \int_{t_2}^{t_2+\delta_0} \sum_{p=2}^{p=m} r_p \left(f_p(v(\tau)) - f_p(v_d(\tau)) \right) d\tau \right| \leq k_{eff} \tag{4.110}$$

STEP 3. CHOOSE SCALING FACTOR, k, IN THEOREM CONDITION (III.) FOR $v_c = 0$

Use the results in appendix (H) in equation (H.8) to obtain an upper bound on the scaling factor, k. Use the lower bound on ϵ_0 in step 2, and use the value of T_{0_D} calculated in lemma (4.2.2), choose scaling factor k small enough to satisfy the following,

$$k < \frac{1}{\epsilon_0 T_{0_D} \dot{v}_{max}} \left(f_{p_{minI_{v_c,v_{max}}}} \right) \left(f_{p_{minI_{v_c,v_{max}}}} \right) \tag{4.111}$$

STEP 4. CHECK P.E. DEGREE

With the bound for the scaling factor k chosen in step 3 and for using k_{eff} from step 2, check if the p.e. level is high enough

$$\epsilon_0 (1 - k - k_{eff}) > \gamma' \nu'_{max} \tag{4.112}$$

If the statement above is true, we are finished. If the statement above is not true,

return to step 2 and iterate again with an increased degree of p.e.

This algorithm will converge. On each pass through steps 2-4, we choose a higher p.e. degree, ϵ_0. In step 2, that means that k_{eff} is smaller. In step 3, a higher degree of p.e. means that k is smaller. Therefore, $k + k_{eff}$ is smaller on each pass. A sequence can be formed of the values on each pass for $1-(k+k_{eff})$. This sequence is monotonically increasing and bounded by one. Therefore, a there exists a degree of input p.e., ϵ_0, for which $1 - k - k_{eff} > 0$.

Finally choose v_c small enough so that the conditions still hold i.e. choose v_c small enough so that

$$0 < \delta_0 \quad < \quad \frac{\frac{k\epsilon_0 T_{0_D}}{\delta_0} - v_c}{\dot{v}_{max}} < \frac{\frac{\epsilon_0 T_{0_D}}{\delta_0} - v_c}{a_{d_{max}}}, \tag{4.113}$$

And use this value in the definition for the saturation function.

This concludes the end of the first part of the theorem. An algorithm exists that converges to values which satisfies the conditions in theorem (4.4.1).

Next we prove the second part, that the error model solution bounds can be calculated.

From equation (4.103), the bounds on the error model solutions are

$$\begin{aligned} ||\tilde{\theta}||^2 &\leq c_1'^2 + (1/4)(\gamma'\nu'_{max})^2\lambda'_Q T_{0_D} \\ ||e||^2 &\leq \frac{1}{\lambda_{P_{min}}}\left(c_1'^2 + (1/4)(\gamma'\nu'_{max})^2\lambda'_Q T_{0_D}\right) \end{aligned} \tag{4.114}$$

where c_1' was defined in equation (4.80) as

$$c_1' \quad = \quad k_1\nu'_{max}/(1 - (ce^{k_2 T_{0_D}})) \tag{4.115}$$

where

$$
\begin{aligned}
k_1 &= \lambda_{P_{max}} b_{max} T_{0_D} e^{k_2 T_{0_D}} \\
k_2 &= \lambda_{P_{max}} b_{max} d_{max}
\end{aligned}
\tag{4.116}
$$

These bounds are a function of T_{0_D}, which can be computed using lemma (4.2.2).

The other terms involved in that the error model solutions bounds are functions of the control terms, A, P and Q and the bounds for the disturbances in the system. These are known apriori to the control designer. So because T_{0_D} can be computed using lemma (4.2.2), error model solution bounds can be computed.

END OF PROOF

REMARK 4.6.1 Although this theorem makes the method implementable to a control designer, conservative conditions may have implications on the practicality of satisfying all the conditions. Instead, a control designer may decide to just increase the level of p.e. in the system until an acceptable tradeoff is reached between tracking error, parameter estimate rates and control gain.

REMARK 4.6.2 Notice that the assumption on the desired trajectory in the stability theorem (equation (4.62)) has implications for the range of usefulness of the control scheme. If the control designer must increase p.e. level to a very high level, then for a given desired trajectory the assumption in equation (4.62) may never be reached. So there is an underlying relationship between p.e. level and capability of the desired trajectory. This is not a serious concern for the friction problem because the method is applied to tasks when the velocity is operating near zero.

4.7 Chapter Summary

In this chapter, we analyzed and proved conditions to guarantee that the solutions of the new type of error model are bounded. These conditions imply that if the input is persistently exciting enough over a small enough interval and if the bandwidth is large enough compared to the level of disturbances, then the tracking and parameter estimates for the adaptive nonlinear friction compensator are bounded. The approach we used was to exploit special properties of first and third quadrant functions so that the errors in the regression vector can be scaled to errors in tracking. We also focused on implementation issues and showed that the p.e. conditions and bounds can be computed for the friction compensation system when the Lipschitz perturbations in the model are small enough.

Chapter 5

Performance of Friction Compensation Algorithm

In this chapter, we input signals to the baseline velocity tasks to boost the level of p.e. in the input trajectory and to verify the results in chapter 4. We show that with sufficient persistent excitation in the input trajectory, the adaptive nonlinear friction compensation algorithm improves tracking performance and the algorithm is stable (i.e. the parameter estimates do not grow unbounded). Because the conditions for bounded tracking and parameter estimates may be conservative, we experimented with the level of p.e. in the system until we got parameter estimates to stay within reasonable ranges over reasonably long times. So in this chapter, 'sufficient' means that the simulation results are reasonable. We show that even if the p.e. levels are not chosen specifically to satisfy the conditions of the theorem, the adaptive nonlinear friction compensation scheme can offer a dramatic improvement in the tracking problems due to friction. Additionally, we find that the design has robustness to some of the typical types of modelling errors which could be present in the friction model.

We return to the three baseline low velocity problematic friction tasks studied. In chapter 2, we observed undesirable tracking performance in a linear control design due to problems with friction. In chapter 3, we observed the adaptive nonlinear friction compensator with insufficient p.e. can be unstable. In the first section of this chapter, we test the adaptive nonlinear friction compensator with the addition of small sinusoidal terms to make the input trajectories have more persistent excitation, and we show that this friction compensation design improves the tracking performance without unreasonably large parameter estimates and without unreasonably large control usage.

In the second section, we compare the adaptive nonlinear friction compensator to a friction compensator based on estimating the internal friction state. We find comparable tracking performance.

In the third section of this chapter, we study the robustness of compensator. Although the method is designed to have robustness to bounded uncertainty in the model, we are also interested in the effects of structural modelling errors in the friction model as well as unmodelled dynamics. This is an important consideration given the variety of different friction models discussed in the literature. In chapter 2 in section (2.2.3), we alluded to some of the alternative methods to model the observed frictional mechanisms. Analyzing the stability of our method with a different structural model or with unmodelled dynamics is very difficult; however, because our method is designed for some bounded modelling uncertainties, we expect to have local robustness properties when the additional modelling uncertainties are small in some sense. We support this hypothesis by including simulations in which we apply the friction compensator we designed to a control system with unmodelled actuator dynamics and a friction model that is structurally different and uses some alternative modelling techniques motivated by the literature.

5.1 Low Velocity Tracking Baseline Tasks with Friction Compensation and P.E.

In this section we investigate how the addition of persistent excitation to the friction compensator improves tracking performance.

We experimented with different levels of p.e., frequency component of p.e. signal , and the rate of decay of V, which can be varied by adjusting the Q and P matrices. Additionally, we also experimented with adaptation gain because multiplying the adaptation laws by a positive constant will not affect the stability analysis in the previous chapter. We were interested in a tradeoffs between p.e. level, tracking error, parameter error levels and parameter convergence rates.

Adaptive control systems can be 'stiff', which means that the performance is sensitive to the initial conditions. Additionally, friction system itself has a sharp nonlinear behavior at zero velocity. These factors make it more difficult for numerical integration packages. Due to this fact, we used 'ode15s.m ', which is a matlab simulation routine specifically written for stiff systems, [26].

In this section, we present runs using levels of p.e. which exhibit improved tracking compared to the linear controller for all three baseline low velocity tasks.

5.1.1 Adaptive Nonlinear Friction Compensation with Sufficient P.E.: A Constant Velocity Task

The first task is a ramp in position, with a constant velocity of .02m/s. To give the trajectory some p.e., we add a small sinusoidal input (1 centimeter 2 Hz)to the desired trajectory.

Tracking performance results are shown in figure 5-1 and tracking results from chapters 2 and 3 are also reprinted and compared in this figure. We see that tracking performance is much improved from the corresponding plots in chapters 2 and 3. The linear controller exhibited a stick slip limit cycle with tracking errors of 5 centimeters or more due to jumps in position, and these are eliminated by the adaptive nonlinear friction compensator with p.e. The tracking performance is also improved compared to the adaptive algorithm with no p.e. which caused initial improvement, but then the mass remained stuck as the parameter errors began to grow large. Because we have added p.e. to the desired trajectory, instead of a constant .02 m/s velocity, the p.e. causes the velocity to oscillate with a 1 centimeter amplitude about this level.

Figure 5-2 shows the other variables of interest for this simulation. The addition of some p.e. causes the parameter errors to stay low. Two of the parameters appear to converge after 100 seconds, while the third, exhibits a slow variation.

At this low velocity, the frictional dynamics terms dominate the friction force. However, the friction compensator is successful in estimating the friction force and the plot shows that the difference between the actual and estimated friction force, which is labelled the friction force error, is low.

The required control usage is not unreasonably large. The plots show that the controller amplitude is only about 2.5 N and the frequency component, due to the p.e. requirement, which is only 2 Hz.

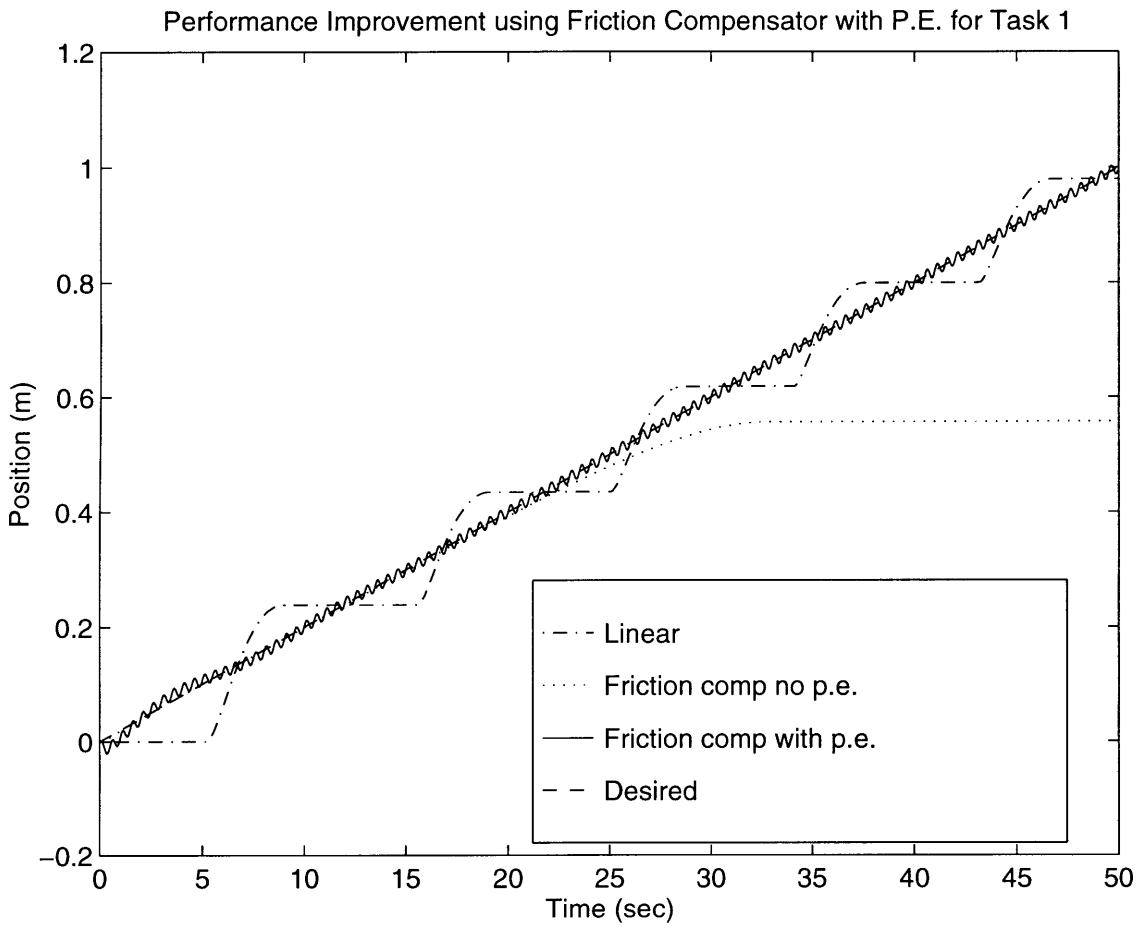

Figure 5-1: The adaptive nonlinear friction compensator with the addition of p.e. inputs eliminates the undesirable stick slip limit cycle which the linear controller exhibits. With insufficient p.e., the friction compensator can not maintain performance improvement. Tracking oscillations about the ramp of about 1 centimeter are present due to the p.e. requirement. The tracking performance is much improved compared to the linear controller, which has errors of 5 cm or more.

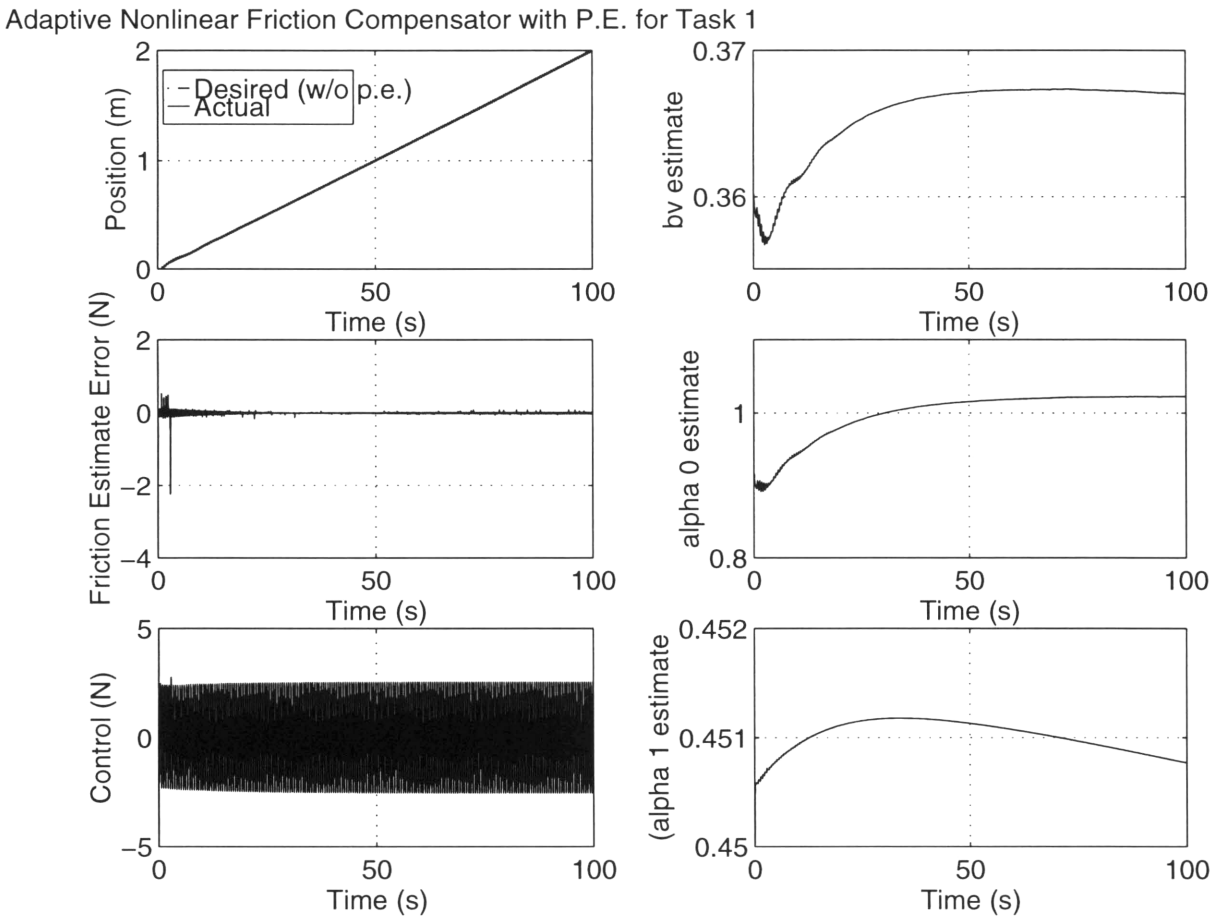

Figure 5-2: The addition of one centimeter 2 Hz sinusoidal input to the desired constant velocity input trajectory eliminates stick slip. None of the parameter estimates grow unbounded. The friction estimate is close to the actual friction force. The control usage required to obtain this performance has an amplitude less than 5 N and dynamics at the p.e. frequency of 2 Hz, which is not excessive.

5.1.2 Adaptive Nonlinear Friction Compensator with Sufficient P.E. for Low Velocity Task 2 - A Task with Repeated Zero Velocity Crossings

The second task is the low velocity sinusoid. We add a 1 centimeter 2 Hz sinusoid to the position sinusoid of $x_d = .05 * sin(.5t)$, which is the same signal that was added to the position ramp input. The amplitude of this additional signal corresponds to twenty percent of the desired signal.

We again see that tracking performance is much improved from the corresponding plots in chapters 2 and 3 as shown in figure 5-3. A linear controller could not follow this low amplitude velocity trajectory because friction forces balanced the low control forces and the mass remained stuck. The friction compensation with no p.e. offers initial improvement but cannot maintain this improvement because the mass gets stuck when the parameters start to diverge too greatly. The friction compensator with p.e. inputs however, offers much better tracking at low velocities.

The addition of p.e. allows the tracking error to periodically grow large enough in every direction so that the parameter update law does not lose effectiveness and the parameter estimates do not grow large and unbounded in a particular direction. Instead, two of the parameters converge and the third exhibits a slow variation as shown in figure 5-4. The figure also shows that the friction compensator successfully estimates the friction force using reasonable control levels of 2.5 N at 2 Hz.

Because this is a sinusoidal tracking task, hysteresis loops can be observed in the friction force vs. velocity curves. Figure 5-5 shows that the friction compensator is estimating this effect. The figure shows a plot of the actual friction force vs. velocity and the estimated friction force vs velocity. The hysteresis effect exhibited in the actual friction force is being captured in the estimated friction force, which also exhibits hysteresis loops.

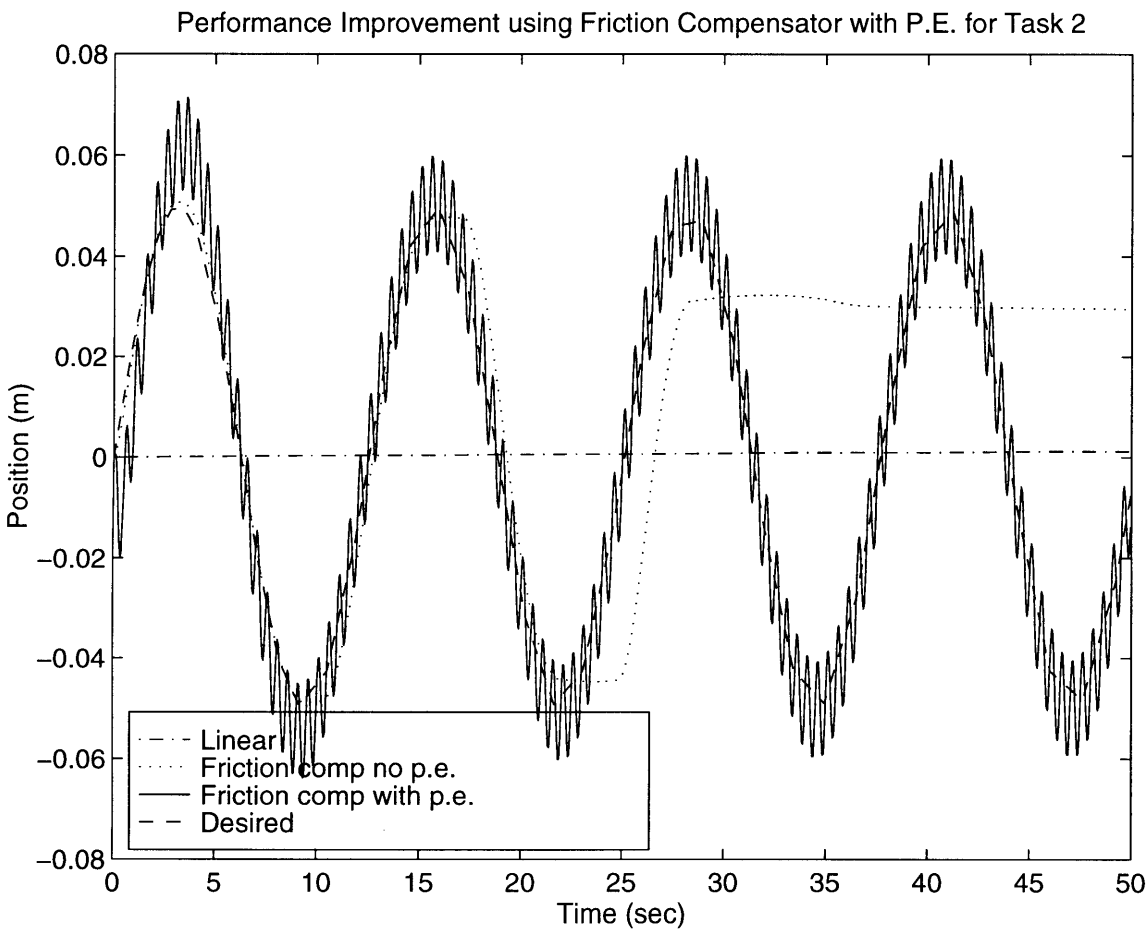

Figure 5-3: The adaptive nonlinear friction compensator with p.e. inputs offers dramatic improvement over the linear controller in the ability to track a low velocity sinusoid better. Under the influence of linear control gets stuck and stays stuck so the tracking errors are on the order of the task, about 5 centimeters. The friction compensator with p.e. oscillates with a 1 centimeter amplitude about the desired sinusoidal trajectory due to the p.e. requirement. Without p.e. the friction compensator can not maintain performance improvement.

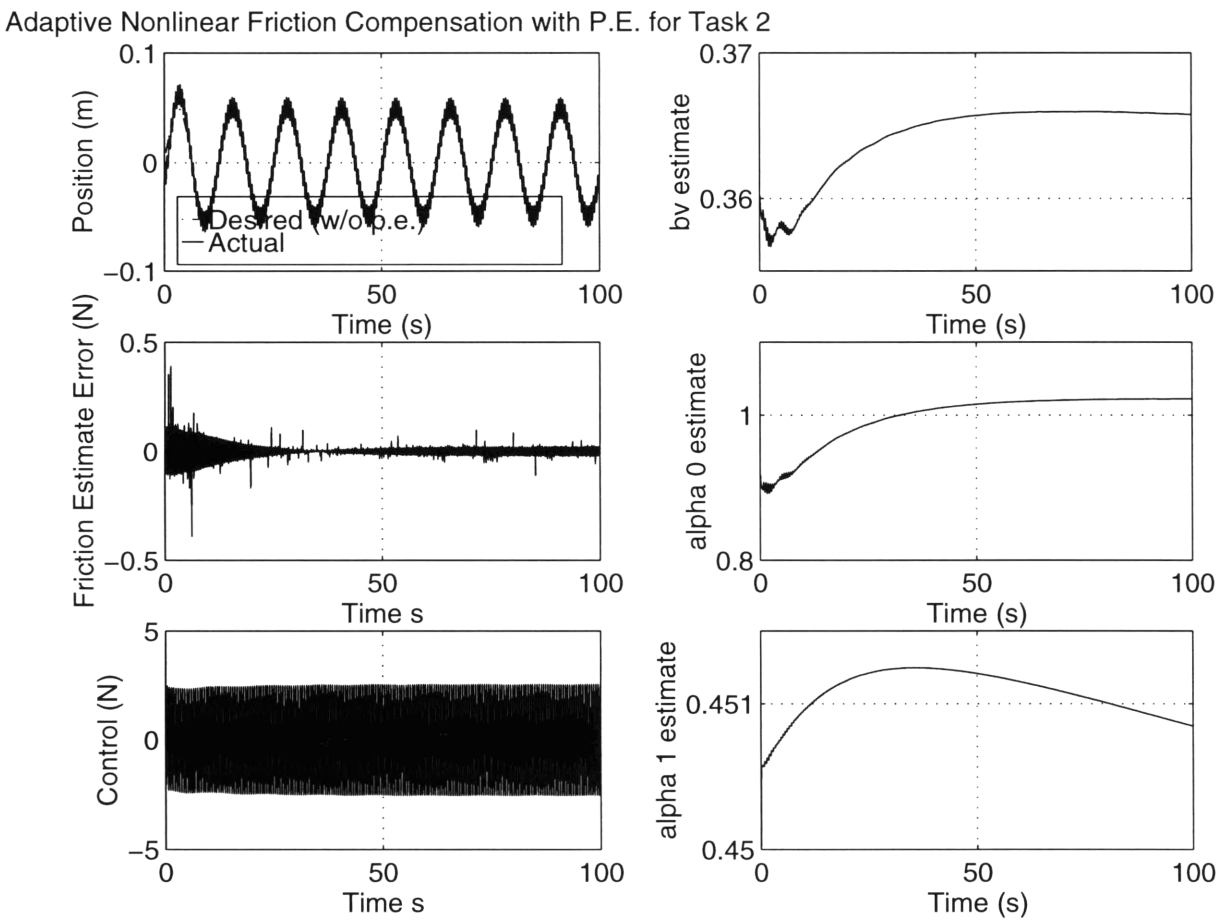

Figure 5-4: The friction compensator with p.e. tracks the sinusoid well. The mass does not get stuck like it does in the linear controller. The parameter estimates remain bounded and and error in the friction estimator is small. The control requirements are reasonable.

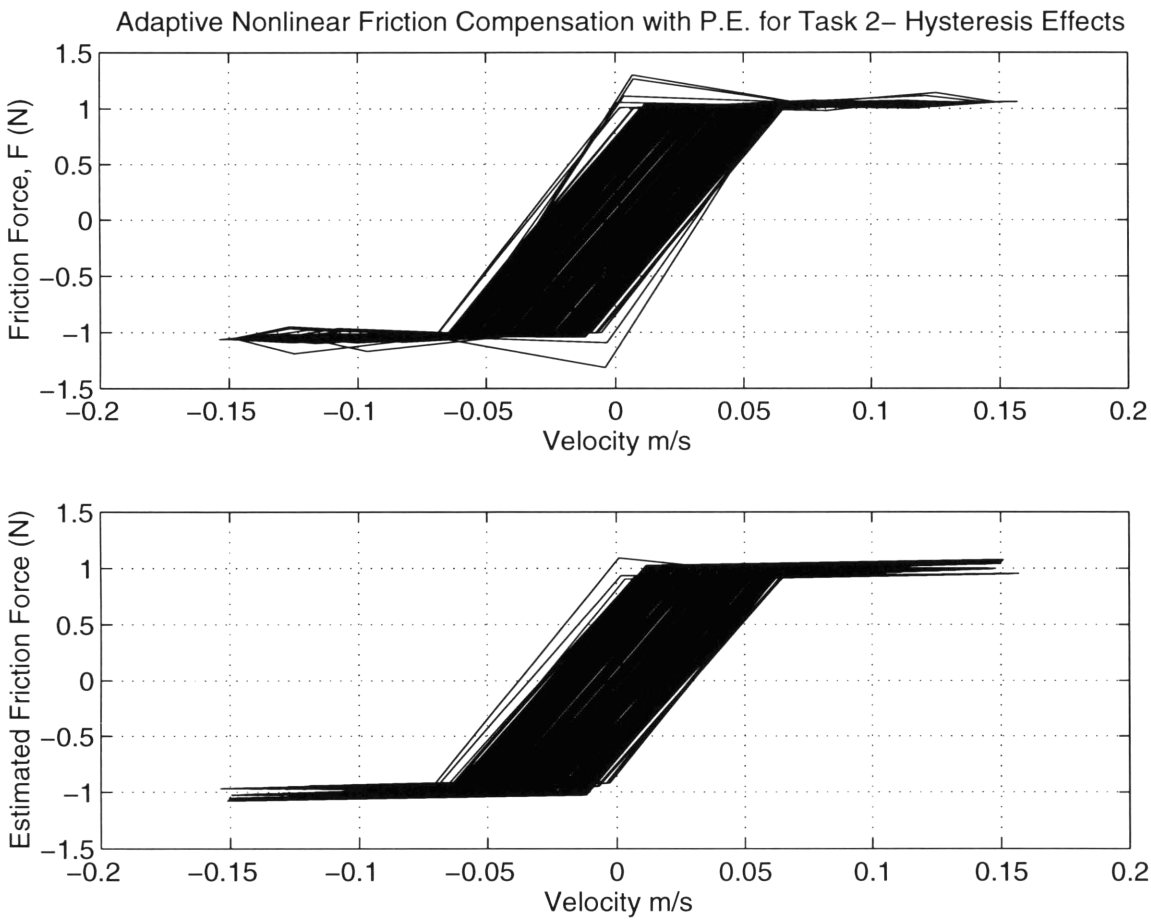

Figure 5-5: The adaptive nonlinear friction estimator is capturing the hysteresis loops which are present in the system. These hysteresis loops operate very close to stick.

5.1.3 Low Velocity Tracking Task 3 with Friction Compensator and Sufficient P.E.: A Step Response

In this section, we examine the third task, which is unit step response. For this set of simulations, we added a higher level of p.e. with an amplitude of 2 centimeters and frequency of 5 Hz.

The step response plots from chapters 2 and 3 are re-plotted along that friction compensator with p.e. inputs in figure 5-6. We see that hunting is eliminated; however, the addition of p.e. causes a two percent oscillatioabout the set point with no stick. This is smaller than the steady state hunting between six and seven percent about the final position exhibited by the linear controller in chapter 2. In chapter 3, the friction compensation without p.e. exhibited a relatively large constant position error of about ten percent when it got stuck and the parameters continued to diverge.

Figure (5-7) shows the parameter estimates, friction force estimate and control for this simulation. Two of the parameter estimates are adjusting very slowly and the third remains relatively constant. A slow reduction in the error between friction force and estimated friction force is shown in the figure which is an oscillating but enveloped by an exponentially decreasing curve. The control is using about 20 N of force, but is increasing slowly as the controller continues to adapt and the force error continues to decrease. When the errors become small, the adaptation rate can also become small.

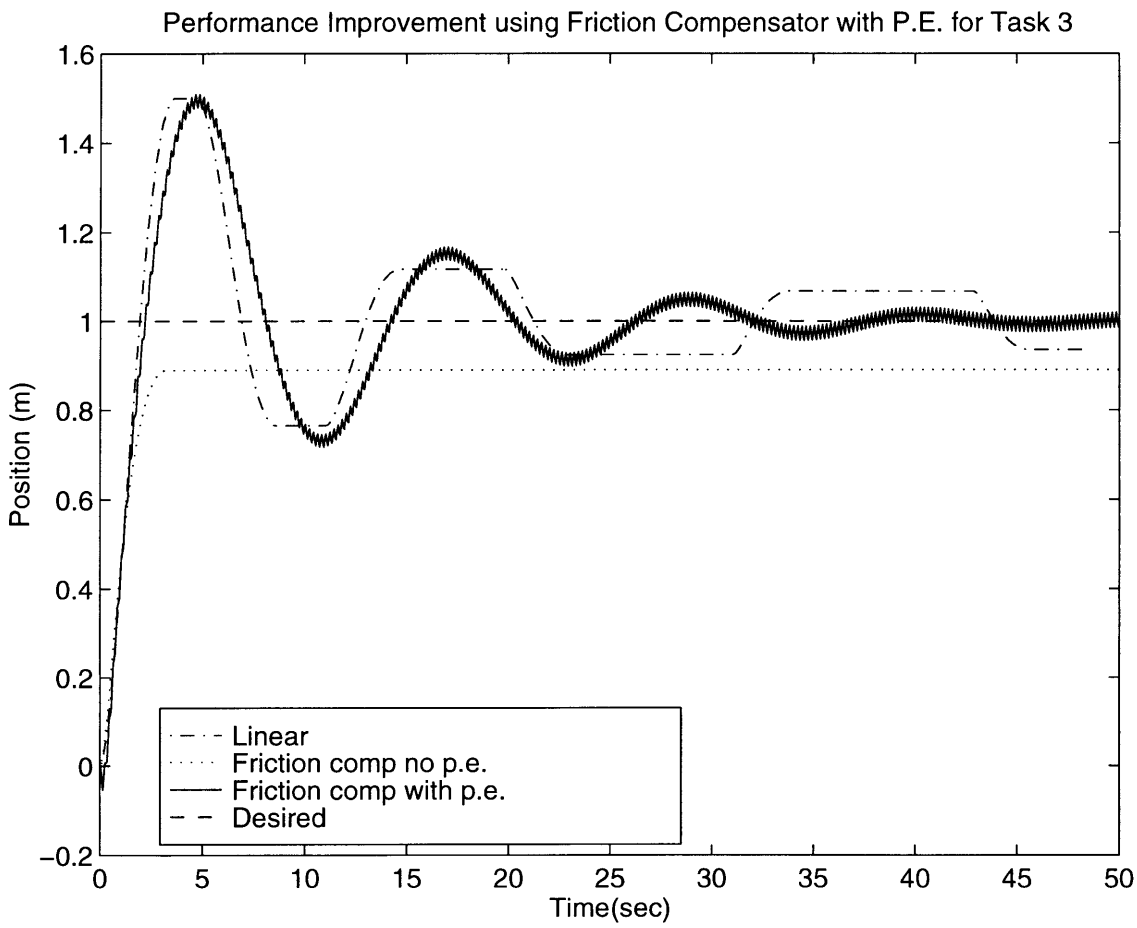

Figure 5-6: The linear controller with integral control exhibits hunting about the set point with steady state levels of about six or seven percent. The adaptive friction estimator with insufficient p.e. has a ten percent tracking error. The addition of p.e. eliminates hunting about the set point. The required p.e. level is about two percent so the oscillation about the set point is an improvement in tracking.

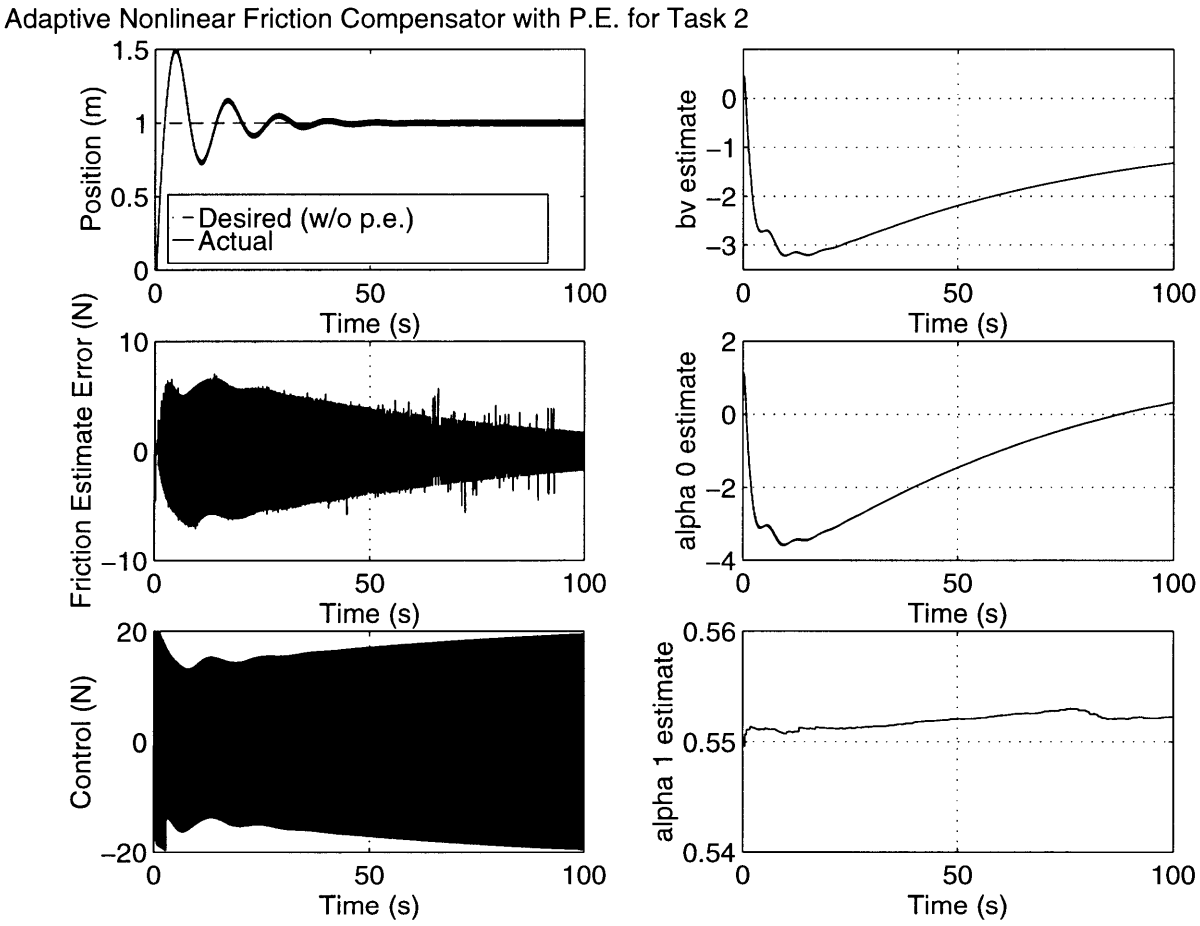

Figure 5-7: The addition of a 2 centimeter 5 Hz sinusoid to the friction compensator eliminates the hunting stick slip limit cycle. Tracking is improved with errors of about two percent due to the p.e. requirement. The parameter estimates stay low and the effects of the friction estimation error are reduced. The control levels required for this task are 20 N at about 5 Hz, which is larger than the other tasks but still within reasonable limits. After 100 seconds, the controller is still adjusting slowly.

5.2 Comparison of Nonlinear Adaptive Controller using P.E. Inputs with Nonlinear Fixed Detuned Controller

In the previous section, we showed the adaptive nonlinear friction compensator improved the tracking performance compared to the baseline linear controller, which was the goal of this study. In this section, we would like to compare the adaptive nonlinear friction compensator to a nonlinear controller with detuned parameters. We choose the second control design at the end of chapter 2 in section (2.3.2), because the first clearly does not perform as well as the adaptive nonlinear friction compensator. Recall that the second compensator was designed using an estimate for the internal friction state, z. Although it is similar to the design in [4], we wanted to compare designs based on a lower bandwidth control, and at this bandwidth, this controller does not meet the restrictive stability requirements.

We compare these controllers in terms of tracking performance to the three baseline tasks. After increasing the frequency content of the added p.e. from the previous section for the adaptive nonlinear compensator with p.e., we find that the tracking performance is comparable.

Because the focus of this study is on the design and stability analysis of the adaptive nonlinear controller, this is not an extensive comparison study. We include these plots more to show that the friction compensator designed here is comparable to other modern approaches.

For the nonlinear adaptive controller, we increased frequency content of the added signal as follows. For task 1, the constant velocity task, we added a 1/4 cm sinusoid at 2 Hz and a 1/4 cm sinusoid at 3 Hz. For task 2, we added at 4/10 cm sinusoid at 2 Hz and and 1/10 cm sinusoid at 5 Hz. For task 3, we added a 1/2 cm sinusoid at 10

Hz and a 1/10 cm sinusoid at 5 Hz. The initial parameter estimates were estimated as fifty percent above the true values.

For the nonlinear controller using an estimator for the internal friction state, we detuned the parameter estimates used in the compensator by increasing them by fifty percent above the true values as well.

Figure 5-8 is a comparison of the tracking errors for the adaptive nonlinear compensator and the nonlinear compensator which uses an estimate for the internal friction state, z. The tracking errors are about 1/2 cm for tasks 1 and 2 which were the constant velocity and the repeated zero velocity tasks respectively. The tracking errors for task 3 are about 1/2 cm for the adaptive nonlinear compensator and slowly reducing from 1 cm for the detuned nonlinear compensator. The times plotted for the various plots are different because the controllers reach steady state at different times, with the adaptive controller taking longer as it adapts. The control levels used in these simulations are not shown here but both controller use reasonable control forces of about 10 N for the step response plots. Tracking performance is comparable for these two controllers.

5.3 Robustness Simulations

In this set of simulations, we examine the effect of additional modelling uncertainties. We include unmodelled actuator dynamics at 10 Hz. We also include two types of errors in our friction model, a positive ten percent error in the Stribeck parameter, v_0, and a low frequency variation in the parameter $\alpha_1(t) = .5 + .5 * .1 * cos(.1t)$.

We have made these choices to reflect what may be reasonable errors motivated by the discussion in chapter 2 section (2.2.3). Unmodelled dynamics are always present. Additionally, as we have seen in chapter 2, there are many types of friction

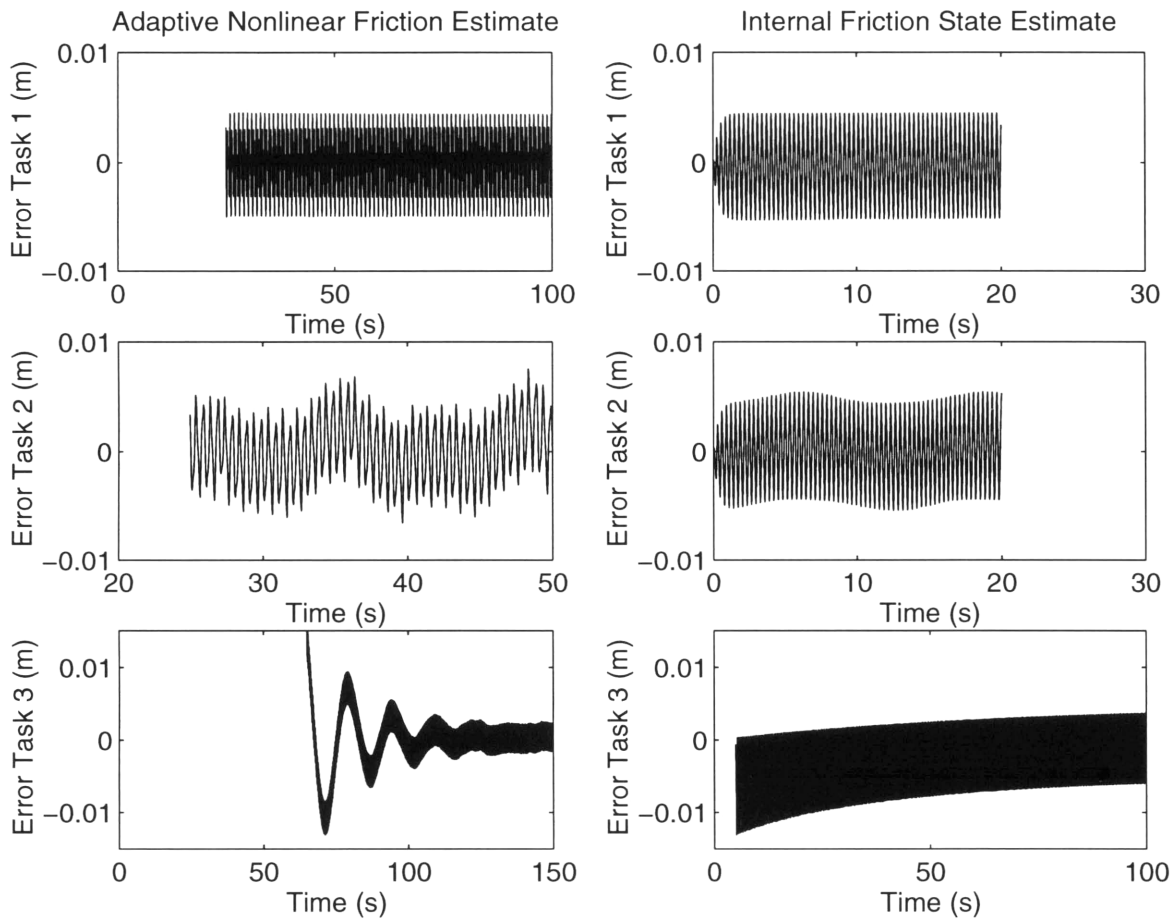

Figure 5-8: The adaptive nonlinear friction compensator and the detuned nonlinear friction compensator which is based on an internal friction state estimate have similar tracking performance. Errors are on the order of 1/2 to 1 cm for all three baseline tasks, which were task 1, the low velocity task, task 2, the task with repeated zero velocity crossings and task 3 the regulation task.

models available. We have chosen the error in Stribeck parameter because our method currently assumes that the Stribeck parameter is known. So our model could be incorrect in modelling the steepness of the Stribeck effect in the static friction model. Additionally, while many models use the exponential model, some use a different functional form. However, the differences in the Stribeck effect in models, is really a bounded disturbance with a maximum at some low velocity. We would expect our method to have some robustness to this because it was designed to handle bounded disturbances.

The second type of friction modelling error included is a low frequency variation in the parameters α_1. This term, as well as the Stribeck parameter, affects the rising static friction phenomena. Some models, for example [2], fit the rising static to a curve as a function of time in the stuck position.

We added a 5 Hz sinusoidal component which has an amplitude of 4 centimeters for the step response task. This corresponds to twice the amplitude of the step response simulation in the first section of this chapter. Higher p.e. level was needed in order to handle the additional disturbances in the system.

Figure 5-9 shows that the controller is robust to these modelling errors. Hunting is still eliminated and the tracking errors are low. Two of the parameter estimates, b_v and α_0 are converging to relatively large values. In general, it is preferable when the parameter estimates are closer to their true values; however, the transients in this simulation do not seem unreasonable. The third parameter, which we have made time-varying in this simulation, is converging to about 4 times its average true value. The error in estimated force is bounded and the control levels used are not excessively high.

We also simulated tasks 1 and 2 for the modelling uncertainties described in this section. The adaptive nonlinear friction compensator used the following signals added to the baseline trajectories. For task 1, the constant velocity task, a 3 cm 5 Hz and

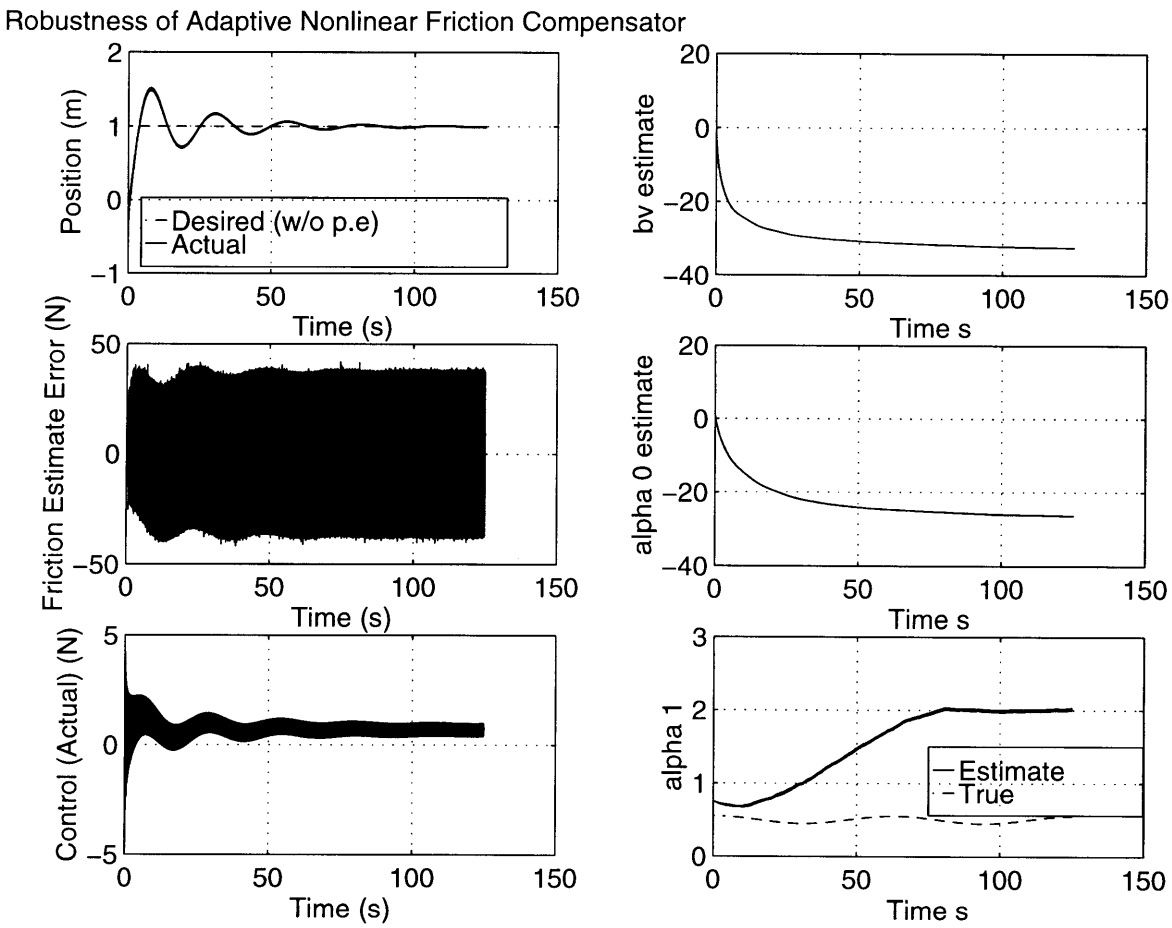

Figure 5-9: This simulation tests the ability of the adaptive nonlinear friction compensator with p.e. for several types of modelling errors, including unmodelled actuator dynamics, error in Stribeck parameter, and a time-varying parameter. Because it was designed for robustness, the friction compensator still performs well under these different types of modelling perturbations. Hunting about the set point is eliminated, and the parameter estimates do not grow unbounded.

a 2 cm 10 Hz signal were added. For task 2, the trajectory with repeated velocity crossings, a 1/2 cm 1 Hz sinusoid and a 1/2 cm 6 Hz sinusoid were added.

The results are shown in figure 5-10. Tracking performance is good for both tasks 1 and 3, the ramp and the step. For the sinusoid, there is about a 50 percent error in the peaks and the phase is shifted, which may be more desirable than the linear controller which remained stuck.

These results are promising. The controller is exhibiting some robustness properties when small amounts of p.e. are added to the input trajectories.

5.4 Chapter Summary

Simulation results for the adaptive nonlinear friction compensator with p.e. inputs look very promising. We saw that tracking performance is greatly improved over the linear controller for a set of representative baseline tasks. Undesirable limit cycling is eliminated and tracking errors are reduced. The algorithm is stable and the parameter estimation errors stay within reasonable limits. We also compared the adaptive nonlinear friction compensator to a nonlinear friction compensator that operates by estimating the internal friction state. Tracking performance was comparable.

Practical design issues arise with the use of this control. One is how much of the p.e. requirement is reasonable. Increasing the p.e. can enhance performance, however, it makes sense to use p.e. that is commensurate with the desired task. If the additional amount of p.e. required is higher than the errors in a linear controller, it is better to use the linear controllers. However, many types of tasks for which friction effects are problematic include trajectories with repeated zero velocities and these types of tasks have some naturally-occurring p.e.. Some tasks will perform well naturally, while others may need more added p.e. than is reasonable for the task.

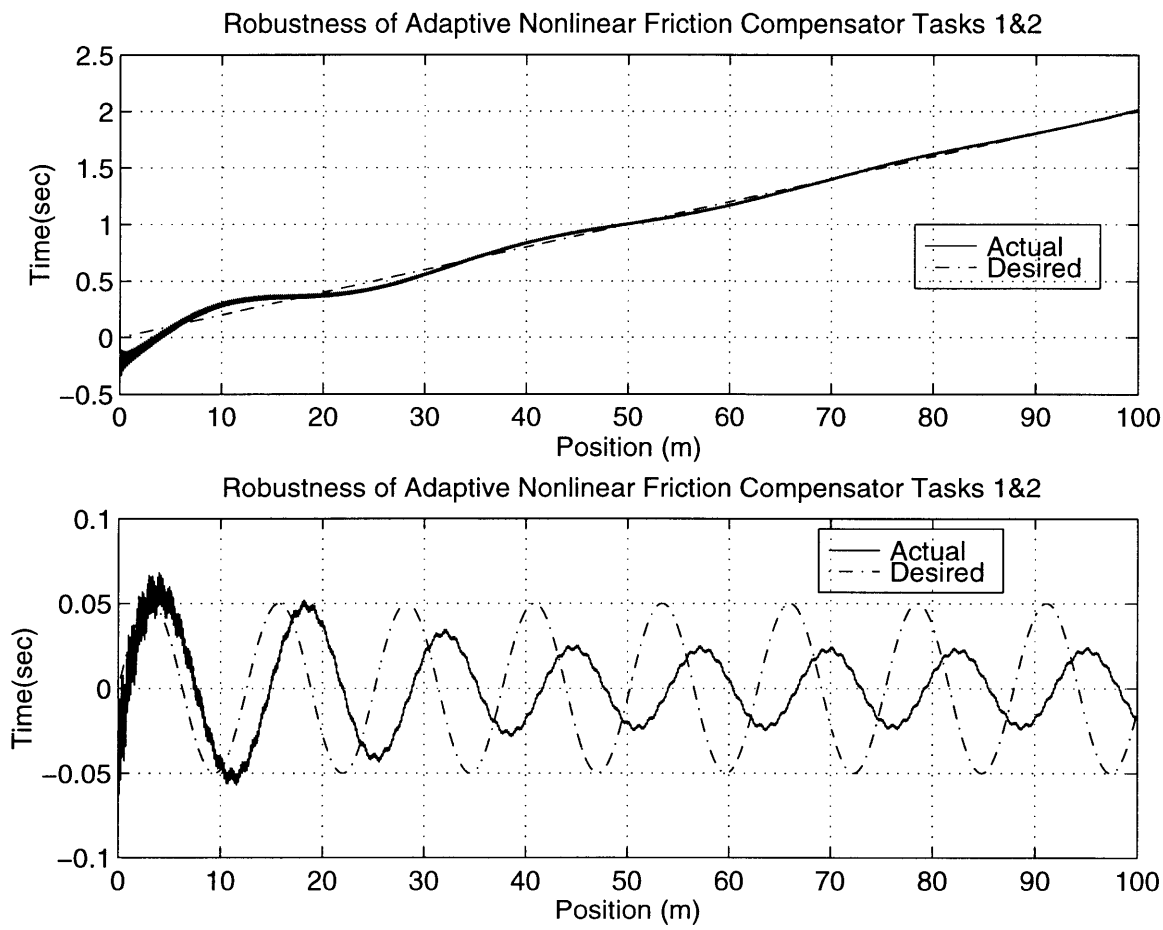

Figure 5-10: These simulations are for the constant velocity and the repeated zero velocity crossings tasks in the presence of the modelling uncertainties. The constant velocity task performs well. The sinusoidal task has about 50 percent peaks compared to the desired trajectory and is out of phase. However, this is better than the linear controller which barely moved at all.

Chapter 6

Conclusions

In this thesis, we have shown that due to nonlinearities, modelling uncertainties and lack of feedback about the internal state, it is difficult to compensate for the effects of friction, which include undesirable stick-slip limit cycles, tracking errors and hunting about a set point, in control applications involving high precision, low velocity tasks.

We designed an adaptive nonlinear friction compensation scheme especially to provide stable compensation for a friction model which captures more of the problematic friction effects, including Stribeck effect, frictional lag, stick-slip, presliding displacements and rising static friction, than previous friction compensation methods. The design strategy for the design was to compensate for the static, Coulomb and viscous components of the friction force, while remaining robust to dynamic perturbations in the model.

Our friction compensation scheme resulted in a new type of error model which relates tracking error, parameter error and disturbances perturbations due to the friction dynamics. The new error model is different from error models previously considered in adaptive control work because it has a regression vector which contains first and third

quadrant nonlinearities. Additionally, the disturbances include Lipschitz as well as bounded disturbances. We illustrated that stability questions for the error model are important issues which must be addressed to achieve good performance of the friction compensation scheme, and we identified robust adaptive theory using persistently exciting (p.e.) inputs as an appropriate tool for addressing these issues. And we showed that without the use of sufficient p.e. inputs, the adaptive nonlinear friction compensation design could have stability problems, but with the use of sufficient p.e. the friction compensator does not have these stability problems.

We extended robust adaptive theory using persistent excitation inputs to include the new type of error model. We proved a stability theorem which states that if the input is persistently exciting enough over a small enough subinterval, and if the bandwidth of the linear portion of the controller is high enough relative to the Lipschitz disturbance bounds, then conditions can be chosen to ensure bounded tracking and parameter errors. We prove a second theorem for the friction system which makes this method useful for control designers because it shows if the level of Lipschitz disturbances in the system are small enough, there is an algorithm which will converge to p.e. conditions which will satisfy the conditions of the stability theorem and the bounds on the error model solution can be computed.

We simulated a position control system for a mass with the dynamic nonlinear friction model. Linear control was shown to have large tracking errors for low velocity tracks. Three types of low velocity tasks, a constant low velocity trajectory position ramp task, a low velocity sinusoidal tracking task and finally a step response task were examined. For the ramp task, stick slip limit cycling is evident for the linear controller. For the sinusoid task, we observed that control gains for the linear controller are not large enough to counter the friction force and consequently, the mass stays stuck. For the step response task, we observed undesirable limit cycling about a set point.

By using our friction compensation method without the required p.e. inputs, we

illustrate by simulation that stability issues are indeed a problem and the parameters errors can grow without bound.

Finally, we add p.e. to the desired trajectory inputs and show that the friction compensation design offers dramatic improvement the tracking problems presented using reasonable control levels and having reasonable parameter convergence properties. Stick slip limit cycling is eliminated in the ramp response. The mass can follow a low velocity trajectory with repeated zero velocity crossings. And finally hunting about a set point is eliminated.

We also compare the compensator designed here to a different type of nonlinear controller. Tracking performance is comparable.

We also evaluate the robustness of our controller. We test for several different types of modelling uncertainties including the steepness of the Stribeck effect, a time varying parameter. These errors are motivated by alternative models in the literature. We also include unmodelled dynamics. The simulations verify that this controller has some robustness properties.

The results of this study show that adaptive nonlinear friction compensation using p.e. inputs is a promising approach to control of systems in which friction plays an important role such as high precision low velocity tasks.

Furthermore, the design resulted in an extension of robust adaptive theory using persistent excitation.

Appendix A

Boundedness of Internal Friction State, z

The following is a proof of boundedness for the internal friction state, z, which is stated in lemma (2.2.1)

PROOF A.0.1 *First we use a Lyapunov function argument to show that the internal friction state, z, i s bounded. Let V_z be defined as*

$$V_z = z^2 \tag{A.1}$$

Taking the derivative we obtain

$$\dot{V}_z = 2\left(vz - \sigma_0 \frac{h(v)z^2}{\alpha_0 + \alpha_1 e^{-(\frac{v}{v_0})^2}}\right)$$

$$
\begin{aligned}
\dot{V}_z &\leq 2|z||v|\left(1+\sigma_0\frac{sign(v)}{sat(v)}\frac{1}{\alpha_0+\alpha_1 e^{-(\frac{v}{v_0})^2}}|z|\right) \\
\dot{V}_z &\leq 2|z||v|\left(1+\frac{sign(v)}{sat(v)}\frac{1}{z_s}|z|\right)
\end{aligned}
\tag{A.2}
$$

The derivative is negative when $|z| > z_s$. *Furthermore, assuming bounds on the parameters are known,* z_s *is bounded by*

$$
z_{s_{max}} \leq \frac{\alpha_{0_{max}}+\alpha_{1_{max}}}{\sigma_{0_{min}}} \tag{A.3}
$$

Therefore $|z|$ *is bounded by* $max(|z(t_0)|, z_{s_{max}})$.

Appendix B

Bounds for dynamic model perturbation effects, F_{unest}, in the friction model

To quantify the difference between the actual and static friction force, we can write the friction force in terms of an error, ϵ, which is defined as the difference between the internal friction state, z, and its static value, z_s.

$$\epsilon = z - z_s \tag{B.1}$$

Then, in terms of the error, ϵ, the friction force can be written

$$\begin{aligned} F &= F_s + \sigma_0 \epsilon \left(1 - \sigma_1 \frac{h(v)}{\alpha_0 + \alpha_1 e^{-(\frac{v}{v_0})^2}}\right) \\ F_{unest} &= \sigma_0 \epsilon \left(1 - \sigma_1 \frac{h(v)}{\alpha_0 + \alpha_1 e^{-(\frac{v}{v_0})^2}}\right) \end{aligned} \tag{B.2}$$

The unestimated part of the friction, F_{unest}, quantified above, can be bounded as in the figure (3-3) shown in chapter 3 because $h(v)$ is a Lipschitz bounded function and the error, ϵ, is bounded. We showed in chapter 2 that given bounds on the parameter values, then z and z_s are a bounded quantities, therefore ϵ is bounded. That is,

$$|\epsilon| \leq \epsilon_{max} = 2\max(|z(t_0)|, z_{s_{max}}) \tag{B.3}$$

This leads to bounds on the unestimated part of the friction force as follows,

$$\begin{aligned} |F_{unest}| &\leq \nu_{max} + d_{max}||e|| \\ \nu_{max} &\leq \sigma_{0_{max}}\epsilon_{max}(1 + \frac{\sigma_{1_{max}}}{\alpha_{0_{min}} + \alpha_{1_{min}}} max(v_c, \dot{x}_{d_{max}})) \\ d_{max} &\leq \sigma_{0_{max}}\sigma_{1_{max}}\epsilon_{max}\frac{1}{\alpha_{0_{min}} + \alpha_{1_{min}}} \end{aligned} \tag{B.4}$$

Appendix C

A Property About First and Third Quadrant Continuous Functions

In this section we prove property (4.1.1). First we establish that the conditions of the property imply that v must reach a threshold in the subinterval. Next we show that δ_0 is small enough so that v does not reach zero in the subinterval. Finally, we compute the minimum value of the integral of the first and third quadrant function over the subinterval and choose the scaling factor small enough to ensure the desired result.

C.1 Threshold for v

If the integral of a continuous signal over an interval is 'large', then the signal is at least a threshold magnitude somewhere on the interval.

The signal v must reach a threshold value somewhere on the interval $\begin{bmatrix} t_2 & t_2 + \delta_0 \end{bmatrix}$.

Or, equivalently, as shown in figure C-1, if it did not, the integral would be smaller.

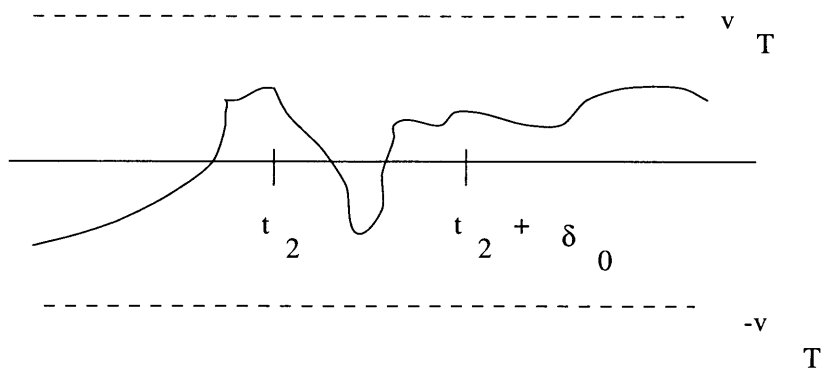

Figure C-1: If v does not reach threshold value in subinterval, then the integral of v over the subinterval is less than $v_T \delta_0$

LEMMA C.1.1 *If $v(\tau)$ is a continuous function of τ and*

$$\left| \int_{t_2}^{t_2+\delta_0} v(\tau) d\tau \right| \geq k\epsilon_0 T_{0_D}$$

then there is a $t' \in \left[\begin{array}{cc} t_2 & t_2+\delta_0 \end{array} \right]$ such that the magnitude $|v(t')|$ is at least a threshold value

$$|v(t')| \geq v_T$$

where

$$v_T = \frac{k\epsilon_0 T_{0_D}}{\delta_0} \tag{C.1}$$

PROOF OF LEMMA (C.1.1)

We prove the contrapositive. Suppose $|v(t)|$ does not reach the threshold value, v_T, in the subinterval

$$|v(t)| < v_T \qquad \text{for } t \in \left[\begin{array}{cc} t_2 & t_2+\delta_0 \end{array} \right] \tag{C.2}$$

Then

$$\begin{aligned}
\left| \int_{t_2}^{t_2+\delta_0} v(\tau)d\tau \right| &\leq \int_{t_2}^{t_2+\delta_0} |v(\tau)|d\tau < v_T\delta_0 \\
\left| \int_{t_2}^{t_2+\delta_0} v(\tau)d\tau \right| &< k\epsilon_0 T_{0_D} \qquad \text{(C.3)}
\end{aligned}$$

END OF PROOF OF LEMMA (C.1.1)

C.2 v DOES NOT CHANGE SIGN FOR $t \in [t_2\ t_2 + \delta_0]$

The next section shows that given the property conditions, then $v(t)$ does not reach zero in the subinterval.

LEMMA C.2.1 *Let $v : \Re^1 \to \Re^1$ be a continuous differentiable function satisfying the condition in the previous lemma:*

$$\left| \int_{t_2}^{t_2+\delta_0} v(\tau)d\tau \right| \geq k\epsilon_0 T_{0_D}$$

Assume we are given upper bounds for $|v(t)|$ and $|\dot{v}(t)|$, on the subinterval $t \in \left[\ t_2 \quad t_2 + \delta_0\ \right]$ such that

$$\begin{aligned}
|v(t)| &\leq v_{max} \qquad \text{for } t \in \left[\ t_2 \quad t_2 + \delta_0\ \right] \\
|\dot{v}(t)| &\leq \dot{v}_{max} \qquad \text{for } t \in \left[\ t_2 \quad t_2 + \delta_0\ \right] \qquad \text{(C.4)}
\end{aligned}$$

Let $v_T = \frac{k\epsilon_0 T_{0_D}}{\delta_0}$ *be the threshold value defined in the previous lemma and let* $0 < v_c < v_T$ *be a small positive number. If* δ_0 *is such that*

$$\delta_0 < \frac{v_T - v_c}{\dot{v}_{max}} \tag{C.5}$$

then $v(t)$ *does not change sign for* $t \in \left[\begin{array}{cc} t_2 & t_2 + \delta_0 \end{array}\right]$. *More specifically, either* $v(t) \in \left[\begin{array}{cc} v_c & v_{max} \end{array}\right]$ *or* $v(t) \in \left[\begin{array}{cc} -v_c & -v_{max} \end{array}\right]$ *for* $t \in \left[\begin{array}{cc} t_2 & t_2 + \delta_0 \end{array}\right]$.

PROOF OF LEMMA (C.2.1)

By lemma (C.1.1), let $t' \in \left[\begin{array}{cc} t_2 & t_2 + \delta_0 \end{array}\right]$, so that $|v(t')| \geq v_T$. Let $t \in \left[\begin{array}{cc} t' - \delta_0 & t' + \delta_0 \end{array}\right]$

$$v(t') - \dot{v}_{max}\delta_0 \leq v(t) \leq v(t') + \dot{v}_{max}\delta_0 \tag{C.6}$$

If $v(t') > 0$, then $v(t') \geq v_T$,

$$\begin{aligned} v_T - (v_T - v_c) &< v(t') - \dot{v}_{max}\delta_0 \leq v(t) \\ v_c &< v(t) \\ v_c &< |v_T| \text{ for } t \in \left[\begin{array}{cc} t' - \delta_0 & t' + \delta_0 \end{array}\right] \end{aligned} \tag{C.7}$$

If $v(t') < 0$, then $v(t') \leq -v_T$,

$$\begin{aligned} v(t) &\leq v(t') + \dot{v}_{max}\delta_0 < -v_T + (v_T - v_c) \\ v(t) &< -v_c \\ v_c &< |v_T| \text{ for } t \in \left[\begin{array}{cc} t' - \delta_0 & t' + \delta_0 \end{array}\right] \end{aligned} \tag{C.8}$$

Then of the two cases above

$$v_c < |v_T| \text{ for } t \in \left[\begin{array}{cc} t' - \delta_0 & t' + \delta_0 \end{array}\right] \subset \left[\begin{array}{cc} t_2 & t_2 + \delta_0 \end{array}\right] \tag{C.9}$$

END OF PROOF OF LEMMA (C.2.1)

C.3 BOUNDS FOR $\left|\int_{t_2}^{t_2+\delta_0} f_p(v(\tau))d\tau\right|$

Define

$$f_{p_{min}} = min|f_p(v)| \text{ for}$$
$$[-v_{max} \quad -v_c]\cup[v_c \quad v_{max}]$$
$$v \in \left[-v_{max} \quad v_c\right] \cup \left[v_c \quad v_{max}\right] \tag{C.10}$$

$$f_{p_{max}} = max|f_p(v)| \text{ for}$$
$$[-v_{max} \quad -v_c]\cup[v_c \quad v_{max}]$$
$$v \in \left[-v_{max} \quad -v_c\right] \cup \left[v_c \quad v_{max}\right] \tag{C.11}$$

REMARK C.3.1 The above bounds exist because $|f_p(v)|$ is a continuous function defined on the compact set $\left[-v_{max} \quad -v_c\right] \cup \left[v_c \quad v_{max}\right]$. The advantage of the notation is that it allows for generality when the functions f_p are not monotonic and also when the functions are not symmetric. For monotonic functions, the bounds depend on the value of the function at the endpoints of the intervals.

C.4 PROOF OF PROPERTY 4.1.1

In this section, we prove property (4.1.1). By the conditions in the property, the previous two lemmas apply and we can conclude that v is in a compact set on the

subinterval.

$$v(t) \in \left[\begin{array}{cc} -v_{max} & -v_c \end{array} \right] \cup \left[\begin{array}{cc} v_c & v_{max} \end{array} \right] \text{ for } \left[\begin{array}{cc} t_2 & t_2 + \delta_0 \end{array} \right] \tag{C.12}$$

By definition above, on this set, the continuous function $f_p(v)$ which we can use that to derive the following bound

$$\left| \int_{t_2}^{t_2+\delta_0} f_p(v(\tau))d\tau \right| \geq f_{p_{min}} \Big|_{[\ -v_{max} \quad -v_c\ ]\cup[\ v_c \quad v_{max}\ ]} \delta_0 \tag{C.13}$$

For all $p = 2, ...m$, choose

$$\frac{1}{f_{p_{min}} \Big|_{[\ -v_{max} \quad -v_c\ ]\cup[\ v_c \quad v_{max}\ ]}} k\epsilon_0 T_{0_D} \leq \delta_0 < \frac{\frac{k\epsilon_0 T_{0_D}}{\delta_0} - v_c}{\dot{v}_{max}} \tag{C.14}$$

End of Proof of Property (4.1.1)

This concludes the proof of property (4.1.1). We have chosen the subinterval width, δ_0 small enough so that v does not change sign in the subinterval. Then we have chosen the scaling factor, k, small enough so that we can relate a measure of the signal to a measure of a first and third quadrant function of the signal.

Appendix D

A Property About a Vector of First and Third Quadrant Continuous Functions

PROOF OF LEMMA (4.1.1)

For all possible cases of the unit vector r, we have to find out the size of the tracking error. First consider a 'corner case', i.e. when r is a standard unit basis vector,

THE SIMPLER DIRECTIONS - WHEN r IS A STANDARD UNIT BASIS VECTOR

First we consider cases when r is a standard unit basis vector, the pth element of r is one and the other elements of r are zero. This corner case is equivalent to

$$\left| \int_{t_2}^{t_2+\delta_0} f_p(v(\tau))d\tau \right| < k\epsilon_0 T_{0_D} \tag{D.1}$$

where $f_p(v)$ is the pth element of the regression vector $\omega(v)$ and v is the jth state variable. Now we consider two subcases that encompass all possibilities:

SUBCASE 1.

$$\left| \int_{t_2}^{t_2+\delta_0} v(\tau)d\tau \right| < k\epsilon_0 T_{0_D} \tag{D.2}$$

Since the assumed condition on $\omega(v_d)$ implies that

$$\left| \int_{t_2}^{t_2+\delta_0} v_d((\tau)d\tau \right| \geq \epsilon_0 T_{0_D} \tag{D.3}$$

Then a positive lower bound can be obtained as desired.

$$\epsilon_0 T_{0_D}(1-k) \leq \left| \int_{t_2}^{t_2+\delta_0} (v_d(\tau) - v(\tau))d\tau \right| \tag{D.4}$$

SUBCASE 2.

$$\left| \int_{t_2}^{t_2+\delta_0} v(\tau)d\tau \right| \geq k\epsilon_0 T_{0_D} \tag{D.5}$$

To handle this subcase we use the results established in property (4.1.1) to choose conditions

$$\frac{1}{f_{p_{min}}\Big|_{[-v_{max} \quad -v_c]\cup[v_c \quad v_{max}]}} k\epsilon_0 T_{0_D} \leq \delta_0 < \frac{v_T - v_c}{\dot{v}_{max_{I_{i_P}}}} \tag{D.6}$$

where

$$v_T = \frac{k\epsilon_0 T_{0_D}}{\delta_0} \tag{D.7}$$

Then

$$\left| \int_{t_2}^{t_2+\delta_0} v(\tau)d\tau \right| \geq k\epsilon_0 T_{0_D} \quad \rightarrow \quad \left| \int_{t_2}^{t_2+\delta_0} f_p(v(\tau))d\tau \right| \geq k\epsilon_0 T_{0_D} \tag{D.8}$$

Because this is a contradiction to our original assumption for this corner case (Equation (D.1)), we will be able to conclude that this subcase can not happen.

THE MORE GENERAL DIRECTIONS -WHEN r IS A UNIT VECTOR IN $\Re^m$

For this case, there exists a unit vector $r \in \Re^m$ such that

$$\left| \int_{t_2}^{t_2+\delta_0} r_1 v(\tau) + \sum_{p=2}^{m} r_p f_p(v(\tau))d\tau \right| < k\epsilon_0 T_{0_D} \tag{D.9}$$

where the *pth* element of r is denoted by r_p.

SUBCASE 1.

$$\left| \int_{t_2}^{t_2+\delta_0} v(\tau)d\tau \right| < k\epsilon_0 T_{0_D} \tag{D.10}$$

Similarly to the corner case, the assumed condition on $\omega(v_d)$ together with the above condition implies that the tracking error satisfies a p.e. condition.

$$\epsilon T_{0_D}(1-k) \leq \left| \int_{t_2}^{t_2+\delta_0} (v_d(\tau) - v(\tau))d\tau \right| \tag{D.11}$$

SUBCASE 2.

$$\left| \int_{t_2}^{t_2+\delta_0} v(\tau)\, d\tau \right| \geq k\epsilon_0 T_{0_D} \tag{D.12}$$

In the corner cases, we have used the results of property (4.1.1) to construct a situation that ensures that v does not change sign in the subinterval $\left[\begin{array}{cc} t_2 & t_2+\delta_0 \end{array} \right]$. It will

turn out be useful if we make the same nice property to hold for the model trajectory, v_d. We want

$$\left| \int_{t_2}^{t_2+\delta_0} v_d(\tau)\, d\tau \right| \geq \epsilon_0 T_{0_D} \tag{D.13}$$

to imply that v_d does not change sign in the subinterval $\left[\begin{array}{cc} t_2 & t_2+\delta_0 \end{array}\right]$. So we pick

$$\delta_0 \;\leq\; \frac{\frac{\epsilon_0 T_{0_D}}{\delta_0} - v_c}{a_{d_{max}}} \tag{D.14}$$

where we define $a_{d_{max}}$ as an upper bound for the rate of change of the desired state variable v_d,

$$|\dot{v}_d(t)| \leq a_{d_{max}} \quad \text{for } t \geq 0 \tag{D.15}$$

By construction, δ_0 is small enough so that neither v nor v_d change sign in $\left[\begin{array}{cc} t_2 & t_2+\delta_0 \end{array}\right]$. Additionally because we are given the p.e. condition on v_d, we can conclude that $v_d \neq 0$ in $\left[\begin{array}{cc} t_2 & t_2+\delta_0 \end{array}\right]$. Similarly, by the Subcase 2 assumption in equation (D.12), we can conclude that $v \neq 0$ in $\left[\begin{array}{cc} t_2 & t_2+\delta_0 \end{array}\right]$. We have to consider only two cases:

A. $\text{sign}(v) \neq \text{sign}(v_d)$ in $\left[\begin{array}{cc} t_2 & t_2+\delta_0 \end{array}\right]$
B. $\text{sign}(v) = \text{sign}(v_d)$ in $\left[\begin{array}{cc} t_2 & t_2+\delta_0 \end{array}\right]$

<u>CASE A. $\text{sign}(v) \neq \text{sign}(v_d)$ in $\left[\begin{array}{cc} t_2 & t_2+\delta_0 \end{array}\right]$</u> Because the signums of v and v_d are not equal in $\left[\begin{array}{cc} t_2 & t_2+\delta_0 \end{array}\right]$,

$$\left| \int_{t_2}^{t_2+\delta_0} (v_d(\tau) - v(\tau))\, d\tau \right| \;=\; \left| \int_{t_2}^{t_2+\delta_0} (|v_d(\tau)|\text{sgn}(v_d(\tau)) - |v|\text{sgn}(v(\tau)))\, d\tau \right|$$

$$= \left| \int_{t_2}^{t_2+\delta_0} (|v_d(\tau)| + |v(\tau)|)\, d\tau \right| \tag{D.16}$$

By the assumed persistent excitation of $\omega(v_d)$ and the fact that v_d does not change sign in $\left[\begin{array}{cc} t_2 & t_2+\delta_0 \end{array}\right]$, we have

$$\left| \int_{t_2}^{t_2+\delta_0} v_d(\tau) d\tau \right| = \int_{t_2}^{t_2+\delta_0} |v_d(\tau)| d\tau \geq \epsilon_0 T_{0_D} \tag{D.17}$$

Similarly, v does not change sign in $\left[\begin{array}{cc} t_2 & t_2+\delta_0 \end{array}\right]$ gives

$$\left| \int_{t_2}^{t_2+\delta_0} v(\tau) d\tau \right| = \int_{t_2}^{t_2+\delta_0} |v(\tau)|\, d\tau \geq k\epsilon_0 T_{0_D} \tag{D.18}$$

By combining equations (D.16), (D.17), (D.18), we obtain

$$\begin{aligned} \left| \int_{t_2}^{t_2+\delta_0} (v_d(\tau) - v(\tau)) d\tau \right| &= \int_{t_2}^{t_2+\delta_0} (|v_d(\tau)| + |v(\tau)|) d\tau \\ &= \int_{t_2}^{t_2+\delta_0} |v_d(\tau)|\, d\tau + \int_{t_2}^{t_2+\delta_0} |v(\tau)|\, d\tau \\ &\geq \epsilon_0 T_{0_D}(1+k) \end{aligned} \tag{D.19}$$

Thus we have a positive lower bound for $\left| \int_{t_2}^{t_2+\delta_0} (v_d(\tau) - v(\tau)) d\tau \right|$ as desired. In this case in which we know the signs of v and v_d are different, the positive lower bound for the measure of the tracking error, is larger than in the next case in which the signs are the same.

<u>CASE B. $\text{sign}(v) = \text{sign}(v_d)$ in $\left[\begin{array}{cc} t_2 & t_2+\delta_0 \end{array}\right]$</u> Let r_p denote the *pth* element of the unit vector r. Add and subtract $\omega(v_d)r$ to equation (D.9),

$$\left| \int_{t_2}^{t_2+\delta_0} r_1(v(\tau) - v_d(\tau)) + r_1 v_d(\tau) + \sum_{p=2}^{p=m} r_p \left(f_p(v(\tau)) - f_p(v_d(\tau))\right) + r_p f_p(v_d(\tau)) \right|$$

$$< k\epsilon_0 T_{0_D} \tag{D.20}$$

We use the p.e. of $\omega(v_d)$ and the lower triangle inequality to obtain

$$(1-k)\epsilon_0 T_{0_D} - \left| \int_{t_2}^{t_2+\delta_0} \sum_{p=2}^{p=m} r_p \left(f_p(v(\tau)) - f_p(v_d(\tau)) \right) d\tau \right|$$

$$< \left| \int_{t_2}^{t_2+\delta_0} r_1(v(\tau) - v_d(\tau)) d\tau \right| \tag{D.21}$$

The second term in the left-hand side of the above equation has a maximum because it is a continuous function defined on the compact set, $v \in \begin{bmatrix} -v_{max} & -v_c \end{bmatrix} \cup \begin{bmatrix} v_c & v_{max} \end{bmatrix}$ and $v_d \in \begin{bmatrix} -v_{d_{max}} & -v_c \end{bmatrix} \cup \begin{bmatrix} v_c & v_{d_{max}} \end{bmatrix}$. An upper bound for this maximum, k_{eff} is defined such that

$$\left| \int_{t_2}^{t_2+\delta_0} \sum_{p=2}^{p=m} r_p \left(f_p(v(\tau)) - f_p(v_d(\tau)) \right) d\tau \right| \leq k_{eff}\epsilon_0 T_{0_D} \tag{D.22}$$

By condition in the lemma statement, ϵ_0 is chosen large enough so that the term $1 - k - k_{eff} > 0$. Then a positive lower bound for a measure of the tracking error is

$$0 < \epsilon_0 T_{0_D} \left(1 - k - k_{eff}\right) \leq \left| \int_{t_2}^{t_2+\delta_0} (v_d(\tau) - v(\tau)) d\tau \right| \tag{D.23}$$

End of Proof of Lemma (4.1.1)

Remark D.0.1 We could proceed directly with the general r case and omit the special case when r is a standard unit basis vector. However, analyzing the standard unit basis case first is instructive because it illustrates the basic idea we follow in the more general case.

Appendix E

A Property About the Conditions Required to Exploit First and Third Quadrant Function Properties

PROOF OF LEMMA (4.1.2)

First we consider condition (i.) on the p.e. level, ϵ_0. By assumption,

$$v_{max_{I_{i_P}}} \leq v_{max} \tag{E.1}$$

By definition

$$\begin{aligned} k_{eff_{I_{i_P}}} &\leq k_{eff} \\ 1 - k - k_{eff_{I_{i_P}}} &\geq 1 - k - k_{eff} \end{aligned} \tag{E.2}$$

By definition, this is equivalent to

$$\frac{\gamma'\nu'_{max}}{\gamma'\nu'_{max} + \delta + \delta_{eff_{I_{i_P}}}} \geq \frac{\gamma'\nu'_{max}}{\gamma'\nu'_{max} + \delta + \delta_{eff}} \tag{E.3}$$

So condition (i.) on the p.e. level also satisfies condition (i.')

$$\gamma'\nu'_{max} + \delta + \delta_{eff_{I_{i_P}}} \leq \gamma'\nu'_{max} + \delta + \delta_{eff} < \epsilon_0 \tag{E.4}$$

Next consider condition (ii.) which is an upper bound on the p.e. subinterval width, δ_0

$$\delta_0 \quad < \quad min\left(\frac{\frac{\epsilon_0 T_{0_D}}{\delta_0} - v_c}{a_{d_{max}}}, \frac{\frac{k\epsilon_0 T_{0_D}}{\delta_0} - v_c}{\dot{v}_{max}}\right) \tag{E.5}$$

The first term on the right hand side is not a function of the upper bounds on v and $\dot{v}$. So it is automatically satisfied for both sets of lower bounds. For the second term because

$$\frac{1}{\dot{v}_{max}} \leq \frac{1}{\dot{v}_{max_{I_{i_P}}}} \tag{E.6}$$

and also because

$$\frac{k\epsilon_0 T_{0_D}}{\delta_0} - v_c > 0 \tag{E.7}$$

we conclude condition (ii.') is also satisfied

$$\delta_0 < \frac{\frac{k\epsilon_0 T_{0_D}}{\delta_0} - v_c}{\dot{v}_{max}} \leq \frac{\frac{k\epsilon_0 T_{0_D}}{\delta_0} - v_c}{\dot{v}_{max_{I_{i_P}}}} \tag{E.8}$$

Next consider condition (iii.) on the smallness of the scaling factor, k.

The terms in the denominator of the the left-hand side of the condition involve the minimum of a the function f_p over a closed bounded set (see definition in section (C.3) of appendix (C) in equation (C.10)) The set for the lower bounds is a subset of the set for the upper bounds.

$$\left[-v_{max_{I_{i_P}}} \quad -v_c \right] \cup \left[v_c \quad v_{max_{I_{i_P}}} \right] \subseteq \left[-v_{max} \quad -v_c \right] \cup \left[v_c \quad v_{max} \right] \tag{E.9}$$

This means that for $p = 2, ...m$

$$\frac{1}{f_{p_{min}}\left[v_c \quad v_{max_{I_{i_P}}} \right] \cup \left[-v_c \quad -v_{max_{I_{i_P}}} \right]} \leq \frac{1}{f_{p_{min}}\left[v_c \quad v_{max} \right] \cup \left[-v_c \quad -v_{max} \right]} \tag{E.10}$$

and this means that condition (iii.') is satisfied for every $p = 2, ..m$, we have

$$\frac{1}{f_{p_{min}}\left[v_c \quad v_{max_{I_{i_P}}} \right] \cup \left[-v_c \quad -v_{max_{I_{i_P}}} \right]} k\epsilon_0 T_{0_D}$$

$$\leq \frac{1}{f_{p_{min}}\left[v_c \quad v_{max} \right] \cup \left[-v_c \quad -v_{max} \right]} k\epsilon_0 T_{0_D} \delta_0$$

END OF PROOF

Appendix F

Properties about the 'Unforced' Error Model System

In this appendix, we prove property (4.2.1) and lemma (4.2.2). Before proceeding, we briefly summarize proof ideas.

Property (4.2.1) says that the regression vector satisfies a p.e. condition on an interval, then an interval can be constructed over which the positive definite function, V_u, of the errors decreases. The first part of the proof follows exactly from [16]. Because of the lemma in [16], we know that $||\tilde{\theta}||$ must eventually get small. In this situation, if V_u is 'large', then $||e_u||$ must be large, which implies that V_u will decrease and an upper bound on the amount of decrease can be given as a function of the interval size, γ. This is in equation (F.11) below.

At this point the analysis departs slightly from [16] because we are particular in characterizing the behavior of the function γ for the proof of lemma (4.2.2).

The idea of the proof of lemma (4.2.2) is to choose the smallest value for the level of

decrease in V_u that we can because the smaller the level of decrease, the higher the level of Lipschitz disturbances we can have for which we can satisfy the constraint in equation (4.46).

F.1 Proof of Property 4.2.1

In this section we prove property (4.2.1).

For $t > t_i$,

$$||q_u(t)||^2 \leq \sqrt{\frac{\lambda_{P_{max}}}{\lambda_{P_{min}}}}||q(t_i)||^2 \tag{F.1}$$

Choose positive constants ϵ_2, c_1 and δ_s

$$\begin{aligned} 0 < \epsilon_2 &< c\epsilon_1 < \epsilon_1 \\ 1 - c_1 &> 0 \\ \delta_s &= \sqrt{\epsilon_2 c_1} \end{aligned} \tag{F.2}$$

There is a lemma, which is proved in [16] and stated below, which states that there is a time, $T(\epsilon_1, \delta_s)$ by which $\tilde{\theta}$ gets 'small', $||\tilde{\theta}_u|| \leq \delta_s$.

Lemma F.1.1 *If $\omega(v(t))$ satisfies a p.e. condition on an interval $\begin{bmatrix} t_i & t_i + T_{0_P} \end{bmatrix}$, i.e. positive constants δ_0, k, and ϵ_0' exist such that on a subinterval $\begin{bmatrix} t_2 & t_2 + \delta_0 \end{bmatrix}$*

$$\int_{t_2}^{t_2+\delta_0} \omega(v(\tau))^T r d\tau \geq k\epsilon_0' T_{0_P} \tag{F.3}$$

for any unit vector $r \in \Re^3$.

Then there is a $T = T(\epsilon_1, \delta_s)$ such that if $q_u(t)$ is a solution to equation (4.36) with $||V_u(q_u(t_i), t_i)|| \leq \epsilon_1$, then there exists a $t_2' \in \left[\ t_i, t_i + T\ \right]$ such that $||\tilde{\theta}_u(t_2')|| \leq \delta_s$.

Next, we construct a T_c such that V_u decreases by a specified amount over the interval $\left[\ t_i, t_i + T(\epsilon_1, \delta_s) + \delta_0 + T_c\ \right]$. We will define $T_{0_D} = T_(\epsilon_1, \delta_s) + \delta_0 + T_c$.

If $V_u(q_u(t_2')) \leq \epsilon_2$, we are done. Assume that $V_u(q(t_2')) > \epsilon_2$. Then if V_u is 'large' and $\tilde{\theta}_u$ is 'small', then $||e_u||$ must be 'large', i.e.

$$||e_u(t_2')||^2 \geq \frac{1}{\lambda_P}(V_u(q_u(t_2') - \delta_s^2) \geq V_u(q_u(t_2'))\frac{1 - c_1}{\lambda_P} \tag{F.4}$$

If $t > t_2'$ derive the maximum decrease in $||e_u||$ using the dynamic equation (equation (4.36)) as

$$||e_u(t_2')|| - ||e_u(t)|| \leq ||e_u(t) - e_u(t_2')|| \ \leq \ \int_{t_2'}^{t} ||Ae_u - b\omega(v(\tau))^T\tilde{\theta}_u||d\tau \tag{F.5}$$

Now we consider the maximum value for $||\omega(v(\tau))||$ where v represents the solution for the forced system. In [16], this term is a bounded quantity. For our problem an upper bound for this term can be denoted as follows.

$$||\omega(v(\tau))|| \leq \omega_{max_{I_{i_D}}} \qquad \text{for } \tau \in I_{i_D} \tag{F.6}$$

This term exists because it is a continuous function defined on a compact set. Substituting into (F.5), we obtain

$$||e_u(t_2')|| - ||e_u(t)|| \ \leq \ (A_{max} + b_{max}\omega_{max_{I_{i_D}}})\frac{\sqrt{\lambda_{P_{max}}}}{\sqrt{\lambda_{P_{min}}}}||q_u(t_2')||(t - t_2') \tag{F.7}$$

Combining this result with that in equation (F.4), for some $T_c > 0$, we can represent

the maximum decrease in $||e_u(t_2' + T_c)||$ in terms of $V_u(q_u(t_2'))$.

$$||e_u(t_2' + T_c)|| \geq \sqrt{V_u(q_u(t_2')}\left(\frac{\sqrt{1-c_1}}{\sqrt{\lambda_P}} - (A_{max} + b_{max}\omega_{max_{I_{i_D}}})\frac{\sqrt{\lambda_P}}{\lambda_{P_{min}}}T_c\right) \tag{F.8}$$

Notice $||e_u(t_2' + t)||$ can only decrease until it gets to zero. Now we would like to obtain the minimum decrease in V_u over time T_c.

$$V_u(q_u(t_2')) - V_u(q_u(t_2' + T_c)) \geq \lambda_{Q_{min}} \int_{t_2'}^{t_2'+T_c} ||e(\tau)||^2 d\tau \tag{F.9}$$

$$\lambda_{Q_{min}} \int_{t_2'}^{t_2'+T_c} ||e(\tau)||^2 d\tau \geq \lambda_{Q_{min}} T_c V_u(q_u(t_2'))\left(\frac{\sqrt{1-c_1}}{\sqrt{\lambda_P}} - (A_{max} + b_{max}\omega_{max_{I_{i_D}}})\frac{\sqrt{\lambda_P}}{\lambda_{P_{min}}}T_c\right)^2$$

Again we notice that because $||e_u||$ can only decrease until it gets to zero, V_u can only decrease until it gets to zero.

Rewrite the inequalities

$$V_u(q_u(t_2' + T_c)) \leq \gamma V_u(q_u(t_2')) \tag{F.10}$$

where γ is defined as follows as an upper bound on the amount of decrease in V_u for the specified interval

$$\gamma = \left(1 - \lambda_{Q_{min}} T_c \left(\frac{\sqrt{1-c_1}}{\sqrt{\lambda_P}} - (A_{max} + b_{max}\omega_{max_{I_{i_D}}})\frac{\sqrt{\lambda_P}}{\lambda_{P_{min}}}T_c\right)^2\right) \tag{F.11}$$

To satisfy the property, we choose conditions so that $\gamma < 1$. The value of γ depends on $\lambda_{Q_{min}}$ and T_c. However, $\lambda_{Q_{min}}$ is fixed by the system parameters, i.e. the A, P and Q matrices, and we will also choose it based on the the level of disturbances (see condition (i.) of theorem (4.4.1). So we must pick T_c so that $\gamma < 1$. Then we will have constructed the interval of width $T_{0_D} = T(\epsilon_1, \delta_s) + \delta_0 + T_c$ on which the function

V_u decreases.

Notice, however, that to pick T_c, the value of $\omega_{max_{I_{i_D}}}$ matters. Because this quantity depends on the interval I_{i_D}, we are trying to pick T_c, and therefore T_{0_D}, based on a quantity that is dependent on T_{0_D}. Therefore T_{0_D} is implicitly defined.

This is not a problem, however, and we maintain that we can always choose an appropriate T_{0_D}. This turns out to be true because $\omega_{max_{I_{i_D}}}$ is a nondecreasing function, i.e. if the interval I_{i_D} gets larger, than the value of $\omega_{max_{I_{i_D}}}$ stays the same or gets larger.

Define

$$c_3 = \frac{\sqrt{1-c_1}}{\sqrt{\lambda_P}} \tag{F.12}$$

$$k_1(T_{0_D}) = (A_{max} + b_{max}\omega_{max_{I_{i_D}}})\frac{\sqrt{\lambda_P}}{\lambda_{P_{min}}} \tag{F.13}$$

Note that because the function k_1 is a monotonically increasing function of T_{0_D} then because $T_{0_D} > T(\epsilon_1, \delta_s)$ implies

$$\frac{1}{k_1(T_{0_D})} < \frac{1}{k_1(T(\epsilon_1, \delta_s))} \tag{F.14}$$

Substituting the definitions for $k_1(T_{0_D})$ and c_3 into the equation for γ, we have

$$\gamma = 1 - \lambda_{Q_{min}} T_c \left(c_3 - k_1(T_{0_D})T_c\right)^2 \tag{F.15}$$

Next we would like to examine the behavior of the γ as a function of T_c. At $T_c = 0$ and $T_c = \frac{c_3}{k_1(T_{0_D})}$, $\gamma = 1$. Because $T_{0_D} = T(\epsilon_1, \delta_s) + \delta_0 + T_c$ is a function of T_c, let

$$k_1' = \frac{d\gamma(T_c)}{dT_c} \tag{F.16}$$

Because k_1 is a nondecreasing function of T_c,

$$k_1' \geq 0 \tag{F.17}$$

Then the derivative of γ is as follows

$$\frac{d\gamma}{dT_c} = (c_3 - k_1(T_{0_D})T_c)\,(T_c k_1(T_{0_D})(1 + 2k_1') - c_3)\,\lambda_{Q_{min}} \tag{F.18}$$

The derivative of γ is zero at $T_c = \frac{c_3}{k_1(T_{0_D})}$ and at $T_c = \frac{c_3}{k_1(T_{0_D})(1+2k_1')} \leq \frac{c_3}{k_1(T_{0_D})}$. There is a local minimum at $T_c = \frac{c_3}{k_1(T_{0_D})(1+2k_1')}$ and a local maximum of $\gamma = 1$ at $T_c = \frac{c_3}{k_1(T_{0_D})}$.

The first term in the equation for the derivative of γ with respect to T_c is negative and the second term is positive for $T_c > \frac{c_3}{k_1(T_{0_D})}$ Therefore γ is a strictly decreasing function of T_c for $T_c > \frac{c_3}{k_1(T_{0_D})}$.

Figure F-1 shows how the γ as a function of T_c can behave. Note that γ is the upper bound on amount of decrease in V_u as T_c varies, it is not the actual decrease. Because $\dot{V}_u \leq \lambda_{Q_{min}}||e_u||^2$, the actual decrease is a monotonically decreasing function.

We must find one value of T_c so that the corresponding value of γ in equation (F.11) is less than one.

We can choose any $0 < T_c < \frac{c_3}{k_1(T_{0_D})}$, because the corresponding value of γ is less than one.

END OF PROOF OF PROPERTY (4.2.1)

F.2 PROOF OF LEMMA 4.2.2

In this section we prove lemma (4.2.2).

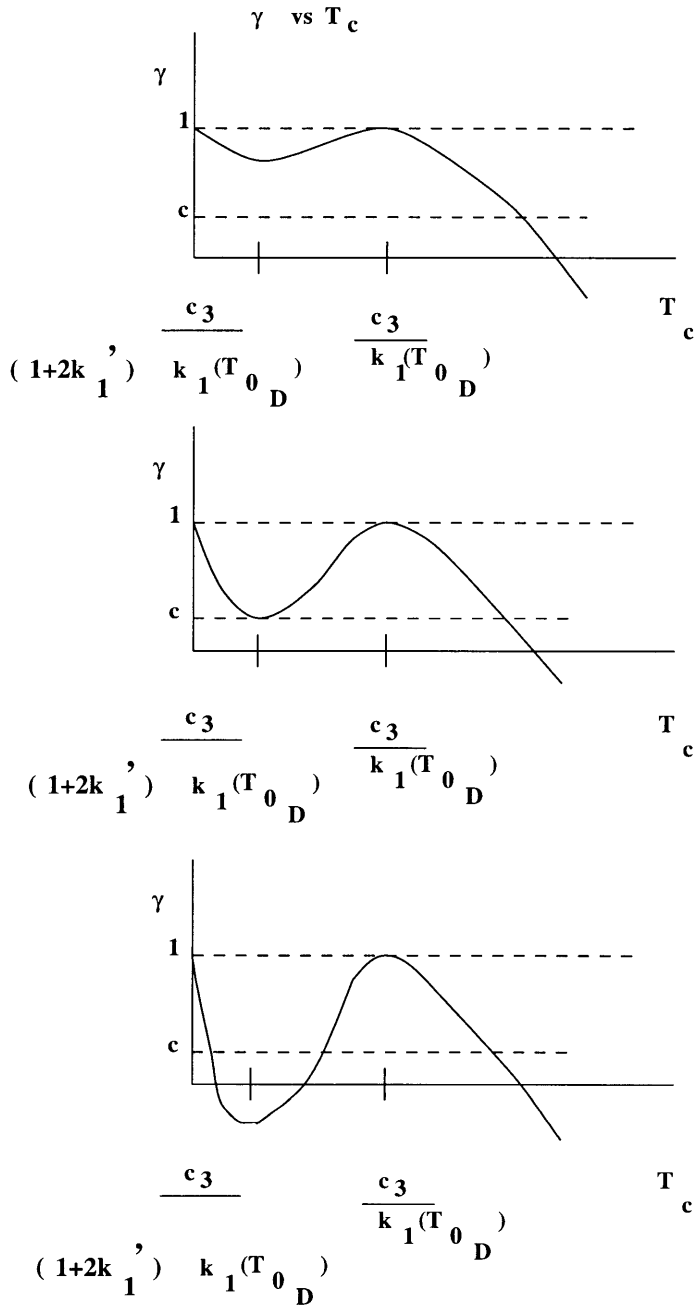

Figure F-1: The function, γ, which depends on T_c, is an upper bound on the amount of decrease in V_u on an interval. The function has a local minimum which is less than one at $T_c = \frac{c_3}{k_1(T_{0_D})(1+2k_1')}$.

PROOF OF LEMMA (4.2.2)

We continue from the proof of property (4.2.1).

We would like to choose the smallest value of decrease in V_u that we can in order to satisfy the constraint for the largest level of Lipschitz disturbances, k_2.

Although the function γ is strictly decreasing for T_c, it could be decreasing arbitrarily slowly and we need to quantify the relationship between c and T_{0_D}.

So for the smallest decrease in V_u, we choose the value of T_c at the local minimum and define the corresponding value for γ as, c^*, the lowest level of decrease we can compute.

Choose

$$\begin{aligned} T_c^* &= \frac{c_3}{k_1(T_{0_D})(1+2k_1')} < \frac{c_3}{k_1(T(\epsilon_1,\delta_s))} \\ c^* &= 1 - \lambda_{Q_{min}} T_c^* \left(c_3 - k_1(T_{0_D})T_c^*\right)^2 \end{aligned} \tag{F.19}$$

Note that this has to be computed iteratively because of the functional dependence on T_{0_D}. However, it can be computed because T_c^* is bounded by a known quantity as shown in the equation above.

Now in order to satisfy the constraint we must choose $0 < k_2^*$ small enough so that

$$\gamma(T_c^*) < e^{-k_2^*(T(\epsilon_1,\delta_s)+\delta_0+T_c^*)} \tag{F.20}$$

END OF PROOF OF LEMMA (4.2.2)

Appendix G

Properties Bounding the Error Model State and the Function, V, on an Interval

G.1 Proof of Property 4.3.1

We showed in chapter 3 in equation (3.15) that for this error model

$$\dot{V} \leq -\lambda'_Q ||e||^2 + 2\lambda_{P_{max}} \nu'_{max} ||e|| \tag{G.1}$$

The function, V, can only increase when the error has a small magnitude, $||e|| \leq 2\frac{\nu'_{max}\lambda_{P_{max}}}{\lambda'_Q}$.

We find the maximum rate of change of V,

$$\frac{d\dot{V}}{d||e||} = -2\lambda'_Q||e|| + 2\lambda_{P_{max}}\nu'_{max} \tag{G.2}$$

The maximum value of $\dot{V}$ occurs when

$$||e|| = \frac{\lambda_{P_{max}}\nu'_{max}}{\lambda'_Q} \tag{G.3}$$

$$\dot{V}_{max} = \frac{(\nu'_{max}\lambda_{P_{max}})^2}{\lambda'_Q} \tag{G.4}$$

The maximum increase of V over a time interval of length T_{int} is therefore

$$\begin{aligned} V(z(t_i + T_{int})) - V(z(t_i)) &= \frac{\lambda^2_{P_{max}}\nu'^2_{max}}{\lambda'_Q}T_{int} \\ &= \frac{\gamma'^2\nu'^2_{max}}{4}\lambda'_Q T_{int} \end{aligned} \tag{G.5}$$

End of Proof of Property (4.3.1)

G.2 Proof of Property 4.3.2

The absolute value of jth state and derivative, v and $\dot{v}$ respectively, are continuous (v is continuous because it is differentiable and a differentiable function is continuous. $\dot{v}$ is continuous because the error model dynamic equation for $\dot{v}$ is defined to be continuous). A continuous function has a maximum on the compact set I_{int}. Therefore, $v_{max_{I_{int}}}$ and $\dot{v}_{max_{I_{int}}}$ exist.

To find upper bounds on interval I_{int}, we use the result obtained in (equation (G.5)).

$$\begin{aligned} V(q(t_i+t)) &\leq V(q(t_i)) + \leq \frac{\gamma'^2 \nu'^2_{max}}{4} \lambda'_Q t \text{ for } t_i + t \in I_{int} \\ &\leq V(q(t_i)) + \frac{\gamma'^2 \nu'^2_{max}}{4} \lambda'_Q T_{int} \end{aligned} \tag{G.6}$$

So by definition of V

$$\begin{aligned} e^T(t_i+t)e(t_i+t) &\leq \frac{1}{\lambda_{P_{min}}} \left(V(q(t(i)) + \frac{\gamma'^2 \nu'^2_{max}}{4} \lambda'_Q T_{int} \right) \quad \text{for } t_i + t \in I_{int} \\ \tilde{\theta}^T(t_i+t)\tilde{\theta}(t_i+t) &\leq V(q(t_i)) + \frac{\gamma'^2 \nu'^2_{max}}{4} \lambda'_Q T_{int} \quad \text{for } t_i + t \in I_{int} \end{aligned} \tag{G.7}$$

Define $||e||_{max_{I_{int}}}$ and $||\tilde{\theta}||_{max_{I_{int}}}$ as upper bounds for $||e(t)||$ and $||\tilde{\theta}(t)||$ respectively for $t \in I_{int}$.

$$\begin{aligned} ||e||_{max_{I_{int}}} &= \frac{1}{\lambda_{P_{min}}} \sqrt{V(q(t_i)) + \frac{\gamma'^2 \nu'^2_{max}}{4} \lambda'_Q T_{int}} \\ ||\tilde{\theta}||_{max_{I_{int}}} &= \sqrt{V(q(t_i)) + \frac{\gamma'^2 \nu'^2_{max}}{4} \lambda'_Q T_{int}} \end{aligned} \tag{G.8}$$

Because we have derived a bound for $||e||$ on the interval, we can use it to get a bound for the jth element of the state. By definition of e we obtain

$$v_{max_{I_{int}}} \leq \frac{1}{\lambda_{P_{min}}} \sqrt{V(q(t_i)) + \frac{\gamma'^2 \nu'^2_{max}}{4} \lambda'_Q T_{int}} + v_{d_{max}} \tag{G.9}$$

where $v_{d_{max}}$ is defined as the maximum magnitude of the v_d, which is jth element of the desired trajectory vector x_d, i.e.

$$|v_d(t)| \leq v_{d_{max}}(t) \qquad \text{for all } t \geq 0 \tag{G.10}$$

Since $|v(t)| \in \begin{bmatrix} 0 & v_{max_{I_{int}}} \end{bmatrix}$ for $t \in I_{int}$, then a maximum for $||\omega(v(t))||$ exists because a continuous function on a compact set has a maximum. Let an upper bound for this

maximum as be as follows,

$$||\omega(v(t))|| \leq \omega_{max_{I_{int}}} \tag{G.11}$$

Using the error model equation and the assumed disturbance bounds, we can derive a bound for $\dot{v}_{max_{I_{int}}}$ for $t_i + t \in I_{int}$.

$$\begin{aligned} |\dot{v}(t_i + t)| \quad < \quad & a_{d_{max}} + A_{max}||e||_{max_{I_{int}}} \\ & + b_{max}(||\tilde{\theta}||_{max_{I_{int}}} \omega_{max_{I_{int}}}) \\ & + \nu'_{max} + b_{max} d_{max} ||e||_{max_{I_{int}}} \end{aligned} \tag{G.12}$$

Using the above result and the bounds obtained in equation (G.7), we can obtain the desired result.

End of Proof of Property (4.3.2)

Appendix H

Choice of p.e. subinterval width, δ_0, and scaling factor, k

In this appendix, given a value for the p.e. level, ϵ_0, we make choices for the p.e. subinterval width, δ_0, the scaling factor, k, in order to satisfy condition (iii.) of the stability theorem. The upper bounds for δ_0 and k can be decoupled from each other. Additionally, the p.e. subinterval width can be decoupled from the p.e. level.

The following notation will be used,

$$I_{v_c,v_{max}} = \left[\begin{array}{cc} -v_{max} & v_c \end{array} \right] \cup \left[\begin{array}{cc} v_c & v_{max} \end{array} \right] \tag{H.1}$$

The value for v_c will be assumed to be zero in this section as explained in the proof of theorem (4.6.1).

From condition (iii.) of theorem (4.4.1), the p.e. subinterval width, δ_0, and a scaling

factor, $0 < k < 1$, must be small enough to satisfy the following

$$\begin{aligned} 0 &< k < 1 \\ 0 &< max_{p=2,..m}\left(\frac{1}{f_{p_{minI_{v_c},v_{max}}}} k\epsilon_0 T_{0_D}\right) \leq \delta_0 \\ 0 &< \delta_0 < min\left(\frac{\frac{\epsilon_0 T_{0_D}}{\delta_0}}{a_{d_{max}}}, \frac{\frac{k\epsilon_0 T_{0_D}}{\delta_0}}{\dot{v}_{max}}\right) \end{aligned} \tag{H.2}$$

Because $k < 1$, $\dot{v}_{max} > a_{d_{max}}$ by definition, we have

$$\left(\frac{\frac{\epsilon_0 T_{0_D}}{\delta_0}}{a_{d_{max}}}\right) > \left(\frac{\frac{k\epsilon_0 T_{0_D}}{\delta_0}}{\dot{v}_{max}}\right) \tag{H.3}$$

Define an upper bound for δ_0,

$$0 < \delta_{0_{max}} = \sqrt{\left(\frac{\epsilon_0 T_{0_D}}{a_{d_{max}}}\right)} \tag{H.4}$$

Both of the equations in condition (iii.) involve both δ_0 and k. First we break up condition (iii) into two conditions. Let condition (iiia.) be the inequality in condition (iii.) which can be represented as an upper bound for the scaling factor k. Let condition (iiib.) be the inequality in condition (iii.) which is an upper bound on δ_0.

(iiia.) For $p = 2, ...m$

$$\begin{aligned} 0 &< k < 1 \\ k\epsilon_0 T_{0_D} &\leq \delta_0 f_{p_{minI_{v_c},v_{max}}} \end{aligned} \tag{H.5}$$

(iiib.)

$$0 < \delta_0 < \frac{\frac{k\epsilon_0 T_{0_D}}{\delta_0}}{\dot{v}_{max}} \tag{H.6}$$

Note that (iiib.) also implies that $\delta_0 < \delta_{0_{max}}$

We decouple the conditions. Substituting condition (iiia.) into (iiib.), we obtain a decoupled equation for the p.e. subinterval width, δ_0,

$$0 < \delta_0 < \frac{1}{\dot{v}_{max}} \left(f_{p_{minI_{v_c,v_{max}}}} \right) \tag{H.7}$$

Substituting the result (equation (H.7)) into condition (iiia.) we obtain a decoupled equation for the scaling factor, k.

$$k < \frac{1}{\epsilon_0 T_{0_D} \dot{v}_{max}} \left(f_{p_{minI_{v_c,v_{max}}}} \right) \left(f_{p_{minI_{v_c,v_{max}}}} \right) \tag{H.8}$$

Bibliography

[1] A.M. Annaswamy, F.P. Skantze, and A.P Loh. Adaptive control of continuous time systems with nonlinear parameterization. *M.I.T. Adaptive Control Laboratory*, 9602, April 1996.

[2] B. Armstrong-Helouvry, P. Dupont, and C. Canudas de Wit. A survey of models, analysis tools and compensation methods for the control of machines with friction. *Automatica*, 30(7), 1994.

[3] F.P. Bowden and D. Tabor. The area of contact between stationary and between moving surfaces. In *Proceedings of the Royal Society, Series A.*, volume 169, 1939.

[4] C. Canudas de Wit, H. Olsson, K.J. Astrom, and P. Lischinsky. A new model for control of systems with friction. *IEEE Transactions on Automatic Control*, 40(3), March 1995.

[5] P.R. Dahl. *A Solid Friction Model*, volume TOR-158. The Aerospace Corporation, El Segundo, CA, 1968.

[6] S. Dasgupta, Y. Shrivastava, and G. Krenzer. Persistent excitation in bilinear systems. *IEEE Transactions on Automatic Control*, 36(3), March 1991.

[7] B. Egardt. *Stablilty of Adaptive Controllers.* Spinger-Verlag, Berlin, 1979.

[8] J. Halling. *Principles of Tribology.* Macmillan, London, 1975.

[9] Soom A. Hess D.P. Friction at a lubricated line contact operating at oscillating sliding velocities. *Journal of Tribology Transactions of the ASME*, 112, 1990.

[10] P.A. Ioannou and P.V. Kokotovic. *Adaptive Systems with Reduced Models.* Springer-Verlag, NY, 1983.

[11] I. Kanellakopoulos, P.V. Kokotovic, and A.S. Morse. Systematic design of adaptive controllers for feedback linearizable systems. *IEEE Transactions on Automatic Control*, 36(11), November 1991.

[12] G. Kreisselmeier and K.S. Narendra. Stable model reference adaptive control in the presence of bounded disturbances. *IEEE Transactions on Automatic Control*, 27, December 1982.

[13] N. E. Leonard and P.S. Krishnaprasad. Adaptive friction compensation for bidirectional low-velocity position tracking. In *Proceedings of the 31st Conference on Decision and Control*, Tucson, AZ, December 1992.

[14] W. Li and X. Cheng. Adaptive high-precision control of positioning tables-theory and eexperiments. *IEEE Transactions on Control Systems Technology*, 2(3), September 1994.

[15] R.V. Monopoli. Model reference adaptive control with an augmented error signal. *IEEE Transactions on Automatic Control*, 19, 1974.

[16] A.P. Morgan and K.S. Narendra. On the stability of nonautonomous differential equations $\dot{x} = [A + B(t)]x$, with skew symmetric matrix $B(t)$. *Siam Journal of Control and Optimization*, 15(1), January 1977.

[17] K.S. Narendra and A.M. Annaswamy. Robust adaptive control in the presence of bounded disturbances. *IEEE Transactions on Automatic Control*, AC-31(4), April 1986.

[18] K.S. Narendra and A.M. Annaswamy. A new adaptive law for robust adaptation without persistent excitation. *IEEE Transactions on Automatic Control*, AC-32(2), February 1987.

[19] K.S. Narendra and Y.H. Lin. *Design of Stable Model Reference Adaptive Controllers.* Academic Press, New York, 1980.

[20] K.S. Narendra and L.S. Valavani. Stable adaptive controller design-direct control. *IEEE Transactions on Automatic Control*, 23, August 1978.

[21] E. Rabinowicz. *Friction and Wear of Materials.* John Wiley and Sons, NY, 1965.

[22] C.J. Radcliffe and S.C. Southward. A property of stick-slip friction models which promotes limit cycle generation. In *ACC*, San Diego, 1990.

[23] C. Rohrs, L. Valavani, M. Athans, and G. Stein. Robustness of continuous-time adaptive control algorithms in the presence of unmodelled dynamics. *IEEE Transactions on Automatic Control*, AC-30(9), September 1985.

[24] C Samson. Stability analysis of adaptively controlled systems subject to bounded disturbances. *Automatica*, 19, 1983.

[25] D. Seto, A.M. Annaswamy, and J. Baillieul. Adaptive control of a class of nonlinear systems with a triangular structure. *IEEE Transactions on Automatic Control*, 39(7), July 1994.

[26] L.F. Shampine and M.W. Reichelt. The matlab ode suite. *Math Department SMU, TX*, 94-6, 1994.

[27] Fredrik Petter Skantze. Model-based algorithms for nonlinear systems identification. Master's thesis, Massachusetts Institute of Technology, February 1996.

[28] N.P. Suh. *Tribophysics.* Prentice Hall, Englewood Cliffs, NJ, 1986.